ISSN 0503-1540

La mer

Tome 43 Numéro 1–2 Mai 2005

La Société franco–japonaise

d'océanographie

Tokyo, Japon

Note pour la présentation des manuscrits

La mer, organe de la Société franco-japonaise d'océanographie, publie des articles et notes originaux, des articles de synthèse, des analyses d'ouvrages et des informations intéressant les membres de la société. Les sujets traités doivent avoir un rapport direct avec l'océanographie générale, ainsi qu'avec les sciences halieutiques.

Les manuscrits doivent être présentés avec un double, et dactylographiés, en *double interligne*, et au recto exclusivement, sur du papier blanc de format A4 (21×29.7 cm). Les tableaux et les légendes des figures seront regroupés respectivement sur des feuilles séparées à la fin du manuscrit.

Le manuscrit devra être présenté sous la forme suivante:

1° Il sera écrit en japonais, français ou anglais. Dans le cadre des articles originaux, il comprendra toujours le résumé en anglais ou français de *200 mots* environs. Pour les textes en langues européennes. il faudra joindre en plus le résumé en japonais de *500 letters* environs. Si le manuscrit est envoyé par un non-japonophone, le comité sera responsable de la rédaction de ce résumé.

2° La présentation des articles devra être la même que dans les numéros récents; le nom de l'auteur précédé du prénom *en entier*, en minuscules; les symboles et abréviations standards autorisés par le comité; les citations bibliographiques seront faites selon le mode de publication: article dans une revue, partie d'un livre, livre entier, etc.

3° Les figures ou dessins originaux devront être parfaitement nettes en vue de la réduction nécessaire. La réduction sera faite dans le format 14.5×20.0 cm.

La première épreuve seule sera envoyée à l'auteur pour la correction.

Les membres de la Société peuvent publier 7 pages imprimées sans frais d'impression dans la mesure à leur manuscrit qui ne demande pas de frais d'impression excessift (pour des photos couleurs, par exemple). Dans les autres cas, y compris la présentation d'un non-membre, tous les frais seront à la charge de l'auteur.

Cinquante tirés-à-part peuvent être fournis par article aux auteurs à titre gratuit. On peut en fournir aussi un plus grand nombre sur demande, par 50 exemplaires.

Les manuscrits devront être adressés directement au directeur de publication de la Société: J. YOSHIDA, Université des Pêches de Tokyo, Konan 4-5-7, Minato-ku, Tokyo, 108 Japon; ou bien au rédacteur étranger le plus proche: H. J. CECCALDI, EPHE, Station marine d'Endoume, rue Batterie-des-Lions, 13007 Marseille, France; E. D. GOLDBERG, Scripps Institution of Oceanography, La Jolla, California 92093, Etats-Unis; L. SEURONT, ECRG, Station marine de Wimereux, CNRS UMR 8013 ELICO, Université des Sciences et Technologies de Lille, 28 avenue Foch, F-62930 Wimereux, France. ou T. R. PARSONS, Institute of Ocean Sciences, P.O.Box 6000, 986OW, Saanich Rd., Sidney, B. C., V8L 4B2, Canada.

編集委員長よりのお知らせ

日頃からLa merにご支援を賜り有り難うございます。今後ともよろしくご支援お願いいたします。さて、La mer発刊に関してですが、昨年度後半より大幅な遅れが生じております。これも編集委員長の不徳の致すところと深くお詫び申し上げます。そこで、誠に申し訳ありませんが、2004年度42巻3，4に関しましては休刊させていただき、2005年度43巻1—2合併号を発刊させていただくことに致しました。会員諸兄におかれましては御理解いただきたくお願い申しあげます。今後はこの様な事態が出来致さぬよう、迅速な編集業務をはかりますので、よろしくお願いいたします。

From the editor

Thank you so much for your supporting La mer. Because of the delaying of issuing La mer(2004, Vol.42, 3–4), we decided to skip these two numbers, and will issue Vol.43(1–2)as soon as possible. I must express my deep apologies in this matter, and ask for your permission.

La mer 43 : 1-7, 2005
Société franco-japonaise d'océanographie, Tokyo

Short-term, seasonal, and tidal variations in the Yellow River plume

Tetsuo YANAGI* and Taka-aki HINO**

Abstract : The short-term, seasonal and spring-neap tidal variations of the Yellow River plume in the Bohai Sea were investigated using NOAA AVHRR visible band images in 2002. As a result, the followings are revealed, that is, the Yellow River plume spreads mainly from Laizhou Bay to Bohai Bay with the coast on the left hand side due to the Lagrangean tide-induced residual current and its spreading area during spring tide was wider than that during neap tide due to the re-suspension by the strong tidal current. There was no distinct seasonal variation in the Yellow River plume spreading in the Bohai Sea during 2002.

Keywords : *Yellow River, river plume, Bohai Sea, NOAA AVHRR*

1. Introduction

The river discharge of the Yellow River has decreased from 1970's due to the overuse of water on land (e.g. HAYASHI *et al.*, 2004). Yearly averaged river discharge was about 3,000 m^3/sec in 1960's but it was 1,000 m^3/sec in 1990's, and there were more than 150 days in 1996 when there was no-water-discharge at Lijin near the Yellow River mouth (see Fig. 1). Such decrease of the river discharge may affect the spreading of the Yellow River plume and the marine environment in the Bohai Sea because the Yellow River is the largest river which empties to the Bohai Sea.

There have been many studies on the tide (XIE *et al.*, 1990), the tidal current (WAN *et al.*, 1998), the residual flow (FENG, 1987), the water mass (LEE *et al.*, 2002) in the Bohai Sea, and the water discharge and the sediment discharge from the Yellow River (SAITO and YANG, 1994). However, the characteristics of the spreading of the Yellow River plume and its effect on the marine environment of the Bohai Sea have not been clarified yet.

Using NOAA AVHRR visible images obtained in 2002, we investigate the short-term, seasonal and spring-neap tidal variations in the Yellow River plume in this paper.

2. Used data

Used NOAA images were processed at the NPEC (North Pacific Environmental Center), Toyama, Japan. In case of NOAA infrared image (Bands 4 and 5), the analysis method is already established for the users (e.g. SAKAIDA *et al.*, 2000). However, it is meaningless to directly compare and/or average visible images (Band 1) of NOAA because the signal of NOAA visible image (it expresses the brightness of the sea surface) depends on the sun altitude, the air condition, the sea surface condition and so on, but no correction was made for the signal of the visible Band 1 image of NOAA. Therefore we normalized the signal of the visible Band 1 of each image by designating the signal at the river mouth of the Yellow River as 10 and that at the deepest part of the Bohai Strait as 0 because it was considered that the direct effect of the Yellow River plume did

* Research Institute for Applied Mechanics, Kyushu University
** Interdisciplinary Graduate School of Engineering Sciences, Kyushu University

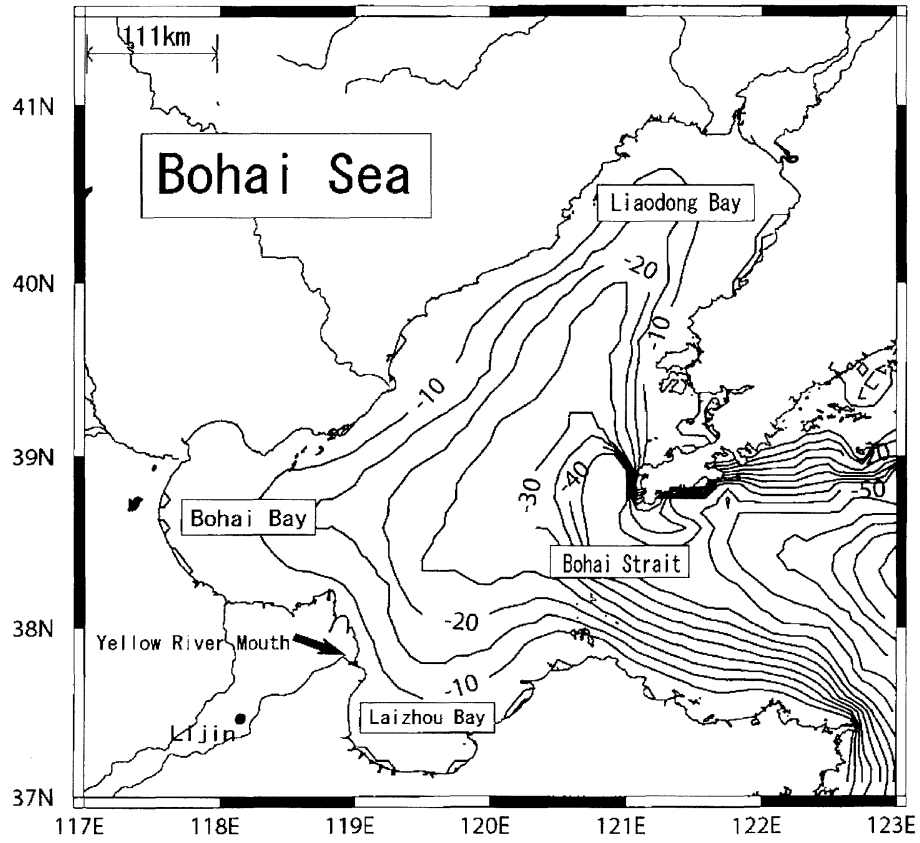

Fig. 1. The Bohai Sea. Numbers show the depth in meters.

not reach to the Bohai Strait. Large normalized number means high turbidity with large effect of the Yellow River plume and small one low turbidity with small effect of the Yellow River plume as shown in Fig. 3. Minus normalized number means lower turbidity than that at the Bohai Strait. The coverage area of each image is 37°N–41°N and 117°E–123°E, and the spatial resolution of each image is 1.1 km × 1.1 km (Fig. 1). Every snapshot images during the daytime from 30 January 2002 to 31 December 2002 with the cloud less than 50 % were analyzed. The data from 1 January to 29 January 2002 were lacking due to the problem of NPEC.

3. Results

The temporal variations in the water level, the river discharge, and the sediment load at Lijin (see Fig. 1) of the Yellow River in 2002 are shown in Fig. 2, which is obtained from HP (http://www.yellowriver.gov.cn/other/hhsq/hhsq.asp). There was no distinct seasonal variation in water discharge and sediment load except an artificial outflow in July when the water level was high, the river discharge was large and the sediment load was also large. The reason of intermittent large sediment load without high water level and large water discharge in late September 2002 is not clear now.

3.1 Short-term variation

The short-term variation in the Yellow River plume spreading related to the artificial outflow in July 2002 is shown in Fig. 3. There was no turbid water near the Yellow River mouth on 27 June (Moon age of 16) before the artificial outflow but a small area of turbid water (shown by the dark color from the Yellow River mouth in Fig. 3) existed on 6 July (Moon age of 25) just after the beginning of the artificial outflow on 29 June. It mainly spread southeastward along the coast of Laizhou Bay

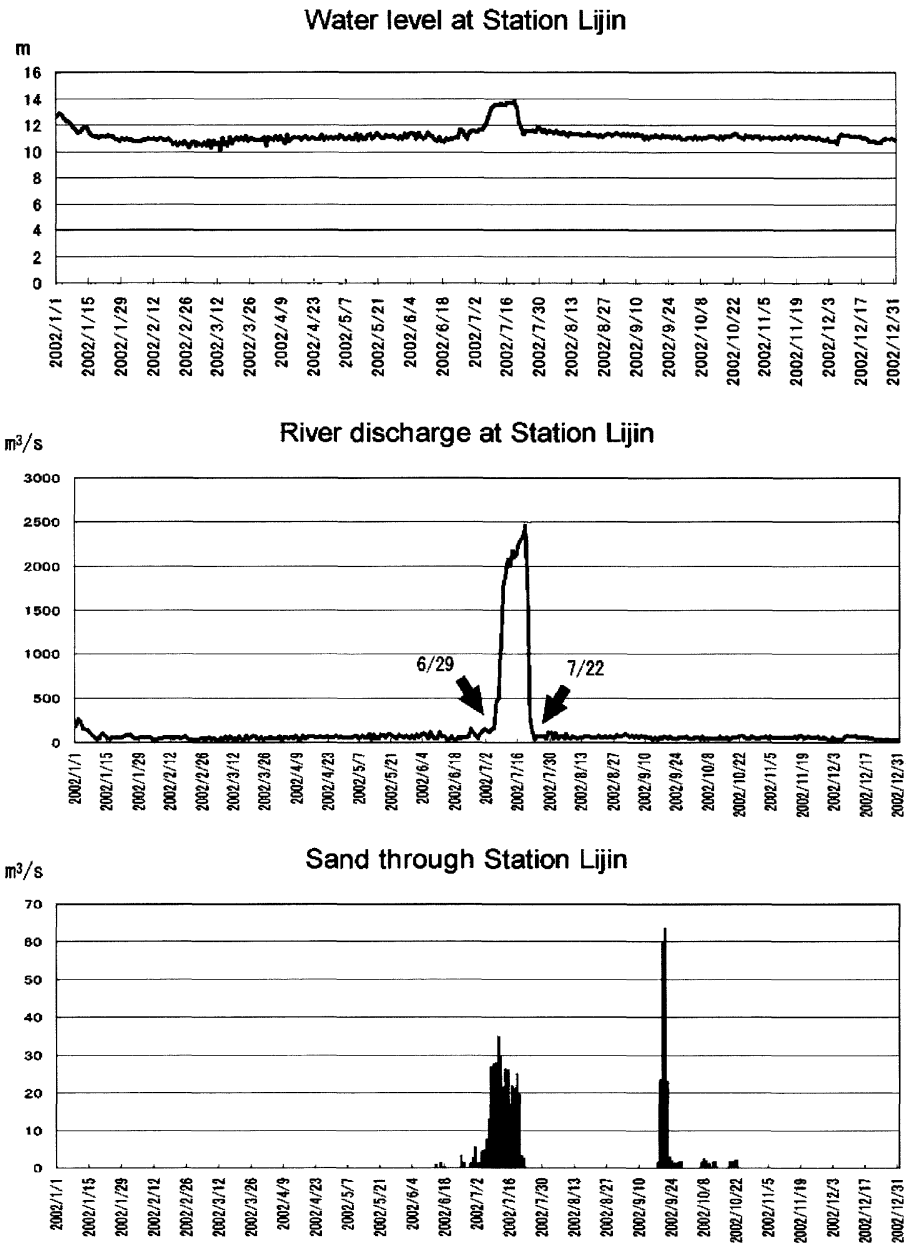

Fig. 2. Temporal variations in water level, discharge, and sediment load of the Yellow River at Lijin in 2002.

on 6 July, northwestward along the coast of Bohai Bay on 10 July (Moon age of 28; spring tide). The spreading area of turbid water took the maximum on 14 July (Moon age of 4) and its area shrank on 15 July (Moon age of 5; neap tide). There was no turbid water on 1 August (Moon age of 22; neap tide) after the end of artificial outflow on 22 July as shown in Fig. 3.

3.2 Seasonal variation

The monthly composite images from February to November 2002 are shown in Fig. 4. Ten to twenty images were composited every month except December. The image in December is not shown in Fig.4 because only one image was obtained because of too many cloudy days in December 2002. The turbid water from the Yellow

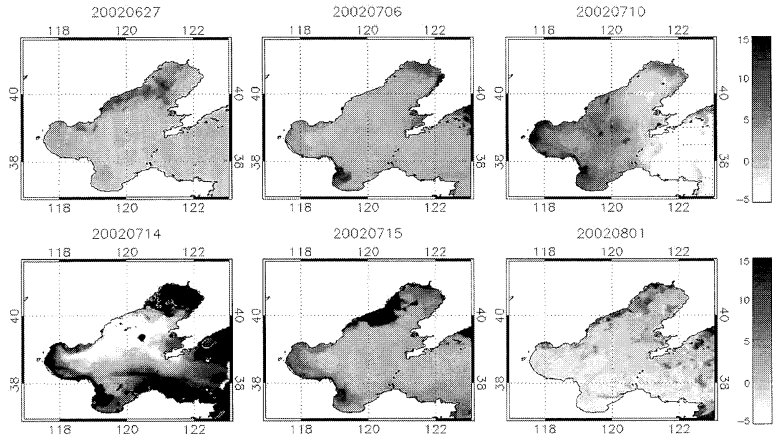

Fig. 3. Short-term variation in the Yellow River plume spreading related to the artificial outflow in July 2002.

River mouth (shown by the dark color from the Yellow River mouth in Fig. 4) spread mainly along the southwestern coasts of Laizhou Bay and Bohai Bay, and there was no distinct seasonal variation in its spreading pattern. The effect of artificial outflow in July 2002 was not distinct from Fig. 4, i.e., the turbidity was not highest in July. This suggests that the effect of re-suspension is large for the spreading pattern of the Yellow River plume, which will be discussed in the next section.

It is interesting that the Yellow River plume spread with the coast on the left hand side because the river plume usually spreads with the coast on the right hand side in the northern hemisphere (e.g. GRIFFITHS, 1986). We will discuss on this point later.

3.3 Spring-neap tidal variation

The average spreading pattern during the spring tide (which was obtained by averaging images during moon ages from 12.0 to 18.0 or from 27.0 to 2.0) and that during the neap tide (which was obtained by averaging images during moon ages from 5.0 to 9.0 or from 20.0 to 24.0) from February to November in 2002 are shown in Fig.5. The river discharge in 2002 was nearly constant except in July as shown in Fig.2. The turbidity was higher during the spring tide than during the neap tide and the spreading area was wider during the spring tide than during the neap tide. This suggests that the re-suspension by the strong tidal current during the spring tide plays an important role in the turbidity of the sea surface along the shallow coastal areas of Bohai Bay and Laizhou Bay.

4. Discussion

The yearly averaged image of the spreading of the Yellow River plume is shown in Fig. 6 (a). We consider that this image should be the characteristic feature of the spreading of the Yellow River plume, because it has the characteristic between those during spring tide and neap tide shown in Fig. 5 and there was no distinct seasonal variation on the spreading of the Yellow River plume as was shown in Fig. 4. The turbid water from the Yellow River mouth spread mainly northwestward to Bohai Bay with the coast on the left hand side. This is interesting from the viewpoint of the dynamics of the density-driven current, that is, the river plume usually spreads with the coast on the right hand side in the northern hemisphere due to the Coriolis effect. Wind may affect the river plume spreading but its effect is not large for the Yellow River plume because there was no distinct seasonal variation in the Yellow River plume spreading as shown in Fig. 4 under the distinct seasonal variation of monsoon wind in the Bohai Sea.

The preliminary calculation of Lagrangean tide-induced residual current by M_2, S_2, K_1, and O_1 constituents in the surface layer is shown in

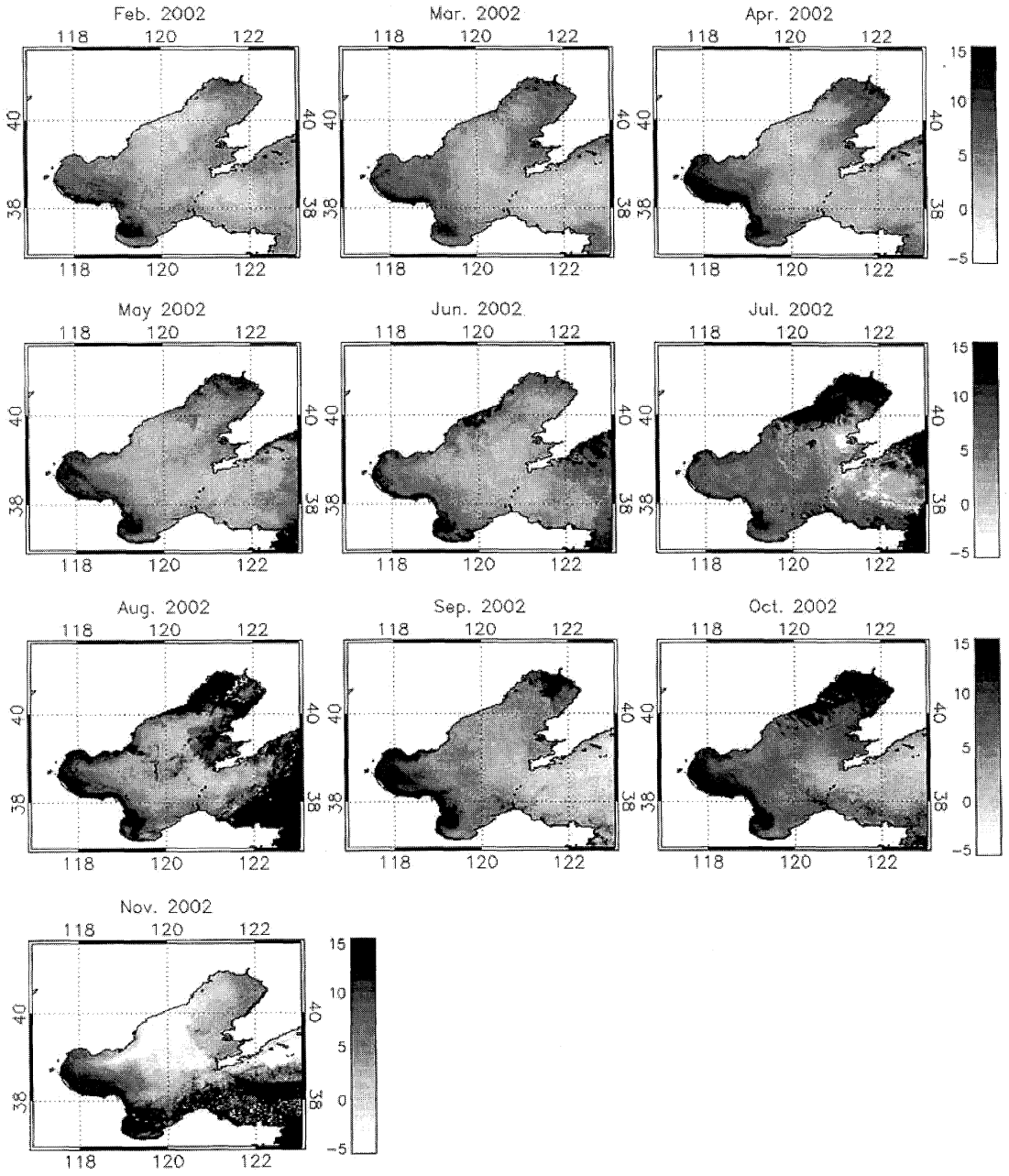

Fig. 4. Monthly composite images of the Yellow River plume spreading in 2002.

Fig. 6 (b) (CUI and YANAGI, 2005). Their numerical model is a three-dimensional one and the tides in the Bohai Sea are well reproduced. The Lagrangean tide-induced residual current in the surface layer was calculated based on the calculated M_2, S_2, K_1, and O_1 tidal currents. It directs northwestward from the Yellow River mouth and it qualitatively explains the spreading pattern of the Yellow River plume shown in Fig. 6 (a). The quantitative numerical experiment on the Yellow River plume spreading is under conducting now.

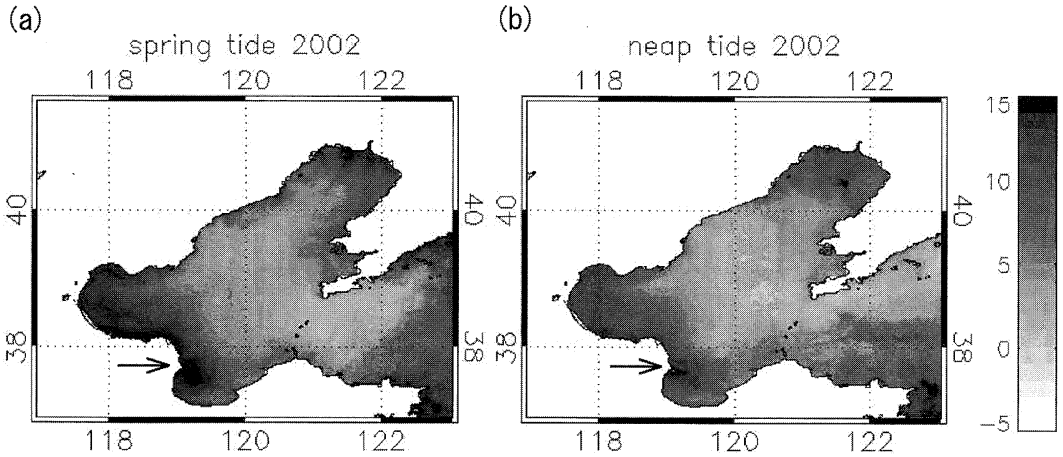

Fig. 5 The Yellow River plume spreading in spring tide (a) and neap tide (b). Arrow shows the position of the Yellow River mouth.

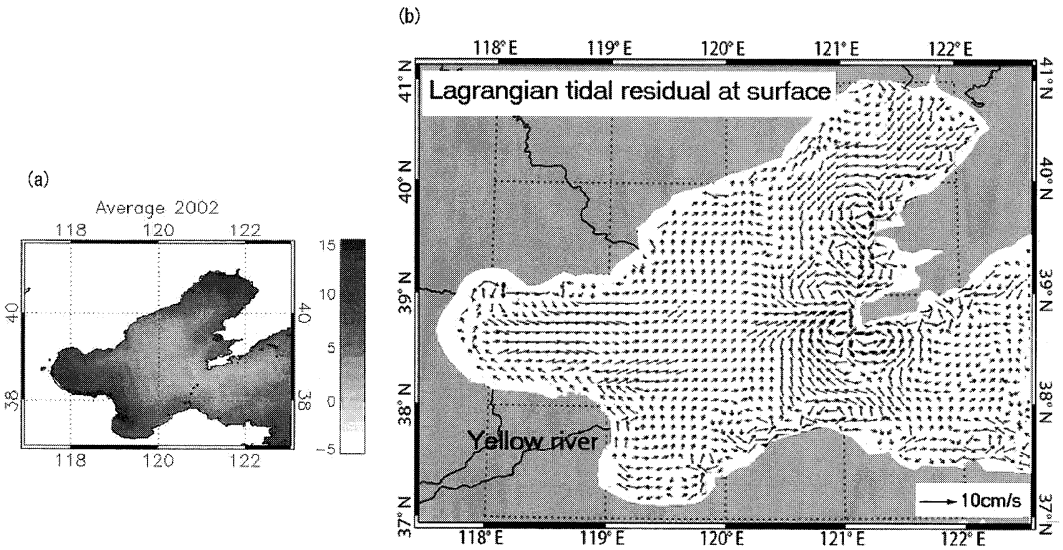

Fig. 6. Yearly average of the Yellow River plume spreading in 2002 (a) and the Lagrangean tide-induced residual current by M_2, S_2, K_1, and O_1 constituents (b) (Cui and Yanagi, 2005).

5. Conclusion

We may conclude from this study that the Yellow River plume spreads mainly from Laizhou Bay to Bohai Bay with the coast on the left hand side due to the Lagrangean tide-induced residual current and the turbidity of the river plume during the spring tide is higher than that during the neap tide due to the re-suspension by the strong tidal current. There was no distinct seasonal variation of the Yellow River plume spreading in the Bohai Sea in 2002.

Acknowledgements

The authors express their sincere thanks to the staff of NPEC at Toyama, Japan who processed NOAA images and kindly provided them to us, and the editor and anonymous reviewer for their useful comments to the first draft. This is a part of "The Yellow River Studies" sponsored by the National Institute for Human and Nature, Japan.

References

CUI, Q and T.YANAGI (2005): Tide and tidal current in the Bohai Sea. (to be submitted).

FENG, S. (1987): A three-dimension weakly nonlinear model of tide-induced Lagrangean residual current and mass transport with an application to the Bohai Sea. *In* "Three-dimensional model of marine and estuarine dynamics", NIHOUL, J. and B.JAMART (eds.), Elsevier Science Pub., 471–488.

GRIFFITHS, R. W., (1986): Gravity currents in rotating systems. Annu. Rev. Fluid Mech. **18**, 59–89.

HAYASHI, M., T.YANAGI and X.GUO (2004): Difference of nutrients budgets in the Bohai Sea between 1982 and 1992 related to the decrease of the Yellow River discharge. J.Korean Soc. of Oceanogr., **39**, 14–19.

LEE, J.H., B.WAN and G.H. HONG (2002): Water residence time for the Bohai and Yellow Seas. *In* "Impact of interface exchange on the biogeochemical processes of the Yellow and East China Seas", HONG G.H. *et al.* (eds.), Bum Shin Press, 385–401.

SAITO, Y. and Z.YANG (1994): The Huanghe (Yellow) River: its water discharge, sediment discharge, and sediment budget. J.Sed.Soc.Japan, **40**, 7–17.

SAKAIDA, F., J.I. KUDOH and H. KAWAMURA (2000): A HIGHERS—The system to produce the high spatial resolution sea surface temperature maps of the western North Pacific using the AVHRR/NOAA. J.Oceanogr., **56**, 707–716.

WAN, Z.W., F.L. QIAO, and Y.L. YUAN, (1998): Three-dimensional numerical modeling of tidal waves in the Bohai Sea. Oceanologia et Limnologia Sinica, **29 (6)**, 611–616.

XIE, L., W. W. HSIEH, and J. A. HELBIG, (1990): A tidal model of Bohai. Continental Shelf Research, **10**, 707–721.

Received January 31, 2005
Accepted April 7, 2005

La mer 43 : 9-17, 2005
Société franco-japonaise d'océanographie, Tokyo

Feeding habits of two sillaginid fishes, *Sillago sihama* and *S. aeolus*, at Sikao Bay, Trang Province, Thailand

Prasert TONGNUNUI,* Mitsuhiko SANO* and Hisashi KUROKURA*

Abstract : The feeding habits of juveniles and adults of two sympatric sillaginid fishes, *Sillago sihama* and *S. aeolus*, were examined on the basis of 892 (127 juveniles and 765 adults) and 734 (159 and 575) specimens, respectively, collected from the sandy bottom at Sikao Bay, Trang Province, Thailand, from May 2003 to April 2004. The diets of juveniles (<130 mm in standard length) of both species changed progressively with increasing body size, with a shift from capturing small zooplankton, such as calanoid copepods, to larger benthic prey, such as polychaetes, shrimps, and crabs. The latter three items were also the most important prey of adults of the two species, together constituting >70% of stomach contents by volume. Pronounced seasonal changes in adult diet were not detected in either fish species. In addition, considerable overlaps of juvenile and adult diets between the two coexisting *Sillago* species were found during the study period, indicating that there may be little or no competition between them at Sikao Bay.

Keywords : *feeding habits, Sillago sihama, Sillago aeolus, Sikao Bay*

1. Introduction

Sillaginidae is a commercially and recreationally important fish family in many regions, two species, *Sillago sihama* and *S. aeolus*, being widely distributed throughout coastal waters in the west-central Pacific and Indian oceans (MCKAY, 1999). In Sikao Bay, Trang Province, Thailand, our preliminary observations indicated that these two species were the most dominant sillaginids, coexisting in shallow sandy areas throughout the year.

Despite their abundance and popularity as food fishes, little is known about the feeding habits of *S. sihama* and *S. aeolus*, except for studies of the former from Taiwan (LEE, 1976) and North Queensland, Australia (GUNN and MILWARD, 1985). Studies on the feeding habits of juvenile and adult sillaginids should be useful for understanding the overall ecology of sillaginids and determining future management strategies.

The objectives of the present study were (1) to describe the stomach contents of juvenile and adult *S. sihama* and *S. aeolus*, (2) to clarify dietary differences among different size classes of juveniles of each species, (3) to determine monthly changes in the diets of adults of each species, and (4) to compare feeding habits between the sympatric congeners.

2. Materials and Methods

The study site, Sikao Bay (7°30′ N, 99°13′ E), opening broadly to the Andaman Sea, is located in Trang Province on the southwest coast of Thailand. It is a large-sized bay, with a length and mouth width of approximately 40 km and 30 km, respectively. The bay has a relatively flat sand surface with several small rocky reefs along the coast. Maximum water depth is about 20 m.

Sikao Bay has relatively short dry (January to April) and long rainy (May to December) seasons. Salinity in the sampling area was essentially marine. Water temperatures at a sandy beach (Rajamangala Beach) at Sikao

*Department of Global Agricultural Sciences, Graduate School of Agricultural and Life Sciences, The University of Tokyo, 1-1-1 Yayoi, Bunkyo-ku, Tokyo 113-8657, Japan

varied from 27.0 to 30.9 ℃, but no seasonal trends were apparent.

Individuals of *Sillago sihama* and *S. aeolus* of 130 mm in standard length (SL) or more were defined as adults, following histological examination of the gonads. To examine seasonal dietary differences, adults of the two species were collected monthly from gill net fishery landings conducted within Sikao Bay from May 2003 to April 2004. Gill nets (500 m wide, 1 m deep, and 25 mm × 25 mm square mesh) were set primarily on the sandy bottom in the central area of the bay (water depth about 15 m) between 05:00 and 07:00 hours, and retrieved between 09:00 and 10:00 hours. Both species were collected during the same gill net operations.

To clarify ontogenetic dietary shifts, most juveniles (<130 mm SL) of the two species were captured from Rajamangala Beach using a small seine net (10 m wide, 1 m deep, and 1 mm × 1 mm square mesh with a 4.5 m long central purse-bag). Sampling was conducted monthly at flood tide (water depth about 1 m) between 6:00 and 9:00 hours from December 2003 to February 2004, when juveniles of both species were abundant. Some large juveniles (101–129 mm SL) collected from gill net fishery landings during the above three months were added to the juvenile samples. Juvenile specimens were pooled for each month for dietary analysis. Immediately after collection, adult and juvenile specimens were preserved on ice.

In the laboratory, within 4 hours of collection, SL and body weight were measured for each adult and juvenile specimen to the nearest 1 mm and 0.1 g, respectively. Juveniles were sorted into 5 size classes (≤10 mm SL, 11–40 mm SL, 41–70 mm SL, 71–100 mm SL, and 101–129 mm SL), although no specimens were included in the 71–100 mm SL size class.

Food items from the stomach contents of each specimen were identified to the lowest possible taxon and the percentage volume of each in the diet visually estimated under a binocular microscope, as follows. Initially, the stomach contents were squashed on a slide glass with a 1 mm × 1 mm grid to a uniform depth of 1 mm, and the area covered by each item measured. The measured area was then divided by the total area of the stomach contents in order to calculate the percentage volume of that item in the diet (HORINOUCHI and SANO, 2000; NAKAMURA *et al.*, 2003). Food resource use was expressed as mean percentage composition of each item by volume (%V), which was calculated by dividing the sum of the individual volumetric percentage for the item by the number of specimens examined (HOBSON, 1974; SANO *et al.*, 1984). Specimens with empty guts were excluded from the analysis.

To measure the degree of feeding intensity of each adult in each species, the Stomach Fullness Index (*SFI*) was used:

$$SFI = [SCW/(BW-SCW)] \times 100,$$

where *SCW* is a weight of stomach contents and *BW* is a fish body weight. Specimens with empty stomachs were included in the comparisons of mean *SFI* among months and species (*S. sihama* and *S. aeolus*).

A two-way analysis of variance (ANOVA) with unequal replication (ZAR, 1999) was used to test (1) for species and month effects on percentage composition of main food items in adults and (2) for species and body size effects on percentage composition of main food items in juveniles. Prior to the analyses, homogeneity of variances was improved by transformation of data to arcsin $\sqrt{x}$. If the ANOVA results indicated significant treatment effects ($P<0.05$), the Gabriel test was used to determine which means were significantly different. If ANOVA revealed a significant interaction between species and month for adults or between species and body size for juveniles, a one-way ANOVA and post-hoc Gabriel test were used to compare the mean of one factor separately at each level of the other factor and vice versa (UNDERWOOD, 1997). Some ANOVA results are not presented in the present study because of space limitations.

3. Results

3.1 Juveniles

Of the 127 stomachs of juvenile *Sillago sihama*, 117 individuals contained food items, 10 (8%) being empty. Among 159 stomachs of juvenile *S. aeolus*, 133 contained food items, 26 (16%) being empty.

Table 1. Percentage volume (%V) of food items in the diets of juvenile *Sillago sihama* and *S. aeolus*.

Food items	*S. sihama* %V	*S. aeolus* %V
Copepods	47.2	38.2
Polychaetes	33.5	26.1
Decapods		
Shrimps	5.0	11.1
Crabs	2.3	3.2
Hermit crabs	0.9	0.9
Mud lobsters	0.8	0.3
Larvaceans	4.0	4.4
Fish	3.0	1.6
Trumpet worms	1.6	5.8
Arrow worms	0.7	0
Ostracods	0.3	+
Molluscs	+	1.2
Amphipods	+	0.5
Isopods	+	0.1
Sea anemones	0	5.3
Stomatopods	0	0.3
Unidentified fragments	0.7	1.0
Number of fish with food examined	117	133
Standard lenght (mm)	8–129	7–128

+ : <0.1.

The overall feeding habits of juvenile *S. sihama* and *S. aeolus* are shown in Table 1. The major food items of the two species were calanoid copepods and polychaetes, those categories accounting for 80.7% and 64.3% of the stomach contents by volume in *S. sihama* and *S. aeolus*, respectively.

Based on the %V data, size-related and species differences in the dietary composition of the two major food items (calanoid copepods and polychaetes) were examined. The remaining (minor) prey items were excluded from this analysis. A two-way ANOVA revealed that %V differed significantly among the size classes in each of the two food items, species × size class effects being insignificant for each item (Table 2). In both *S. sihama* and *S. aeolus,* copepods were taken mainly by juveniles in the ≤10 and 11–40 mm SL size classes (Fig. 1, Table 3). In larger size classes, however, this prey item was replaced by polychaetes. The ANOVA results also indicated that the %V of copepods differed significantly between *S. sihama* and *S. aeolus*, with greater %V in the former, whereas that of polychaetes did not (Fig. 1, Table 2).

3.2 Adults

Of the 765 adult specimens of *S. sihama*, 652 contained food items, 113 (15%) being empty. Among the 575 adult specimens of *S. aeolus*, on the other hand, 393 contained food items, 182 (32%) being empty. The overall mean *SFI* of specimens was 0.561 and 0.415 in *S. sihama* and *S. aeolus*, respectively. Monthly changes in *SFI* for each species are shown in Fig. 2. Mean *SFI* values varied little from month to month for both species, except for January in *S. aeolus*.

The overall feeding habits of adult *S. sihama* and *S. aeolus* are shown in Table 4. The two species consumed a variety of food, including small invertebrates and fishes. In both species, polychaetes were the most important prey item, followed by crabs and shrimps, the three categories constituting 80.1% and 74.0% of the stomach contents by volume in *S. sihama* and *S. aeolus*, respectively.

Based on the %V data, seasonal and species differences in the dietary composition of the three major food items (polychaetes, crabs, and shrimps) were examined. The remaining (minor) prey items were excluded from this analysis. A two-way ANOVA revealed that there

Table 2. Results of a two-way ANOVA testing the effects of species and size class on percentage volume of each main food category in the diets of juvenile *Sillago sihama* and *S. aeolus*.

Source	*DF*	*MS*	*F*	*P*
Copepods				
Species	1	0.87	4.72	0.030
Size class	3	16.8	91.7	<0.001
Species×Size class	3	0.41	2.24	0.084
Error	242	0.18		
Polychaetes				
Species	1	0.32	1.98	0.160
Size class	3	11.5	70.8	<0.001
Species×Size class	3	0.23	1.42	0.237
Error	242	0.17		

Data transformed to arcsin $\sqrt{x}$.

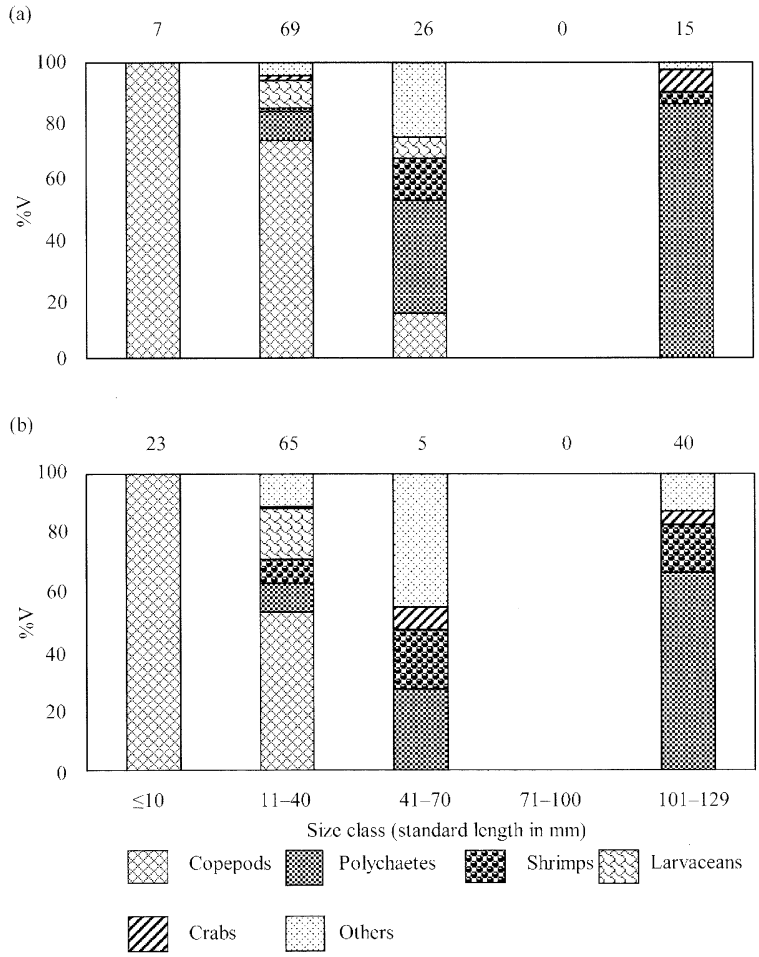

Fig. 1. Percentage volume (%V) of prey items in the diets of four size classes of juvenile *Sillago sihama* (a) and *S. aeolus* (b). Number of individuals containing food given above each column.

Table 3. Results of Gabriel multiple comparison test examining differences in percentage volume of each main food item of juvenile *Sillago sihama* and *S. aeolus* among size classes.

Species	Food item	Size class (standard length in mm)
S. sihama	Copepods	101–129 41–70 1–40 ≤10
	Polychaetes	≤10 11–40 41–70 101–129
S. aeolus	Copepods	101–129 41–70 11–40 ≤10
	Polychaetes	≤10 11–40 41–70 101–129

Size classes not significantly different ($P \geq 0.05$) are linked by underlining and arranged in order of increasing percentage volume.

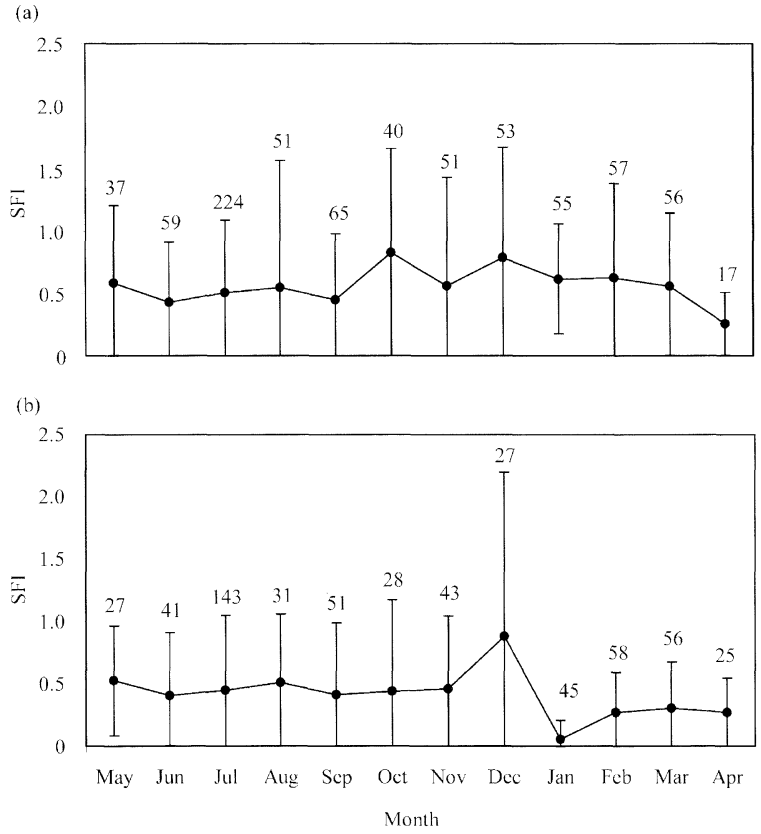

Fig. 2. Monthly changes in Stomach Fullness Index (*SFI*) of adult *Sillago sihama* (a) and *S. aeolus* (b). Bars indicate standard deviation. Number of specimens examined given above each bar.

was a significant interaction between month and species for the major items (Table 5). The %V of each item, therefore, was compared among months for each species, using a one-way ANOVA and post-hoc Gabriel test. These tests indicated that the %V of each of the three items in *S. sihama* and *S. aeolus* differed significantly among the various months of the study, but no apparent seasonal variations were detected (Fig. 3, Table 6). Comparing the %V of each food item between the two species in each month, differences were statistically

Table 4. Percentage volume (%V) of food items in the diets of adult *Sillago sihama* and *S. aeolus*.

Food items	*S. sihama* %V	*S. aeolus* %V
Polychaetes	58.7	46.8
Decapods		
Shrimps	12.4	11.3
Crabs	9.0	15.9
Mud lobsters	4.1	3.9
Hermit crabs	0.9	2.2
Mole crabs	0.4	2.4
Trumpet worms	2.8	6.0
Stomatopods	2.6	3.1
Fish	2.6	0.8
Molluscs		
Bivalves	0.7	1.6
Squids	0.2	0.3
Sea slugs	0.1	0.6
Bristtlestars	0.9	0.6
Sea anemones	0.5	0.8
Amphipods	0.2	0.1
Isopods	0.2	0
Crustacean fragments	3.0	2.1
Unidentified fragments	0.7	1.5
Number of fish with food examined	652	393
Standard lenght (mm)	130–233	130–200

Table 5. Results of a two-way ANOVA testing the effects of species and month on percentage volume of each main food item in the diets of adult *Sillago sihama* and *S. aeolus*.

Source	*DF*	*MS*	*F*	*P*
Polychaetes				
Species	1	7.26	18.1	<0.001
Month	11	1.27	3.16	<0.001
Species×Month	11	1.55	3.86	<0.001
Error	1021	0.40		
Crabs				
Species	1	2.61	12.1	0.001
Month	11	1.17	5.43	<0.001
Species×Month	11	0.64	2.97	0.001
Error	1021	0.21		
Shrimps				
Species	1	0.002	0.01	0.9
Month	11	0.83	6.02	<0.001
Species×Month	11	0.40	2.87	0.001
Error	1021	0.13		

Data transformed to arcsin $\sqrt{x}$

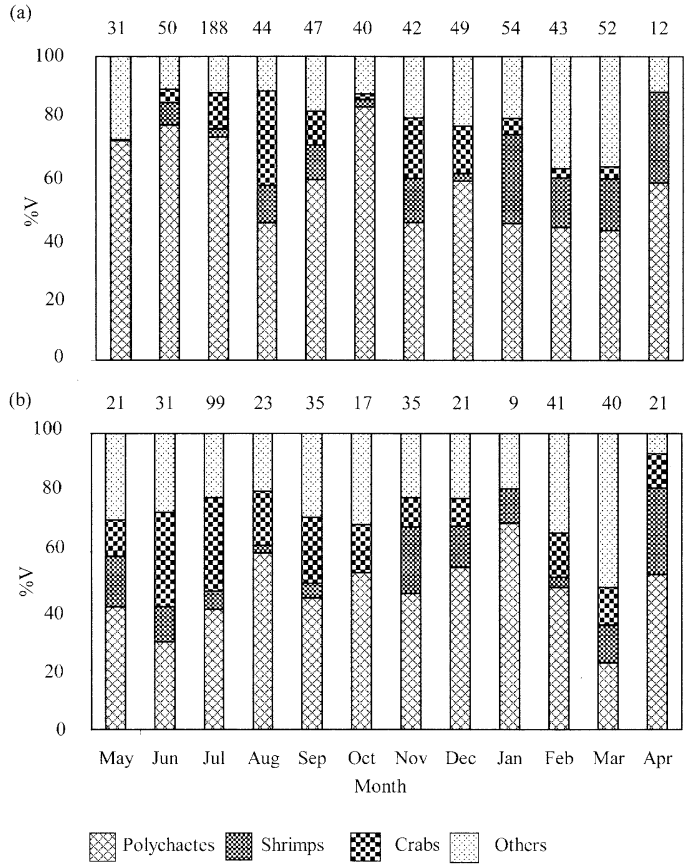

Fig. 3. Monthly changes in percentage volume (%V) of prey items in the diets of adult *Sillago sihama* (a) and *S. aeolus* (b). Number of individuals containing food given above each column.

Table 6. Results of Gabriel multiple comparison test examining differences in percentage volume of each main food item of adult *Sillago sihama* and *S. aeolus* among months.

Species	Food item	Month
S. sihama	Polychaetes	Feb Mar Nov Aug Jan Apr Sep Dec Jul May Jun Oct
	Shrimps	May Dec Jul Oct June Sep Aug Nov Mar Feb Jan Apr
	Crabs	May Apr Oct Feb Jun Mar Jan Sep Jul Dec Nov Aug
S. aeolus	Polychaetes	Mar Jun Jul May Sep Nov Oct Feb Aug Apr Dec Jan
	Shrimps	Oct Aug Feb Sep Jul Jun Jan Mar Dec May Nov Apr
	Crabs	Jan Dec Nov Apr May Mar Oct Feb Sep Jul Aug Jun

Months not significantly different ($P \geq 0.05$) are linked by underlining and arranged in order of increasing percentage volume.

significant in some months: *S. sihama* had higher %V of polychaetes in May, June, July, and October, and of shrimps in January, whereas *S. aeolus* showed greater %V of polychaetes in January, and of crabs in June and July (Fig. 3).

4. Discussion

The dietary compositions of juveniles of both *Sillago sihama* and *S. aeolus* changed progressively with increasing body size. This change included a shift from the ingestion of small zooplankton, such as calanoid copepods, by small juveniles, to the consumption of larger benthic prey, such as polychaetes, shrimps, and crabs, by larger juveniles, the latter diet being similar to those of adults of the two species. Such ontogenetic changes in food items have been found in several other sillaginid species (HYNDES *et al.*, 1997; SCHAFER *et al.*, 2002).

A shift from capturing small zooplankton to larger benthic prey organisms with growth in juveniles of the two *Sillago* species may be partly the result of continuing morphological development of feeding-related characters, including an increase in mouth width (e.g. DE-VRIES *et al.*, 1998; KREBS and TURINGAN, 2003; KANOU *et al.*, 2005) and the ability to extend the jaws downward and forward (GUNN and MILWARD, 1985; HYNDES *et al.*, 1997; SCHAFER *et al.*, 2002). Such protrusible jaws would facilitate the taking of benthic prey on and in the substrate.

The diets of adult *S. sihama* and *S. aeolus* at Sikao Bay consisted mainly of polychaetes, crabs, and shrimps. These food items were essentially similar to those described for *S. sihama* from Taiwan (LEE, 1976) and North Queensland, Australia (GUNN and MILWARD, 1985), and other sillaginid species from tropical and temperate waters (KAKUDA, 1970; BREWER and WARBURTON, 1992; HYNDES *et al.*, 1997; PLATELL and POTTER, 2001; SCHAFER *et al.*, 2002).

Our results showed that the diets of adult *S. sihama* and *S. aeolus* did not undergo pronounced seasonal changes, although the %V of the three major food items in each of the two species differed significantly among some months of the study. The lack of seasonal changes in diet may be attributable to relatively little seasonal fluctuations in food resource abundance at the study site, as also reported in other tropical coastal waters (COLES and MCCAIN, 1990; MCCARTHY *et al.*, 2000). This inference may be supported by the fact that the overall mean *SFI* of specimens varied little from month to month for either species.

In the present study, a considerable overlap in dietary composition in juveniles and adults between the two coexisting *Sillago* species was recognized during the study period, although the %V of major food items was somewhat different between the species in some months, suggesting that there is little or no competition between the two species at Sikao Bay. Several studies have demonstrated that diets among related cohabiting fishes greatly overlap where food resources are relatively abundant, while lower food abundance results in greater trophic and/or habitat segregation through interspecific competition (e.g. ROSS, 1986; HOLBROOK and SCHMITT, 1989; HORINOUCHI *et al.*, 1998). The considerable diet and habitat overlap between the two *Sillago* species at Sikao Bay may be due to the relative abundance of food resources, although we did not examine food resource abundance at the study area. The relationship between diet compositions of the two species and prey abundance appears to be a subject for further research.

Acknowledgments

We are grateful to Ruangrit PANTONG, Suwat TANYAROS, Kou IKEJIMA, Masahiro HORINOUCHI, Takashi INOUE, Tadaomi NAKAI, Pisut KAOBATH, Viwat SAETON, and the Department of Marine Science, Faculty of Science and Fisheries Technology, Rajamangala University of Technology Srivijaya, for assistance in the field work. Constructive comments on the manuscript from Masahiro HORINOUCHI, Yohei NAKAMURA, and Graham HARDY were much appreciated. This study was supported by a Grant-in-Aid for Scientific Research (A) from the Japan Society for the Promotion of Science (No. 15255017).

References

BREWER, D.T. and K. WARBURTON (1992) : Selection of prey from a seagrass/mangrove environment by golden lined whiting, *Sillago analis* (Whitley). J. Fish Biol., **40**, 257–271.

COLES, S.L. and J.C. MCCAIN (1990) : Environmental factors affecting benthic infaunal communities of the western Arabian Gulf. Mar. Environ. Res., **29**, 289–315.

DEVRIES, D.R., R.A. STEIN and M.T. BREMIGAN (1998) : Prey selection by larval fishes as influenced by available zooplankton and gape limitation. Trans. Am. Fish. Soc., **127**, 1040–1050.

GUNN, J.S. and N.E. MILWARD (1985) : The food, feeding habits and feeding structures of the whiting species *Sillago sihama* (Forsskål) and *Sillago analis* Whitley from Townsville, North Queenland, Australia. J. Fish Biol., **26**, 411–427.

HOBSON, E.S. (1974) : Feeding relationships of teleostean fishes on coral reefs in Kona, Hawaii. Fish. Bull., **72**, 915–1031.

HOLBROOK, S.J. and R.J. SCHMITT (1989) : Resource overlap, prey dynamics, and the strength of competition. Ecology, **70**, 1943–1953.

HORINOUCHI, M. and M. SANO (2000) : Food habit of fishes in a *Zostera marina* bed at Aburatsubo, central Japan. Ichthyol. Res., **47**, 163–173.

HORINOUCHI, M., M. SANO, T. TANIUCHI and M. SHIMIZU (1998) : Food and microhabitat resource use by *Rudarius ercodes* and *Ditrema temmincki* coexisting in a *Zostera* bed at Aburatsubo, central Japan. Fish. Sci., **64**, 563–568.

HYNDES, G.A., M.E. PLATELL and I.C. POTTER (1997): Relationships between diet and body size, mouth morphology, habitat and movements of six sillaginid species in coastal waters: implications for resource partitioning. Mar. Biol., **128**, 585–598.

KAKUDA, S. (1970) : Studies on the ecology and fishing stock of *Sillago sihama* (FORSKÅL) through the analysis of its bottom drift-net fishery. J. Fac. Fish. Anim. Husb., Hiroshima Univ., **9**, 1–55 (In Japanese with English summary).

KANOU, K., M. SANO and H. KOHNO (2005) : Ontogenetic diet shift, feeding rhythm and daily ration of juvenile yellowfin goby, *Acanthogobius flavimanus*, on a tidal mudflat in the Tama River estuary, central Japan. Ichthyol. Res., **52**, in press.

KREBS, J.M. and R.G. TURINGAN (2003) : Intraspecific variation in gape-prey size relationships and feeding success during early ontogeny in red drum, *Sciaenops ocellatus*. Environ. Biol. Fish., **66**, 75–84.

LEE, S.C. (1976) : Diet of juvenile *Sillago sihama* (FORSKÅL) from inshore waters near Hsinchu, Taiwan. Bull. Inst. Zool., Academia Sinica, **15**, 31–37.

MCCARTHY, S.A., E.A. LAWS, W.A. ESTABROOKS, J.H. BAILEY-BROCK and E.A. KAY (2002) : Intra-annual variability in Hawaiian shallow-water, soft-bottom macrobenthic communities adjacent to a eutrophic estuary. Estuar. Coast. Shelf Sci., **50**, 245–258.

MCKAY, R.J. (1999) : Sillaginidae. *In* FAO Species Identification Guide for Fishery Purposes. The Living Marine Resource of the Western Central Pacific. Vol. 4. Bony Fishes Part 2 (Mugilidae to Carangidae). CARPENTER, K.E. and V.H. NIEM (eds.), Food and Agriculture Organization of the United Nation, Rome, p. 2614–2629.

NAKAMURA, Y., M. HORINOUCHI, T. NAKAI and M. SANO (2003) : Food habits of fishes in a seagrass bed on a fringing coral reef at Iriomote Island, southern Japan. Ichthyol. Res., **50**, 15–22.

PLATELL, M.E. and I.C. POTTER (2001) : Partitioning of food resources amongst 18 abundant benthic carnivorous fish species in marine waters on the lower west coast of Australia. J. Exp. Mar. Biol. Ecol., **261**, 31–54.

ROSS, S.T. (1986) : Resource partitioning in fish assemblages: a review of field studies. Copeia, **1986**, 352–388.

SANO, M., M. SHIMIZU and Y. NOSE (1984) : Food habits of teleostean reef fishes in Okinawa Island, southern Japan. Univ. Mus. Univ. Tokyo Bull., **25**, 1–128.

SCHAFER, L.N., M.E. PLATELL, F.J. VALESINI and I.C. POTTER (2002) : Comparison between the influence of habitat type, season and body size on the dietary composition of fish species in near shore marine water. J. Exp. Mar. Biol. Ecol., **278**, 67–92.

UNDERWOOD, A.J. (1997) : Experiments in Ecology: Their Logical Design and Interpretation Using Analysis of Variance. Cambridge University Press, Cambridge, 504 pp.

ZAR, J.H. (1999) : Biostatistical Analysis, 4th edn. Prentice Hall, London, 663 pp.

Received March 10, 2005
Accepted April 8, 2005

La mer 43 : 19–32, 2005
Société franco-japonaise d'océanographie, Tokyo

Associations Tintinnides (Ciliophora, Tintinnina) - Dinoflagellés (Dinophyceae) autotrophes potentiellement nuisibles au niveau de la Baie de Tunis et de deux lagunes associées: Ghar El Melh et Tunis Sud (Méditerranée Sud Occidentale)

Mohamed Néjib DALY YAHIA[1*], Ons DALY YAHIA-KEFL[2], Sami SOUISSI[3], Fadhila MAAMOURI[4] et Patricia AISSA[1].

Abstract : Une étude des Tintinnides et des Dinoflagellés autotrophes susceptibles d'être nuisibles a été réalisée mensuellement dans la baie de Tunis et au niveau de deux lagunes associées: Ghar El Melh et Tunis Sud. Les résultats obtenus montrent que du point de vue qualitatif, les communautés lagunaires de Tintinnides sont très influencées par les populations marines avoisinantes. En effet, 61 espèces de Tintinnides ont été recensées dans la baie de Tunis, 15 espèces dans la lagune de Ghar El Melh, et seulement 12 dans la lagune de Tunis Sud. De plus, toutes les espèces rencontrées au moins dans l'une de ces lagunes s'avèrent être présentes dans la baie de Tunis. Le décompte des principales espèces montre que les densités moyennes annuelles atteintes en milieux lagunaires (Lagune de Tunis Sud: 223,1 cellules.litre^{-1} ; Lagune de Ghar El Melh: 62,3 cellules.l^{-1}) sont supérieures à celles enregistrées en mer (baie de Tunis: 49,1 cellules.l^{-1}). Le développement des principales espèces de Tintinnides comme *Favella ehrenbergi, Tintinnopsis* spp et *Stenosemella nivalis* est associé aux poussées de *Dinophysis acuminata, Alexandrium* spp et *Prorocentrum lima.* Cette "hypothèse trophique" a été testée par des classifications hiérarchiques qui ont permis d'identifier des associations spécifiques entre les espèces de Tintinnides dominantes et de Dinoflagellés susceptibles d'être nuisibles.

Keywords : *Tintinnids; Dinoflagellates; Specific Association; SW Mediterranean*

1. INTRODUCTION

Les Tintinnides sont considérés comme un maillon trophique primordial entre les petits producteurs primaires (algues nanoplanctoniques et microplanctoniques) et les producteurs secondaires et tertiaires (CONOVER, 1982; MARGALEF, 1982; LAVAL-PEUTO *et al.*, 1986; CARIOU *et al.*, 1999). Certains d'entre eux sont considérés par STOECKER et GUILLARD (1982) et RASSOULZADEGAN *et al.* (1988) comme des prédateurs exclusifs de Dinoflagellés.

Les Tintinnides, mieux connus que les autres

1) Laboratoire de Biosurveillance de l'Environnement. Groupe de Recherche en Hydrologie et Planctonologie. Département des Sciences de la Vie. Faculté des Sciences de Bizerte. 7021, Zarzouna, Bizerte, Republic of Tunisia. Fax : 216 72 590 566 - E-mail : nejib.daly@fsb.rnu.tn
2) Laboratoire de Planctonologie. Département des Sciences et de la Production Animale et de la Pêche. Institut National Agronomique de Tunisie. 43 Avenue Charles Nicolle, 1082, Tunis, Republic of Tunisia. Fax : 216 71 799 391 - E-mail : dalyyahya.ons@inat.agrinet.tn
3) Ecosystem Complexity Research Group. Station Marine de Wimereux, Université des Sciences et Technologies de Lille, CNRS-UMR 8013 ELICO, 28 avenue Foch, BP 80, F-62930 Wimereux, France. Fax : 33 321 992 901 - E-mail : Sami.SOUISSI@univ-lille1.fr
4) Laboratoire de Biologie Animale. Faculté des Sciences de Tunis. Département des Sciences de la Vie. Campus Universitaire, Tunis, Republic of Tunisia.
* Corresponding author

ciliés, en raison de leur lorica, (LAVAL-PEUTO et BROWNLEE, 1986) sont quantitativement moins nombreux dans les écosystèmes pélagiques (LAVAL-PEUTO *et al.*, 1986; ABBOUD-ABI SAAB, 1989, 2002; DOLAN et MARRASÉ, 1995; DOLAN, 2000; DOLAN et GALLEGOS, 2001).

En raison de leur petite taille comprise généralement entre 20 et 200 μm, ils appartiennent au microzooplancton (CONOVER, 1982; HARRIS *et al.*, 2000) et constituent des proies non négligeables pour des organismes zooplanctoniques tels que les Copépodes, les Cladocères, les Chaetognathes, les Tuniciers, certaines Scyphoméduses ainsi que les larves de Poissons (CONOVER, 1982; KENTOURI et DIVANACH, 1986; AYUKAI, 1987; GIFFORD et DAGG, 1991; GRAIN *et al.*, 1994).

Les données en Méditerranée Sud Occidentale, notamment pour la baie de Tunis et les lagunes de Ghar El Melh et de Tunis Sud restent fragmentaires en ce qui concerne les assemblages spécifiques de Tintinnides et de Dinoflagellés. Ainsi, dans la baie de Tunis, une étude hydrologique antérieure a montré qu'il existe un gradient nutritif croissant depuis la région sud-ouest vers le secteur nord-est, associé à un important développement de Tintinnides dans la zone eutrophe proche de la ville de Tunis (DALY YAHIA, 1998; SOUISSI *et al.*, 2000). Les Dinoflagellés ont fait l'objet de quelques travaux récents du point de vue taxonomique (DALY YAHIA-KEFI et DALY YAHIA, 1997 ; DALY YAHIA-KEFI *et al.*, 2001a) et écologique (ROMDHANE *et al*, 1998 ; DALY YAHIA-KEFI *et al.*, 2001b) et qui concernent surtout la baie de Tunis. Les travaux sur le microzooplancton et plus particulièrement sur les Tintinnides sont plus rares et relatifs à la lagune de Ghar El Melh (BEN FREDJ *et al.*, 2001).

La présente étude se propose de combler cette lacune et d'effectuer un suivi annuel de la taxonomie et de la dynamique des Tintinnides, dans la baie de Tunis et dans deux milieux lagunaires environnants (les lagunes de Ghar El Melh et de Tunis Sud), en parallèle avec une analyse des associations spécifiques entre Tintinnides hétérotrophes et Dinoflagellés autotrophes, ces derniers étant potentiellement nuisibles.

Notre choix des compartiments trophiques pré-cités répond aussi bien à une problématique scientifique que socio-économique. En effet, le domaine des ressources marines et lagunaires en terme de pêches est un secteur socio-économique clé en Tunisie. La production de la pêche est sujette en Tunisie comme d'ailleurs en Méditerranée et dans l'Océan mondial à un déclin en raison d'une surexploitation associée a des captures de tailles de plus en plus petites ("fishing down"). Parallèlement en Tunisie depuis une vingtaine d'année, les milieux lagunaires Tunisiens subissent une importante eutrophisation d'origine anthropique et naturelle. Cette dernière semble être associée à des mortalités massives de poissons sauvages (DALY YAHIA-KEFI and DALY YAHIA, 1997 ; ROMDHANE *et al*, 1998). Déterminer quels sont les facteurs susceptibles d'exercer un contrôle dans la dynamique des efflorescences de Dinoflagellés représente une priorité essentielle dans de tels écosystèmes où les activités de pêche sont développées depuis longtemps.

2. MATERIELS ET METHODES

La zone d'étude fait partie de l'ensemble du golfe de Tunis, compris entre 10° 10′ et 11° 5′ de longitude est et 36° 38′ et 37° 10′ de latitude nord, et situé au sud de la mer Tyrrhénienne, dans le bassin Siculo-Tunisien, sur lequel il s'ouvre largement sur près de 75 miles de côtes (figure 1). Sa limite géographique nord-est est représentée par une radiale joignant Cap Farina au Cap Bon (figure 1).

La baie de Tunis, située au sud du golfe de Tunis, communique directement dans sa région ouest avec la lagune de Tunis Sud. Plus au nord, la lagune de Ghar El Melh s'ouvre sur le littoral ouest du golfe de Tunis (figure 1).

Les caractéristiques géographique, bathymétrique et physico-chimique des trois biotopes étudiés ainsi que les stations d'échantillonnages sont indiquées sur la figure 1 et le tableau 1.

La température et la salinité des eaux de surface sont mesurées, mensuellement, à l'aide d'un salinomètre de terrain type WTW LF196 muni d'une sonde de température.

Les échantillons mensuels de plancton sont

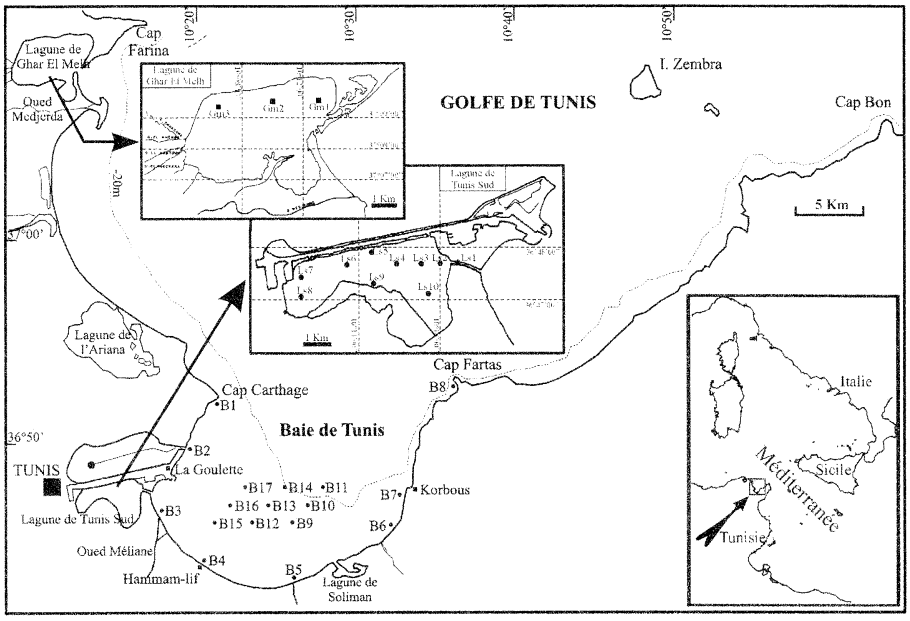

Fig. 1. Situation géographique et emplacement des différentes stations d'étude au niveau de la baie de Tunis et des lagunes de Ghar El Melh et Tunis Sud.

Tableau 1. Caractéristiques générales des différents biotopes étudiés.

Milieux	Superficie (Km^2)	Profondeur moyenne (m)	Période d'étude	Nombre de stations	Température moyenne minimale	Température moyenne maximale	Salinité moyenne minimale	Salinité moyenne maximale
Baie de Tunis	360	15	1993–1994	17	13,2℃ (janvier)	28,9℃ (août)	36,81 (octobre)	37,87 (août)
Lac Sud de Tunis	13	0,35	1996–1997	10	13℃ (janvier)	34℃ (août)	24,5 (février)	40,2 (août)
Lagune de Ghar El Melh	30	1	1994–1995	3	10,4℃ (janvier)	27,4℃ (août)	32,8 (février)	42,24 (août)

prélevés à l'aide d'une bouteille Ruttner (2l) pour l'analyse quantitative et à l'aide d'un petit filet à plancton de forme conique (55 μ m de vide de maille) utilisé pour l'étude qualitative en traits horizontaux de surface en milieu lagunaire, en raison de leur faible profondeur moyenne (Tableau 1) et en traits verticaux fond-surface dans la baie de Tunis. Les échantillons prélevés respectivement au cours des années 1994, 1995 et 1997 au niveau de la Baie de Tunis, de la lagune de Ghar El Melh et de la lagune de Tunis Sud, sont immédiatement fixés au formol neutralisé au borate de soude (2%) puis conservés dans une chambre froide à l'obscurité et à une température de 4° C jusqu'à l'analyse microscopique .

La méthode standard de sédimentation d'Utermöhl (UTERMÖHL, 1958) est utilisée sur microscope inversé (Leitz) pour l'identification et le comptage des Dinoflagellés et des Tintinnides. Sachant qu'il existe une perte significative du nombre de cellules dans les échantillons fixés au formaldéhyde (STOECKER *et al*, 1994 ; GIFFORD et CARON, 2000), une analyse statistique du volume aliquote permettant une stabilisation du nombre

d'individus comptés par échantillon a été réalisée pour chaque écosystème et un volume de 25ml a été choisi pour le comptage des Dinoflagellés et des Tintinnides. Après sédimentation de l'échantillon à analyser, l'ensemble des protistes contenus dans la chambre de comptage sont identifiés et comptés.

L'analyse taxonomique des Tintinnides utilise les travaux de JORGENSEN (1924), de KOFOID and CAMPBELL (1929; 1939), de BALECH (1959) et de MARSHALL (1969) basés sur la structure de la lorica et tient compte des derniers travaux de systématique, édités par LAVAL-PEUTO (1977; 1981; 1983), GRAIN *et al.* (1994) et DE PUYTORAC *et al.* (1993), qui expliquent l'importante variabilité phénotypique de ces organismes.

Les Dinoflagellés quant à eux ont été identifiés spécifiquement dans plusieurs travaux ant érieurs par DALY YAHIA-KEFI et DALY YAHIA (1997), DALY YAHIA-KEFI *et al.* (2001a) et DALY YAHIA-KEFI *et al.* (2001b). Suites aux mortalités massives de poissons sauvages dans divers écosystèmes lagunaires tunisiens (DALY YAHIA-KEFI et DALY YAHIA, 1997 ; ROMDHANE *et al*, 1998), et afin de mieux comprendre les phénomènes enregistrés, seules les espèces autotrophes susceptibles d'êtres nuisibles ont été prises en considération dans ce travail.

Afin de détecter les associations entre Tintinnides hétérotrophes et Dinoflagellés autotrophes des classifications hiérarchiques permettant d'aboutir à des dendrogrammes ont été réalisées sous le logiciel d'analyses statistiques STATISTICA en utilisant la méthode d'agglomération basée sur la moyenne pondérée des groupes associés. Pour chaque site, la matrice de données brutes représentant les abondances des espèces sélectionnées de Tintinnides et Dinoflagellés (p colonnes) en fonction des dates d'échantillonnage (n dates) a été composée. Nous avons calculé la matrice des corrélations (r de Pearson) entre toutes les dates après transformation logarithmique des données brutes. Par la suite la simple transformation arithmétique (1-r Pearson) donne une matrice de distances entre espèces ($p \times p$) qui a été utilisée pour réaliser la classification hiérarchique. Le dendrogramme obtenu est particulier et correspond à un corrélogramme.

3. RESULTATS

Hydrologie

Le cycle de la température montre un minimum en janvier (13,2° C) et un maximum en août (28,9° C) au niveau de la baie de Tunis. L'écart annuel de la température des eaux est plus important en milieu lagunaire en raison de la faible profondeur enregistrée (Tableau 1). Si la salinité moyenne des eaux marines de la baie de Tunis est largement influencée par les eaux Atlantiques (SOUISSI *et al.*, 2000), les écarts halins saisonniers sont beaucoup plus importants. Ainsi, dans les deux lagunes considérées, les minima sont enregistrés en hiver après de fortes pluies tandis que les valeurs les plus élevées ont dépassé 40 psu en saison estivale, au cours du mois d'août caractérisé par les plus fortes températures de l'air et la plus forte insolation.

Il apparaît donc qu'au point de vue physico-chimique, les milieux lagunaires environnants beaucoup plus instables, amplifient les variations climatologiques et anthropiques locales, en raison de leur confinement et de leur faible profondeur moyenne.

Analyse systématique

Du point de vue qualitatif, 61 espèces de Tintinnides ont été inventoriées dans la baie de Tunis, 15 espèces dans la lagune de Ghar El Melh, et seulement 12 dans le Lac Sud de Tunis (Tableau 2).

Du point de vue spécifique, quel que soit le milieu considéré, les deux genres les plus représentés ont été *Tintinnopsis* et *Favella* (Tableau 2). Les espèces correspondantes telles que *Favella ehrenbergi* (CLARAPèDE et LACHMANN, 1858), *Tintinnopsis beroidea* (STEIN, 1867) et *T. campanula* (EHRENBERG, 1840) sont d'après MARSHALL (1969), RASSOULZADEGAN (1979), ABBOUD-ABI SAAB (1989) et MODIGH et CASTALDO (2002) cosmopolites, ubiquistes, biens adaptées aux milieux néritiques côtiers. Ces espèces semblent aussi tolérer les milieux lagunaires fermés sujets à de grandes variations abiotiques.

Les Dinoflagellés ont été quant à eux bien représentés dans l'ensemble du complexe

Tableau 2. Inventaire taxonomique comparé des Tintinnides dans les trois milieux d'études.

Unites systématiques	Blale de Tunis	Lac Sud de Tunis	Lagune de Ghar El Melh
Codonaria cistellula (Fol, 1884)	+	—	—
Codonella galea Haeckel, 1873	+	+	—
Codonella nationalis Brandt, 1906	+	—	+
Codonellopsis ecaudata (Brandt, 1906)	+	+	+
Codonellopsis morchella Jorgensen, 1924	+	—	—
Codonellopsis orthoceras (Haeckel, 1873	+	—	—
Codonellopsis tessellata (Brandt, 1906)	+	—	—
Cyttarocylis cassis (Haeckel, 1873)	+	—	—
Cyttarocylis magna (Bramdt, 1906)	+	—	—
Dadayiella bulbosa (Brandt, 1906)	+	—	—
Dictyocysta lepida Ehrenberg, 1854	+	—	+
Epiplocylis acuminata (Daday, 1887)	+	—	—
Eutintinnus fraknoi (Daday, 1887)	+	—	—
Eutintinnus lusus undae (Entz, 1885)	+	—	—
Eutintinnus macilentus (Jorgensen, 1924)	+	—	—
Eutintinnus sp	+	—	—
Favella azorica (Cleve, 1900)	+	+	—
Favella ehrenbergi (Clarapède et Lachmann, 1858)	+	+	+
Favella markuzowskii (Daday, 1887)	+	—	—
Favella meunieri Kofold et Campbell, 1929)	+	—	—
Favella serrata (Moblus, 1887)	+	+	—
Helicostomella edentata (Fauré-Frémlet, 1908)	+	—	—
Helicostomella kiliensis (Lachmann, 1906)	+	—	—
Helicostomella subulata (Ehrenberg, 1833)	+	+	+
Leprotintinnus bottnicus (Nordqvist, 1890)	+	+	+
Leprotintinnus sp	+	—	—
Metacylis jorgensenii (Cleve, 1902)	+	—	+
Metacylis sp	+	—	—
Parafavella sp	+	—	—
Parundella grandis Kofold et Campbell, 1929	+	—	—
Petalotricha ampulla (Fol, 1881)	+	—	—
Petalotricha major Jorgensen, 1924	+	—	+
Proplectella claparedei (Entz, 1885)	+	—	—
Rhabdonella elegans Jorgensen, 1924	+	—	—
Rhabdonella henseni Brandt, 1906	+	—	—
Rhabdonella spiralis (Fol, 1881)	+	—	—
Salpingella acuminata (Clarapède et Lachmann, 1858)	+	—	—
Salpingella decurtata Jorgensen, 1924	+	—	—
Salpingella gracilis Kofold et Campbell, 1929	+	—	—
Salpingellasecata (Brandt, 1896)	+	—	—
Steenstrupiella steenstrupii (Clarapède et Lachmann, 1858)	+	—	—
Stenosemella nivalis (Meunier, 1910)	+	+	—
Stenosemella ventricosa (Clarapède et Lachmann, 1858)	+	—	—
Tintinnopsis beroidea (Stein, 1867)	+	+	+
Tintinnopsis brandti (Nordquist, 1890)	+	—	—
Tintinnopsis butschli Daday, 1887	+	+	+
Tintinnopsis campanula (Ehrenberg, 1840)	+	+	+
Tintinnopsis cincta (Clarapède et Lachmann, 1858)	+	—	—
Tintinnopsis cyathus Daday, 1887	+	—	—
Tintinnopsis fimbriata Meunier, 1919	+	+	—
Tintinnopsis lobiancoi Daday, 1887	+	—	—
Tintinnopsis major Meunier, 1910	+	—	—
Tintinnopsis radix Imhof, 1886	+	—	+
Tintinnopsis strigosa Meunler, 1919	+	—	—
Tintinnopsis tubulosa Levander, 1900	+	—	+
Tintinnopsis undella Meunier, 1910	+	—	—
Tintinnopsis urnula Meunler, 1910	+	—	—
Tintinnopsis inquilinum (O.F.Muller, 1776)	+	—	—
Undella hyalina Daday, 1887	+	—	+
Xystonella lohmani (Brandt, 1906)	+	—	—
Xystonella treforti (Daday, 1887)	+	—	—
Richesse spécifique	61	12	15

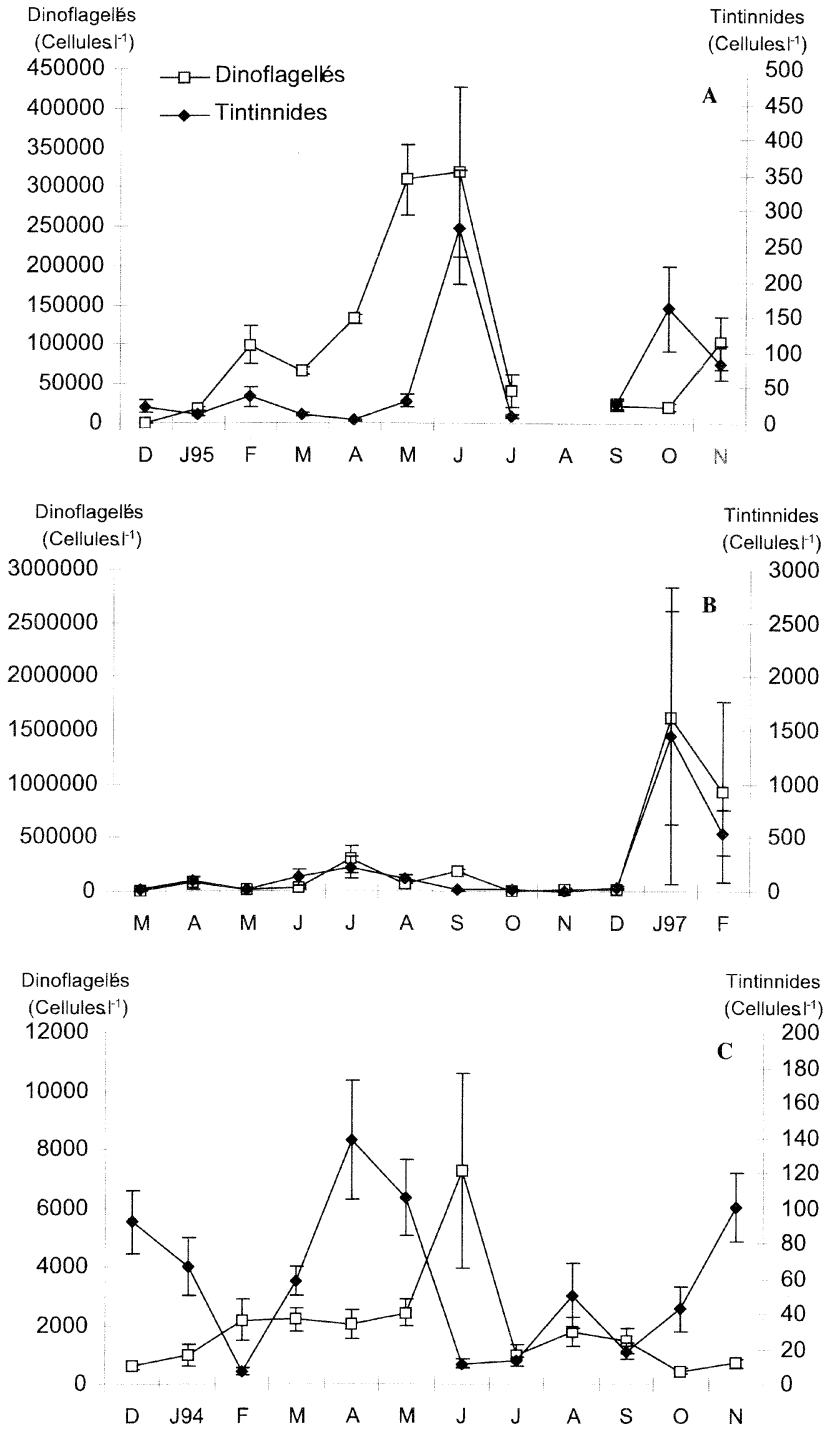

Fig. 2. Variations saisonnières de l'abondance (cell.l $^{-1}$) des Tintinnides et des Dinoflagellés. A : dans la lagune de Ghar El Melh, B : dans le Lac Sud de Tunis, C : dans la baie de Tunis. (Les lignes verticales indiquent l'erreur standard : ES)

Tableau 3. Code spécifique des dinoflagellés et des tintinnides.

Dinoflagellés		Tintinnides	
Unités systématiques	Code	Unités systématiques	Code
Alexandrium spp	ALEX.SPP	*Codonella galea* HAECKEL 1873	CODO.GAL
Dinophysis acuminata Claparde et Lachman 1859	DINO.ACU	*Codonellopsis ecaudata* (BRANDT 1906)	CODO.ECA
Dinophysis caudata Saville-Kent 1881	DINO.CAU	*Dictyocysta lepida* EHRENBERG 1854	DICT.LEP
Dinophysis sacculus STEIN 1883	DINO.SAC	*Eutintinnus fraknoi* (Daday 1887)	EUTI.FRA
Gonyaulax spp	GONY.SPP	*Eutintinnus lusus undae* (Entz 1885)	EUTI.LUS
Gonyaulax verior Sournia 1973	GONY.VER	*Eutintinnus* sp	EUTI.SP
Gymnodinium mikimotoi Miake et Kominami ex Oda 1935	GYMN.MIK	*Favella ehrenbergi* (CLARAPÉDE et LACHMANN 1858)	FAVE.EHR
Gymnodinium sanguineum HIRASAKA 1922	GYMN.SAN	*Favella* spp	FAVE.SPP
Gymnodinium sp	GYMN.SP	*Helicostomella kiliensis* (LACHMANN 1906)	HELI.KIL
Gyrodinium spirale KOFOID et SWEZY 1921	GYRO.SPI	*Leprotintinnus bottnicus* (NORDQVIST 1890)	LEPR.BOT
Peridinium quinquecorne Abé 1936	PERI.QUI	*Leprotintinnus* sp	LEPR.SP
Prorocentrum lima (EHRENBERG) Dodge 1975	PROR.LIM	*Metacylis* sp	META.SP
Prorocentrum mexicanum Taffal 1942	PROR.MEX	*Stenosemella nivalis* (*MEUNIER 1910*)	STEN.NIV
Prorocentrum minimum (Pavillard) SCHILLER 1933	PROR.MIN	Tintinnopsis butschlii Daday 1887	TINT.BUT
		Tintinnopsis campanula (EHRENBERG 1840)	TINT.CAM
		Tintinnopsis sacculus BRANDT 1896	TINT.SAC
		Tintinnopsis spp	TINT.SPP

aquatique étudié, avec 158 espèces recensées dans la baie de Tunis (DALY YAHIA-KEFI *et al.*, 2001a). Parmi ces espèces, 28 se retrouvent au niveau de la lagune Sud de Tunis et 33 dans la lagune de Ghar El Melh (DALY YAHIA - KEFI et DALY YAHIA, 1997).

Distribution quantitative et associations spécifiques entre Tintinnides et Dinoflagellés

Les densités numériques des Tintinnides totaux (figure 2) ont montré d'importantes fluctuations mensuelles avec :

- dans la lagune de Ghar El Melh au cours de l'année 1995 (figure 2A), une densité moyenne annuelle de 62,3 cellules.l^{-1} oscillant entre un minimum en avril de 4,2 cellules.l^{-1} (ES=1,4) et un maximum à la fin du printemps qui atteint 276 cellules.l^{-1} (ES=79,9).

- dans la lagune de Tunis Sud (figure 2B), milieu plus confiné et très pollué, la moyenne annuelle a été durant l'année 1997, de 223,1 cellules.l^{-1}, avec une poussée estivale de Tintinnides de 224,9 cellules.l^{-1} (ES=102,3) en juillet, suivie par un développement hivernal atteignant 1452,5 cellules.l^{-1} (ES=1380,2) en janvier et chutant à 547,5 cellules.l^{-1} (ES=205,4) en février. Le minimum a été relevé en novembre avec 6,3 cellules.l^{-1} (ES=3,2).

- dans la baie de Tunis (figure 2C), l'année 1994 se caractérise par deux périodes de fortes abondances: la première en avril-mai, avec des densités respectives de 138,1 cellules.l^{-1} (ES=34,1) et 105,5 cellules.l^{-1} (ES=22,3); la deuxième en novembre-décembre avec respectivement 100,6 cellules.l^{-1} (ES=19,4) et 92 cellules.l^{-1} (ES=18,2).

Les corrélogrammes obtenus, sur la base des Tintinnides dominants et des Dinoflagellés autotrophes susceptibles d'être nuisibles (Tableau 3), montrent l'existence d'associations entre les espèces de ces deux groupes planctoniques qui pourraient s'expliquer par

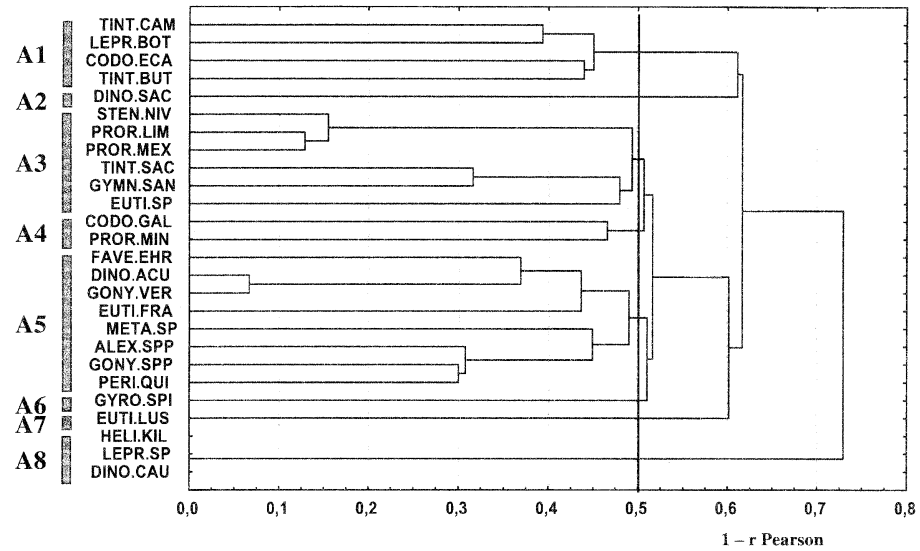

Fig. 3. Corrélogramme représentant les associations spécifiques (Tintinnides–Dinoflagellés toxiques) au niveau de la baie de Tunis.

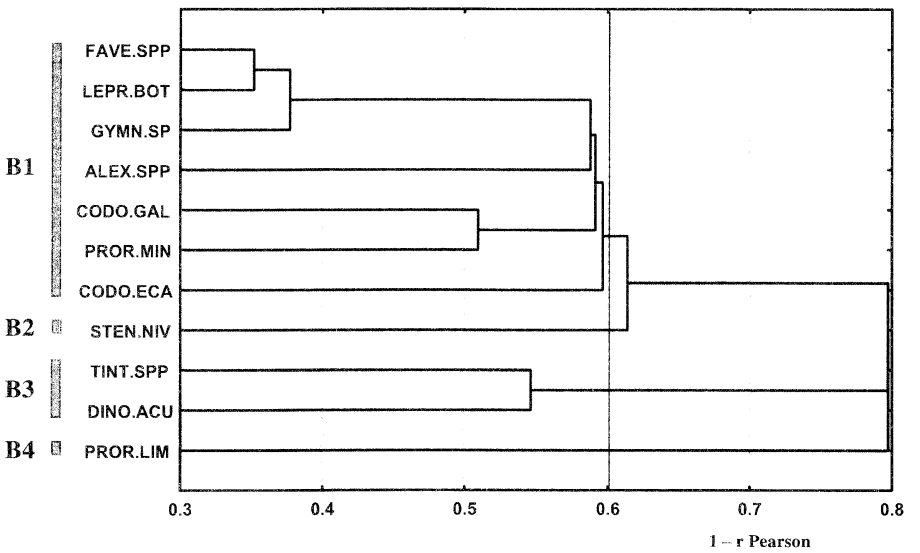

Fig. 4. Corrélogramme représentant les associations spécifiques (Tintinnides–Dinoflagellés toxiques) au niveau de la lagune de Tunis Sud.

des relations trophiques.

En adoptant une coupure au seuil de 0,5 (figure 3) huit assemblages spécifiques ont été identifiés au niveau de la baie de Tunis. Quatre d'entre eux (A3, A4, A5 et A8) regroupent des espèces de Dinoflagellés et de Tintinnides. C'est ainsi que *Prorocentrum lima* (EHRENBERG) Dodge 1975, *P. mexicanum* Tafall 1942 et *Gymnodinium sanguineum* HIRASAKA 1922 sont associés à *Stenosemella nivalis* (MEUNIER, 1910), *Tintinnopsis sacculus* BRANDT, 1896 et *Eutintinnus* sp (A3). Au contraire, *Prorocentrum minimum* (Pavillard) SCHILLER 1933 n'est corrélé qu'avec *Codonella galea*

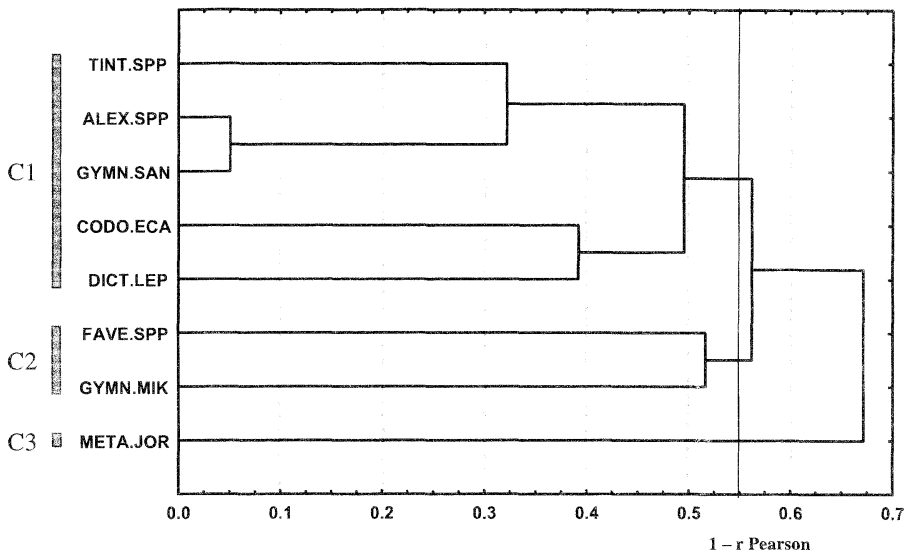

Fig. 5. Corrélogramme représentant les associations spécifiques (Tintinnides–Dinoflagellés toxiques) au niveau de la lagune de Ghar El Melh.

HAECKEL, 1873 (A4).

Le corrélogramme obtenu pour la lagune de Tunis Sud (figure 4) met en évidence quatre groupes d'espèces dont deux (B1 et B3) sont pluri–spécifiques. L'association B1, la plus remarquable, regroupe les Dinoflagellés *Alexandrium* spp HALIM 1960, *Gymnodinium* sp STEIN 1878 et *Prorocentrum minimum* avec les Tintinnides *Favella* spp, *Leprotintinnus bottnicus* (NORDQVIST, 1890), *Codonella galea* et *Codonellopsis ecaudata* (BRANDT, 1906).

Enfin, dans la lagune de Ghar El Melh, trois assemblages dont deux pluri–spécifiques (C1 et C2) ont été mis en évidence (figure 5). L'association spécifique C1 regroupe *Alexandrium* spp et *Gymnodinium sanguineum* avec *Tintinnopsis* spp, *Codonellopsis ecaudata* et *Dictyocysta lepida* EHRENBERG, 1854.

Il faut toutefois éliminer de ces associations *Gymnodinium sanguineum* dont la taille moyenne dépasse le diamètre oral des diffé rentes espèces de Tintinnides auquelle elle est associée. Il en est de même pour *Dinophysis caudata* que l'on retrouve dans l'association A8 (figure 3). La présence de ces deux espèces résulterait plutôt de leurs préférences environnementales.

4. DISCUSSION

Comparé à d'autres écosystèmes côtiers, la Baie de Tunis avec 62 espèces de Tintinnides apparaît plus riche que la Baie d'Alger, la Baie de Villefranche Sur Mer, la Baie de Mali Ston en Adriatique Sud ou encore la Baie de d'Izmir en mer Egée (Tableau 4). De plus c'est sur le littoral Est méditerranéen (côtes Nord libanaises) que le nombre de Tintinnides le plus élevé a été enregistré avec 90 espèces et s'oppose à certains écosystèmes estuariens ou lagunaires confinés et pollués comme la lagune de Tunis Sud et l'estuaire de Bahia Blanca avec respectivement seulement, 13 et 11 espèces inventoriées. Les travaux réalisés par DOLAN (2000) sur l'ensemble de la méditerranée, en période printanière confirment l'existence d'un gradient croissant d'Ouest en Est aussi bien du nombre d'espèces que de l'indice de diversité spécifique H' des Tintinnides. Toutefois, le nombre de 16 espèces récoltées dans la lagune de Ghar El Melh est relativement faible et apparaît proche de celui enregistré dans le golfe de Marseille (TRAVERS, 1973). Cependant, selon TRAVERS (1973) le nombre d'espèces recensées dans son travail ne reflète pas la biodiversité des Tintinnides dans cet écosystème côtier.

Les résultats, obtenus dans notre étude,

Tableau 4. Analyse comparative du nombre d'espèces et de l'abondance des Tintinnides dans quelques écosystèmes du Bassin Méditerranéen et de l'Atlantique (*espèces communes).

Ecosystèmes étudiés	Nombre d'espèces	Abondance moyenne (cellules.l^{-1})	Densités maximales (cellules.l^{-1})	Auteurs
Etang de Thau	21	75,7	276,6	Lam-Hoai (1997)
Estuaire de Bahia Blanca (Argentine)	11	-	2300	Barria De Cao *et al.* (1997)
Golfe de Marseille	15*	375	2000	TRAVERS (1973)
Ville-franche sur Mer	24	146,5	1000	RASSOULZADEGAN (1979)
Ville-franche sur Mer	40	40	500	CARIOU *et al.* (1999)
Baie d'Alger	42	8,1	30,6	Vitiello (1964)
Méditerranée Occidentale et Orientale (milieu océanique)	90	25	115	DOLAN (2000)
Adriatique Sud (Baie de Mali Ston)	60	14,5	1495	Krsinic (1979)
Adriatique Est (Dalmatie)	33	-	123,3	Krsinic (1977)
Liban du Nord	90	10,9	39	Abboud-Abi-Saab (2002)
Côtes libanaises	35	-	200	Lakkis and Novel-Lakkis (1985)
Baie d'Izmir	44	-	-	Koray and Ozel (1983)
Baie de Tunis	62	49,1	138,1	Présent travail
Lac Sud de Tunis	13	223,1	1452,5	Présent travail
Lagune Ghar El Melh	16	62,3	276	Présent travail

mettent aussi en évidence qu'en milieu lagunaire les pics de densités de Tintinnides observés sont largement supérieurs à ceux enregistrés en mer. Plusieurs hypothèses peuvent expliquer ce phénomène :

-Les conditions physico-chimiques, trophiques, ainsi que le confinement et le faible hydrodynamisme des milieux lagunaires opposé à l'importante turbulence constatée dans la baie de Tunis, favoriseraient la croissance et la production des Tintinnides dans ces biotopes.

- Les kystes de Tintinnides qui s'accumulent d'années en années semblent beaucoup plus protégés en milieu lagunaire qu'en milieu marin ouvert.

-L'importante variabilité annuelle et spatiale enregistrée par divers auteurs dans le bassin m éditerranéen doit être prise en compte dans ce travail, d'autant plus que les trois écosystèmes étudiés ont été prospectés à différentes années. En effet, le tableau 4 montre, qu'aussi bien le nombre d'espèces de Tintinnides recensées dans divers écosystèmes côtiers méditerranéens ou atlantiques, que les densités moyennes ou maximales enregistrées varient fortement. C'e st ainsi que dans la Baie de Villefranche Sur Mer, les densités moyennes annuelles ont diminué considérablement après réduction des émissaires d'égouts dans la rade (RASSOULZADEGAN, 1979 ; CARIOU *et al*, 1999).

Les périodes d'abondances des Tintinnides dans les trois biotopes étudiés sont apparues assez différentes. Il semble que ces différences résultent d'une forte variabilité saisonnière liée aux conditions environnementales propres a chaque écosystème. Cette variabilité concerne l'abondance des proies principales de

Tintinnides, les Dinoflagellés, mais aussi de leurs prédateurs et en particulier de deux espèces de scyphoméduses très prolifiques depuis ces dix dernières années, *Rhizostoma pulmo* (MACRI, 1778) et *Cotylorhiza tuberculata* (MACRI, 1778) (données non publiées). En effet, les *figures 2A, 2B et 2C* montrent clairement que les blooms de Dinoflagellés ont généralement lieu au cours des périodes de développement des Tintinnides. Ceci nous permet donc de suggérer une relation de cause à effet, à condition de tenir compte de la taille moyenne des populations de Dinoflagellés associés à la taille moyenne du diamètre oral des Tintinnides qui les contrôlent.

Il ressort nettement de ce travail que, le plus souvent, chaque espèce de Dinoflagellés, susceptibles d'être nuisibles, est associée à un ou plusieurs Tintinnides. De plus, la dynamique de ces Dinoflagellés apparaît beaucoup mieux contrôlée en milieu marin qu'en milieu lagunaire. Ainsi, le nombre de prédateurs potentielsest relativement plus élevé pour un même dinoflagellé en milieu marin. Toutefois, certains Dinoflagellés comme *Dinophysis sacculus* STEIN 1883 et *Gyrodinium spirale* (Bergh) KOFOID et SWEZY 1921 forment au niveau de la baie de Tunis, des entités mono-spécifiques et ne sont associés à aucune espèce de Tintinnides.

Les résultats obtenus nous permettent de comprendre la fragilité de plusieurs lagunes tunisiennes, où des phénomènes d'eaux colorées associés ou non à des mortalités de poissons, s'observent régulièrement en saisons printanière et estivale (DALY YAHIA-KEFI et DALY YAHIA, 1997 ; ROMDHANE *et al.*, 1998). Il apparaît clairement que la dynamique des espèces de Dinoflagellés nuisibles ou susceptibles de l'être est contrôlée par un ou plusieurs Tintinnides. Toutefois, certains maillons de la chaîne semblent fragilisés.

Ce travail nous a permis de préciser l'importance des ciliés Tintinnides au sein du microzooplancton des milieux néritiques. En effet, nous constatons après s'être basé sur la dynamique des principaux Dinoflagellés nuisibles de la baie de Tunis, l'importante structuration du compartiment microzooplanctonique et particulièrement le contrôle effectué par les Tintinnides sur les populations de Dinoflagellés. Ils jouent ainsi un rôle non négligeable dans le transport et le transfert de matière et d'énergie à partir des producteurs primaires jusqu'aux consommateurs de deuxième ordre qui sont essentiellement représentés par les organismes du mésozooplancton (CONOVER, 1982; MARGALEF, 1982).

A l'issue de cette étude, certaines associations spécifiques peuvent être considérées comme des relations prédateurs-proies car elles s'observent dans les trois écosystèmes étudiés, mais aussi car le diamètre oral des Tintinnides considérés correspond au spectre de taille des Dinoflagellés. C'est ainsi que le tintinnide *Codonella galea* semble être le prédateur de *Prorocentrum minimum* (A4 et B1). De même, *Codonellopsis ecaudata* consommerait préférentiellement *Alexandrium* spp(B1 et C1).

Les milieux lagunaires et néritiques tunisiens sont donc propices au développement et à l'étude des ciliés Tintinnides. Leurs proportions élevées dans le zooplancton total (25 à 95%), ainsi que les densités atteintes en pé riode de blooms montrent qu'ils constituent la base de la chaîne alimentaire hétérotrophe. Le confinement naturel, l'eutrophisation et la pollution croissante de ces lagunes en raison des déchets urbains et industriels ont progressivement entraîné une diminution de la diversité spécifique des Tintinnides ainsi que l'ensemble des autres groupes zooplanctoniques (DALY YAHIA et DALY YAHIA -KEFI, 2004 ; DALY YAHIA *et al.*, 2004).

REMERCIEMENTS

Nous tenons à remercier le Professeur Michèle LAVAL-PEUTO de l'Université de Nice-Sophia Antipolis pour avoir bien voulu vérifier l'identification systématique des Tintinnides. Ce travail est une contribution au programme CMCU 2000 de coopération inter-universitaire Tuniso-Française.

References

ABBOUD-ABI SAAB, M. (1989): Distribution and ecology of tintinnids in the plankton of Lebanese costal waters (eastern Mediterranean). J.

Plankton Res., **11** (2), 203–222.

ABBOUD–ABI SAAB, M. (2002): Annual cycle of the microzooplankton communities in the waters surrounding the Palm Island Nature Reserve (north Lebanon), with special attention to tintinnids. Medit. Mar. Sci., **3/2**, 55–76.

AYUKAI, T. (1987): Predation by *Acartia clausi* (Copepoda: Calanoida) on two species of tintinnids. Mar Microb Food Webs, **2** (1), 45–52.

BALECH, E. (1959) : Tintinnoinea del Mediterraneo. Travaux de la station zoologique de Villefranche sur mer, **18** (17), 89pp, 21pl.

BARRIA DE CAO, M.S., R.E. PETTIGROSSO and C. POPOVICH (1997): Planktonic ciliates during a phytoplankton bloom in Bahia Blanca estuary, Argentina. II. Tintinnids. Oebalia, **23**, 21–31.

BEN FREDJ, M., M.N. DALY YAHIA and O. DALY YAHIA–KEFI (2001): Contribution à la connaissance des fluctuations saisonnières qualitatives et quantitatives des Tintinnides dans la lagune de Ghar El Melh. *Bull. Inst. Nat. Sc. Tech. Mer.*, **5** (S), 71–76.

CARIOU, J.B., J.R. DOLAN and S. DALLOT (1999): A preliminary study of tintinnid diversity in the NW Mediterranean Sea. *J Plankton Res,* **21** (6), 1065–1075.

CONOVER, R.J. (1982): Interrelations between microzooplankton and other plankton organisms. *Ann. Inst. Océanogr. Paris,* **58** (S), 31–46.

DALY YAHIA, M.N. (1998): Dynamique saisonnière du zooplancton de la baie de Tunis (Systématique, écologie numérique et biogéographie méditerranéenne). Thèse de Doctorat. Faculté des Sciences de Tunis, Tunis, 247pp.

DALY YAHIA, M.N. and O. DALY YAHIA–KEFI (2004): Structure et dynamique spatio–temporelle du zooplancton de la lagune de Ghar El Melh. Revue de l'I.N.A.T., **19** (1), 59 – 79.

DALY YAHIA, M.N., S. SOUISSI and O. DALY YAHIA–KEFI (2004): Spatio–temporal structure of planktonic copepods in the Bay of Tunis (South Western Mediterranean Sea). Zoological Studies, **43** (2), 8 – 19.

DALY YAHIA–KEFI, O. and M.N. DALY YAHIA (1997): Le phytoplancton toxique dans 3 milieux lagunaires tunisiens: Ghar El Melh, Lac Sud de Tunis et Bou Grara. *In* Gestion et Conservation des Zones Humides Tunisiennes. World Wide fund For Nature (eds.), p.125–131.

DALY YAHIA–KEFI, O., E. NEZAN and M.N. DALY YAHIA (2001a): Sur la présence du genre *Alexandrium* HALIM dans la Baie de Tunis (Tunisie). *Oceanol Acta,* **24** (Supplément), 17–25.

DALY YAHIA–KEFI, O., M.N. DALY YAHIA, S. SOUISSI and M.S. ROMDHANE (2001b) : Les Dinoflagellés de la baie de Tunis: Composition spécifique et numérique. *Rapp Comm Int. Mer Médit,* **36**, 377.

DE PUYTORAC, P.,A. BATISSE, G. DEROUX, A. FLEURY, J. GRAIN, M. LAVAL–PEUTO and M. TRUFFAU (1993) : Proposition d'une nouvelle classification du phylum des protozoaires. Cilophora Doflein, 1901. *C R Acad Sci III–Vie,* **316**, 716–720.

DOLAN, J.R. and C. MARRASÉ (1995): Planktonic ciliate distribution relative to a deep chlorophyll maximum: Catalan Sea, N.W. Mediterranean, June 1993. Deep Sea Res, **I** (42), 1965–1987.

DOLAN, J.R. (2000): Tintinnid ciliate diversity in the Mediterranean Sea: longitudinal patterns related to water column structure in late spring–early summer. Aquat Microb Ecol, 22, 69–78.

DOLAN, J.R. and C.L. GALLEGOS (2001): Estuarine diversity of tintinnids (planktonic ciliates). J *Plankton Res,* **23** (9), 1009–1027.

GIFFORD, D.J. and M.J. DAGG (1991): The microzooplankton–mesozooplankton link: consumption of planktonic protozoa by the calanoid copepods *Acartia tonsa* Dana and *Neocalanus plumchrus* Murukawa. *Mar Microb Food Webs,* **5** (1), 161–177.

GIFFORD, D.J. and D.A. CARON (2000): Sampling, preservation, enumeration and biomass of protozooplankton. *In* ICES Zooplankton Methodology Manual. HARRIS, R.P., H.R. SKJOLDAL, J. LENZ, P.H.WIEBE and M.E. HUNTLEY (eds.), Academic Press, London, p. 193–221.

GRAIN, J., M. LAVAL–PEUTO and G. DEROUX (1994) : La classe des Oligotrichia, Butschlii 1887. *In* Traité de Zoologie, Ciliés. Masson Paris (eds.). (2), p1–219.

HARRIS, R.P., P.H. WIEBE, J. LENZ, H.R. SKJOLDAL and M. HUNTLEY (2000): Zooplankton Methodology Manual. Academic Press, London, 684 pp.

JORGENSEN, E. (1924): Mediterranean Tintinnidae. Report of Danish Oceanographic Expedition 1908 –10 to the Mediterranean and adjacent seas, **2** (Biol.), 1–110.

KENTOURI, M. and P. DIVANACH (1986): Sur l'importance des ciliés pélagiques dans l'alimentation des stades larvaires de poissons. *An Biol,* **25** (4), 307–318.

KOFOID, C.A. and A.S. CAMPBELL (1929) A conspectus of the marine and freshwater Ciliata belonging to the suboerder Tintinnoinea, with descriptions of new species principally from the Agassiz Expedition to the Eastern Tropical Pacific, 1904–1905. *U Calif Publ Zool,* **34**, 1–403.

KOFOID, C.A. and A.S. CAMPBELL (1939): Reports on the scientific results of the expedition to the Eastern Tropical Pacific. The Ciliata: The Tintinnoinea. *Bull Mus Comp Zool Harvard,* **84**, 1–473.

KORAY, T. and I. OZEL (1983): Species of the order Tintinnoinea in Izmir bay and their salinity and temperature dependent distribution. Rapp.

Comm. Int. Mer Médit., **28** (9), 123 – 124.

KRSINIC, F. (1977): Tintinnids of the Eastern coast of Middle Adriatic. Rapp. Comm. Int. Mer Médit., **24** (10), 95–96.

KRSINIC, F. (1979): The tintinnids (Ciliata) from the coastal waters of the Southern Adriatic in the year 1975/76. Nova Thalassia, **3** (suppl.), 199–211.

LAKKIS, S. and V. NOVEL-LAKKIS (1985): Considérations sur la répartition des tintinnides au large de la côte libanaise. Rapp. Comm. Int. Mer Médit., **29** (9), 171–172.

LAM-HOAI, T., C. ROUGIER and G. LASSERRE (1997): Tintinnids and rotifers in a northern Mediterranean coastal lagoon. Structural diversity and function through biomass estimations. Mar. Ecol. Prog. Ser., **152**, 13–25.

LAVAL-PEUTO, M. (1977) : Reconstruction d'une lorica de forme Coxliella par le trophonte nu de *Favella ehrenbergii* (Ciliata, Tintinnina). CR Acad Sci III-Vie, **284**(D), 547–550.

LAVAL-PEUTO, M. (1981): Construction of the lorica in Ciliata Tintinnina. *In vivo* study of *Favella ehrenbergii*: variability of the phenotypes during the cycle, biology, statistics, biometry. Protistologica, **17** (2), 249–272.

LAVAL-PEUTO, M. (1983): Sexual reproduction in *Favella ehrenbergii* (Cilophora, Tintinnina) Taxonomical implications. Protistologica, **19** (4), 503–512.

LAVAL-PEUTO, M. and D.C. BROWNLEE (1986): Identification and systematics of the Tintinnina (Ciliophora): evaluation and suggestions for improvement. *Ann. Inst. Océanogr. Paris,* **62** (1), 69–84.

LAVAL-PEUTO, M., F. HEINBOKEL, O.R. ANDERSON, F. RASSOULZADEGAN and B.F. SHERR (1986): Role of micro- and nanozooplankton in marine food webs. *Insect Sci Appl,* **7** (3), 387–395.

MARGALEF, R. (1982): Some thoughts on dynamics of populations of ciliates. *Ann. Inst. Océanogr. Paris,* **58** (S), 15–18.

MARSHALL, S.M. (1969): Protozoa. Tintinnidae. *In* Fiches d'identification du zooplancton. FRASER, J.H. and V.K. HANSEN (eds), Conseil Permanent International pour l'Exploration de la Mer, 117–127.

MODIGH, M. and S. CASTALDO (2002): Variability and persistence in tintinnid assemblages at a Mediterranean coastal site. *Aquat Microb Ecol,* **28**, 299–311.

RASSOULZADEGAN, F. (1979): Évolution annuelle des Ciliés pélagiques en Méditerranée nord-occidentale. II. Ciliés Oligotriches. Tintinnides (Tintinnina). *Invest Pesq,* **43** (2), 417–448.

RASSOULZADEGAN, F., M. LAVAL-PEUTO and R.W. SHELDON (1988): Partitioning of food ration of marine ciliates between pico and nanoplankton. Hydrobiologia, **159**, 75–88.

ROMDHANE, M.S., H.C. EILERTSEN, O.K. DALY YAHIA and M.N. DALY YAHIA (1998): Toxic dinoflagellate blooms in tunisian lagoons: causes and consequences for aquaculture. *In* Harmful algae. REGUERA, B., J. BLANCO, M.L. FERNÁNDEZ and T. WYATT (eds.), Xunta de Galicia and Intergovernmental Oceanographic Commission of UNESCO, Vigo, 80–83.

SOUISSI, S., O. DALY YAHIA-KÉFI and M.N. DALY YAHIA (2000): Spatial characterisation of nutrient dynamics in the Bay of Tunis (south western Mediterranean) using multivariate analyses: consequences for phyto- and zooplankton distribution. *J Plankton Res,* **22** (11), 2039–2059.

STOECKER, D. and R.L. GUILLARD (1982): Effects of temperature and light on the feeding rate of *Favella* sp. (Ciliated Protozoa, suborder Tintinnina). *Ann. Inst. Océanogr. Paris,* **58** (S), 309–318.

TRAVERS, M. (1973): Le microplancton du golfe de Marseille: Variations de la composition systématique et de la densité des populations. Téthys, **5** (1), 31–54.

UTERMöHL, H. (1958). Zur vervollkommnung der quantitativen Phytoplankton-Methodik. Mitt. d. Internat. Vereinig. f. Limnologie., **9**, 1–38.

VITIELLO, P. (1964): Contribution à l'étude des Tintinnides de la baie d'Alger. Pelagos, **2** (2), 5–39.

Tintinnids (Ciliophora, Tintinnina) and Dinoflagellates (Dinophyceae) associations in the Bay of Tunis and two adjacent lagoons: Ghar El Melh and Tunis South (S W Mediterranean).

Mohamed Néjib DALY YAHIA[1]), Ons DALY YAHIA-KEFI, Sami SOUISSI, Fadhila MAAMOURI and Patricia AISSA.

Abstract : We present here a study of Tintinnids and potentially harmful autotrophic dinoflagellates through monthly sampling of the Bay of Tunis and two associated lagoons: Ghar El Melh and Tunis South. We found that from the qualitative point of view the populations of tintinnids found in lagoons are a subset of those inhabiting the nearby marine environment. 62 species of tintinnids were found in the Bay of Tunis, 16 species in the lagoon of Ghar El Melh, and only 13 in the lagoon of Tunis South. All species found in lagoons were present in the Bay of Tunis. The density of tintinnids is higher in the lagoons (Tunis South: 223.1 cells.liter^{-1} ; Ghar El Melh: 62.3 cells.l^{-1}) than in the open sea (Bay of Tunis: 49.1 cells.l^{-1}). Blooms of the principal tintinnids species such as *Favella ehrenbergi, Tintinnopsis* spp and *Stenosemella nivalis* are associated with *Dinophysis acuminata, Alexandrium* spp and *Prorocentrum lima.* In order to test this hypothesis, hierarchical classifications were realised and allowed the identification of specific associations between the different species of dominant tintinnids and the potentially harmful dinoflagellate species.

– Laboratoire de Biosurveillance de l'Environnement. Groupe de Recherche en Hydrologie et Planctonologie. Département des Sciences de la Vie. Faculté des Sciences de Bizerte, Republic of Tunisia. 7021, Zarzouna, Bizerte. Fax : 216 72 590 566 –
E-mail : nejib.daly@fsb.rnu.tn

Received September 29, 2004
Accepted June 13, 2005

La mer 43 : 33–42, 2005
Société franco-japonaise d'océanographie, Tokyo

Sedimentation rate of dioxins from the mid-1980s to 2002 in a sediment core collected off Ishinomaki in Sendai Bay, Japan

Yutaka OKUMURA[1*], Hiromitsu NAGASAKA[2], Youichi KOHNO[3], Takashi KAMIYAMA[1], Toshiyuki SUZUKI[1], and Yoh YAMASHITA[4]

Abstract : The vertical distribution of dioxins in a sediment core was investigated to elucidate historical trends of dioxins (polychlorinated dibenzo-*p*-dioxins, polychlorinated dibenzofurans and coplanar polychlorinated biphenyls) discharged into Sendai Bay, Japan, from the mid-1980s to 2002. Polychlorinated dibenzo-*p*-dioxins (PCDDs) accounted for approximately 85% of total dioxins. The predominant dioxin congeners in the sediment, 1.3.6.8-tetrachlorodibenzo-*p*-dioxin (1,3,6,8-TeCDD), 1, 3, 7, 9-TeCDD, and octachlorodibenzo-*p*- dioxin (OCDD), accounted for 79% of total PCDDs. The source of dioxins deposited off Ishinomaki in Sendai Bay from the early 1980s to 2002 was mainly impurities in pesticides (chloronitrophen and pentachlorophenol). Sedimentation rates of total dioxins were 161.2 pg g $^{-1}$ year $^{-1}$ during 1992–2002 and 172.6 pg g $^{-1}$ year $^{-1}$ during 1981-1992. Thus, the rate during 1992-2002 was slightly lower than that during 1981–1992, and the dioxin sedimentation rate decreased slightly upward in the core. Furthermore, the sedimentation rate of suspended solids off Ishinomaki, 0.112 g cm $^{-2}$ year $^{-1}$, tended to be lower than those measured in other Japanese ports. The average water content and ignition loss to 60 cm depth were 49.46 ±3.9% and 6.5 ±0.6% (average ±SD), respectively. These data suggest that inorganic suspended solids from rivers contributed more to sedimentation in Sendai Bay than in other Japanese ports.

Keywords : *PCDD/Fs, Co-PCBs, sediment core, historical trend, Sendai Bay*

1. Introduction

Chemicals emitted from the terrestrial environment are carried to the marine environment both by rivers and via the atmosphere (TAKADA 1997). Chemicals reaching the sea are dissolved in seawater or adsorbed onto suspended solids. Those adsorbed onto suspended solids then sink to the sea bottom and accumulate in the bottom sediments. Therefore, sediments are monitored to investigate pollution by heavy metals (MATSUMOTO and YOKOTA 1978) and polycyclic aromatic hydrocarbons (HANDA and OHTA 1983) and to evaluate historical trends in dioxin concentrations (SAKAI *et al.* 1999, KANNAN *et al.* 2000, MASUNAGA *et al.* 2001b, YAO *et al.* 2002) and other chemicals (YAMASHITA *et al.* 2000) and pollution sources, from the point of view of risk assessment. Further, sedimentation rates of suspended solids are calculated so that chemical fluxes in the marine environment can be estimated (MATSUMOTO 1983, TANIMOTO and HOSHIKA 1994, KANAI *et al.* 1997).

Marine sediments in Sendai Bay have been studied to monitor pollution by dioxins (OKUMURA *et al.* 2003) and to evaluate historical trends in dioxin concentrations (OKUMURA *et al.* 2004). However, the surface layers of the sediment core used for the study was mixed, preventing the accurate determination of the historical trend of dioxins in Sendai Bay from the mid-1980s to 2002. Therefore, to complement the estimate of the historical trend of

1) Tohoku National Fisheries Research Institute, Fisheries Research Agency, 3-27-5 Shinhama, Shiogama, Miyagi 985-0001, Japan
2) Metocean Environment Inc., Riemon 1334-5, Ooigawa, Shida, Shizuoka 421-0212, Japan
3) Japan Food Research Laboratories, 6-21-6 Nagayama, Tama, Tokyo 206-0025, Japan
4) Kyoto University, Fisheries Research Station, Nagahama, Maizuru, Kyoto 625-0086, Japan

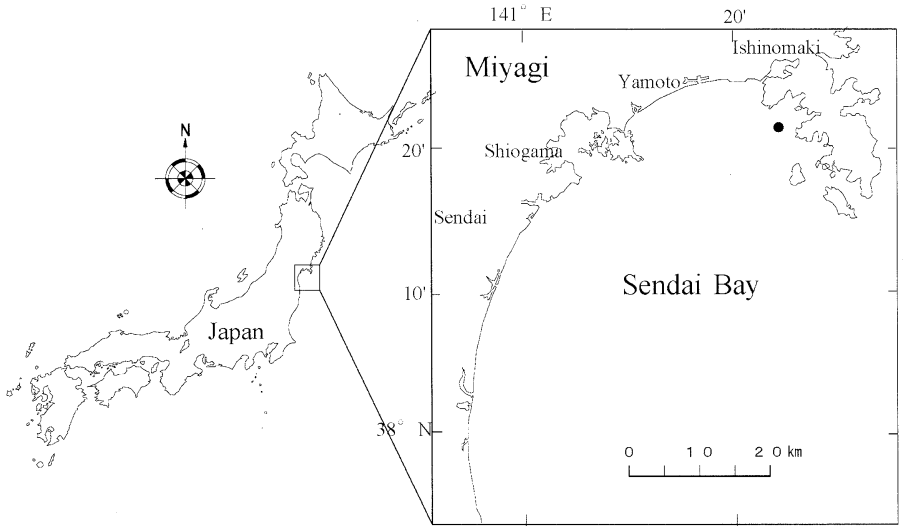

Fig. 1. Location of the sampling site off Ishinomaki in Sendai Bay.

dioxins in Sendai Bay obtained previously, we investigated dioxin concentrations from the mid-1980s to 2002 in another sediment core from Sendai Bay. Moreover, because sedimentation rates of suspended solids are known to vary in different parts of the bay (MINISTRY OF LAND, INFRASTRUCTURE AND TRANSPORT, GOVERNMENT OF JAPAN 2001), we also investigated the sedimentation rate in another part of Sendai Bay.

In this study, density, ignition loss, water content, and ^{210}Pb and ^{137}Cs concentrations in a sediment core collected off Ishinomaki in Sendai Bay were determined, and the sedimentation rate of the suspended solids was calculated. The properties of sediment in Sendai Bay were then compared with data from other parts of Japan. Finally, dioxin concentrations in sediment deposited from the mid-1980s to 2002 were analyzed by high-resolution gas chromatography/high-resolution mass spectroscopy (HRGC/HRMS) in order to clarify trends in the sedimentation rate of dioxins during that period.

2. Materials and Methods

2.1. Sampling

A sediment core approximately 80 cm long was collected with a sediment core sampler (ϕ 20cm × 100cm) from a sampling site in Sendai Bay (lat 38° 21′ N, long 141° 23′ E) on September 19, 2002 (Fig. 1). To protect contamination during sample transfer, the sediment core sampler was tightly sealed and then transferred from the sampling site to the laboratory. In the laboratory, the core was sliced into 2-cm segments, depending on depth. After the outer surface of the sediment, the part which had been in contact with the core sampler, was removed, samples were refrigerated or frozen in glass bottles that had been washed with *n*-Hexane until use.

2.2. Analysis of density, ignition loss, and water content

Density (JAPAN INDUSTRIAL STANDARD 1999a), ignition loss (JAPAN INDUSTRIAL STANDARD 1999b), and water content (JAPAN INDUSTRIAL STANDARD 2000) of the sediments were determined according to methods described by the Japan Industrial Standard. The methods are as follows.

To measure density, refrigerated samples were air-dried overnight, and then the air-dried samples were ground with a mortar and pestle. The sediment powder was transferred to a pycnometer, and distilled water to approximately two-thirds of the total pycnometer volume was added. The pycnometer was warmed in a vessel containing hot water, bubbles in the

pycnometer were removed, and then the pycnometer was removed from the hot water and left at room temperature. Distilled water was added until the pycnometer was full. Then the pycnometer was weighed on an analytical balance (m_b g), and the temperature of its contents was recorded (T °C). The sample was then removed from the pycnometer and dried overnight at 110 °C in a dryer. Dried samples were cooled in a desiccator at room temperature and then weighed on an analytical balance (m_s g). The density of the sediment was calculated as follows:

$$\rho_s = m_s / [m_s + (m_a - m_b)] \times \rho_w(T) \quad (1)$$

where ρ_s is the sediment density (g/cm^3), m_a is the weight of the pycnometer containing a full volume of distilled water without the sediment (g), and ρ_w (T) is the density of distilled water at T °C (g/cm^3).

To measure water content, refrigerated samples were weighed on an analytical balance (m_c g) and then dried overnight in a dryer at 110℃. After the dried samples had cooled in a desiccator to room temperature, they were weighed on an analytical balance (m_d g). The water content in a sediment sample (w %) was calculated as follows:

$$w = [(m_c - m_d)/m_d] \times 100 \quad (2)$$

To measure ignition loss, refrigerated samples were placed in a crucible and dried overnight in a dryer at 110 °C. Dried samples were cooled in a desiccator to room temperature and weighed on an analytical balance (m_e g). Then, the samples were heated at 800 °C in an electric furnace for 6 h, cooled in a desiccator to room temperature, and weighed on an analytical balance (m_f g). Ignition loss in the sediment sample (L_i %) was calculated as follows:

$$L_i = [(m_e - m_f)/m_e] \times 100 \quad (3)$$

Humid density (H_d g/cm^3) was calculated as follows:

$$H_d = 1/[w/100 + (1-w)/100/\rho_s] \quad (4)$$

Interstitial water (I_r %) was calculated as follows:

$$I_r = w / 100 \times H_d \quad (5)$$

Cumulative weight (C_w g/cm^2) was calculated as follows:

$$C_w = (100 - I_r)/100 \times \rho_s \times d_p \quad (6)$$

where d_p is depth of the sample (cm)

2.3. Analysis of ^{210}Pb and ^{137}Cs concentrations

^{210}Pb and ^{137}Cs activities in samples were determined by the methods of MATSUMOTO (1986). Briefly, refrigerated samples were weighed on an analytical balance, air-dried overnight, and ground with a mortar and pestle. The sediment powder was transferred to a crucible and then ignited in an electric furnace.

Lead from the ignited sediment samples was dissolved in nitric acid in an Erlenmeyer flask. The lead solutions were filtered, and lead sulfate was extracted from the filtered lead solution by electrodeposition. The extracted lead sulfate was allowed to stand for 40 days, and then the β-emitter (^{210}Bi, 1.1 MeV) in lead sulfate was measured for 24 h with a low-background gas-flow counter (β-spectrometry; OXFORD, Lb4100-W). ^{210}Pb concentrations were corrected by using the count of the β-emitter standard (712 Bq, Japan Radioisotope Association) for ^{210}Pb.

In addition to ^{210}Pb derived from ^{222}Rn in air, ^{210}Pb is also found in sediment (supported ^{210}Pb). Supported (background) ^{210}Pb is a decay product of the ^{226}Ra found in water and sediment not including ^{210}Pb in the suspended sediments that settled from the sea surface to the sea floor. Accordingly, excess ^{210}Pb (^{210}Pb ex) was calculated as total ^{210}Pb - supported ^{210}Pb. Here, background ^{210}Pb concentrations (supported ^{210}Pb) were calculated by averaging the ^{210}Pb concentrations in sediments from depths of 16–30, 34–36, 38–40, 44–46, 48–50, 62–64, and 76–78 cm.

The sedimentation rate of cumulative weight Sr was calculated as follows:

$$S_r = (0.693/22.2)/|S| \quad (7)$$

where S is the slope of the line describing the relationship between log ^{210}Pb ex and cumulative weight (Fig. 2; −0.278). 0.693 is a disintegration coefficient of ^{210}Pb. 22.2 (year) is a half-life of ^{210}Pb.

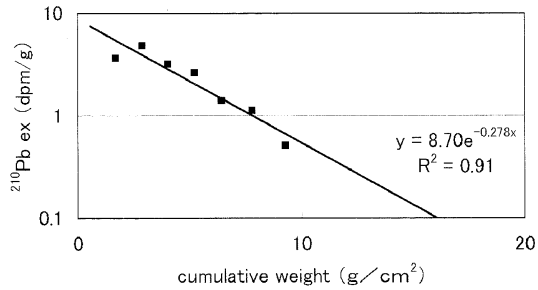

Fig. 2. Relationship between cumulative weight and ^{210}Pb ex in the sediment core collected off Ishinomaki in Sendai Bay. ^{210}Pb ex was calculated as the ^{210}Pb activity concentration of each 2-cm sediment sample less the average ^{210}Pb activity (0.63 ± 0.017 dpm/g) of sediments at depths of 16–30, 34–36, 38–40, 44–46, 48–50, 62–64, and 76–78 cm (used as the background or supported activity).

^{137}Cs (662 keV) in air-dried sediments was also measured with a low-background gas-flow counter (γ-spectrometry; EG & G ORTEC, GMX-25190) and corrected by the count of the γ-emitter standard (mixture of ^{109}Cd, ^{57}Co, ^{139}Ce, ^{51}Cr, ^{85}Sr, ^{137}Cs, ^{54}Mn, ^{88}Y, ^{60}Co, Japan Radioisotope Association) for ^{137}Cs.

2.4. Analysis of PCDDs, PCDFs, and Co-PCBs (dioxins)

Concentrations of polychlorinated dibenzo-*p*-dioxins (PCDDs) and polychlorinated dibenzofurans (PCDFs) with 4-8 chlorine substitutions and those of coplanar polychlorinated biphenyls (Co-PCB) congeners in the sliced surface sediment samples were determined by the method of the Environmental Agency (MINISTRY OF THE ENVIRONMENT 2000), as in the previous study (OKUMURA *et al.* 2004).

The detection limits for the tetra-, penta-, hexa-, hepta-, and octachlorinated PCDD/F congeners in the samples were 1, 1, 2, 2, and 5 pg/g dry weight (dw), respectively. The detection limits of Co-PCBs in the samples were 1 pg/g dw. We observed that the concentrations of the congeners were lower than the detection limits in the blank test.

3. Results and Discussion

3.1. History of the sediment core determined from ^{210}Pb and ^{137}Cs activities

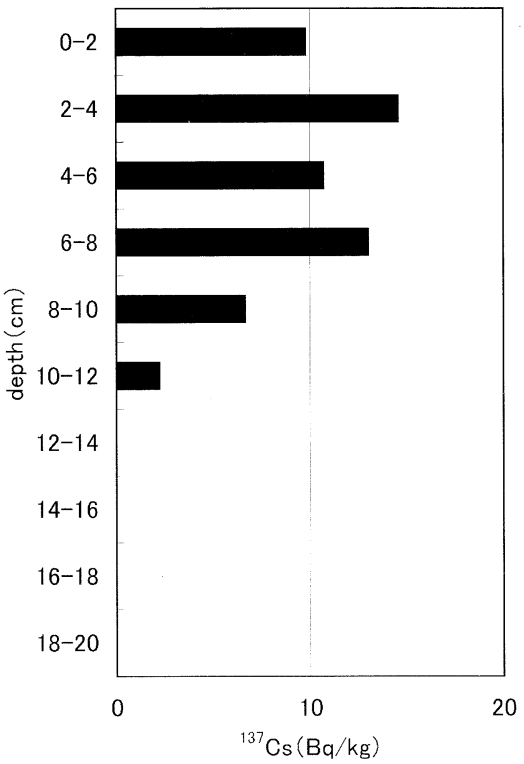

Fig. 2. Vertical distribution of ^{137}CS activity in the sediment core.

^{210}Pb ex values decreased from 2 to 16 cm depth and were significantly correlated with cumulative weight ($r^2 = 0.91$, $p < 0.05$; Fig. 2). We therefore interpreted the layer from 2 to 16 cm depth as not mixed. The sedimentation rate in the layer was calculated from the relationship between cumulative weight and ^{210}Pb ex as 0.112 g cm $^{-2}$ year $^{-1}$ (Eq. 7).

^{137}Cs activity was detected at 10-12 cm depth and above (Fig. 3). Two peaks were observed, at 2-4 and at 6-8 cm depth, and from 2 to 8 cm depth, the activity was higher than 10 Bq/g. We attributed the first ^{137}Cs activity, at 10–12 cm depth, to the detonation of atomic bombs at Hiroshima and Nagasaki in 1945 and to early nuclear testing (e.g., at Bikini Atoll in 1954); thus, we considered the sediments at 10–12 cm depth to have been deposited from the mid-1940s to the early-1950s. We attributed the peak in ^{137}Cs activity at 6–8 cm depth to atmospheric nuclear testing carried out during the 1960s and thus dated those sediments to

Table 1 Properties of the sediment core (0–60cm depth) from off Ishinomaki.

depth (cm)	avarage age (year)	mean date (date)	period of age (years)	time of deposition (date range)	sediment density (g/cm^3)	water content (%)	ignition loss (%)	humid density (g/cm^3)	interstitial water (%)	cumulative (g/cm^2)
					equation1	equation2	equation3	equation4	equation5	equation6
0– 2	4.9	1997	9.7	2002–1992	2.54	59	7.2	1.33	78.51	0.55
2– 4	15.1	1986	10.7	1992–1981	2.54	56	7.5	1.36	76.38	1.69
4– 6	25.5	1976	10.2	1981–1971	2.50	57.5	7.8	1.34	77.18	2.86
6– 8	35.8	1966	10.4	1971–1961	2.51	56.9	7.7	1.35	76.83	4.01
8–10	46.2	1955	10.5	1961–1950	2.60	56.7	7.4	1.36	77.28	5.19
10–12	57.1	1944	11.3	1950–1939	2.53	54.2	7.1	1.38	74.95	6.41
12–14	69.2	1932	13.0	1939–1926	2.54	49.5	6.9	1.44	71.33	7.77
14–16	82.5	1919	13.6	1926–1912	2.53	47.7	6.7	1.46	69.77	9.26
16–18	95.9	1906	13.1	1912–1899	2.60	49.4	6.7	1.45	71.76	10.76
18–20	109.0	1893	13.1	1899–1886	2.52	49.1	6.6	1.44	70.88	12.23
20–22					2.54	48	6.6	1.46	70.07	13.73
22–24					2.57	47	6.2	1.48	69.52	15.27
24–26					2.57	48.5	6.4	1.46	70.78	16.81
26–28					2.53	47.1	6.2	1.47	69.28	18.34
28–30					2.59	47.5	6.2	1.48	70.08	19.89
30–32					2.50	43.6	5.8	1.51	65.90	21.52
32–34					2.58	45.5	5.8	1.50	68.28	23.19
34–36					2.56	47.1	6	1.48	69.52	24.78
36–38					2.64	47.6	6	1.48	70.56	26.34
38–40					2.59	49.9	6.8	1.44	72.06	27.84
40–42					2.55	47.2	6.3	1.47	69.54	29.34
42–44					2.50	47.2	6	1.46	69.11	30.89
44–46					2.57	48.3	6.3	1.46	70.60	32.42
46–48					2.58	48.6	6.2	1.46	70.93	33.93
48–50					2.50	46.3	6.1	1.48	68.32	35.47
50–52					2.54	46.7	6.1	1.48	68.97	37.05
52–54					2.50	48.2	6.1	1.45	69.94	38.59
54–56					2.52	48.3	6.5	1.45	70.15	40.09
56–58					2.52	47.7	6.5	1.46	69.71	41.61
58–60					2.58	47.5	6.3	1.47	69.98	43.15

approximately that time. We related the peak at 2-4 cm depth to the accident at the Chernobyl nuclear power plant in 1986, so we interpreted those sediments to have been deposited in the 1980s.

Assuming that the sediment at 2–4 cm depth was deposited in 1987 [cumulative weight 1.69 g cm^{-2}; Fig. 2; sedimentation period from the surface, 15.1 years (1.69/0.112)], then the time of deposition of the sediment at 10–12 cm depth can be calculated as 1945 [cumulative weight 6.41 g cm^{-2}; Fig. 2; sedimentation period from the surface, 57.2 years (6.41/0.112); 1987−(57.2 −15.1)=1945] by using the sedimentation rate obtained from the ^{210}Pb activities. Thus, the periods of deposition determined from the ^{137}Cs activity peaks agree with those calculated by using the sedimentation rate determined from ^{210}Pb activities.

3.2. Sedimentation rate, water content, and ignition loss in Sendai Bay in comparison with those in other areas of Japan

The sedimentation rates off Ishinomaki and off Yamoto in Sendai Bay were 0.112 g cm^{-2} $year^{-1}$ (this study) and 0.314 g cm^{-2} $year^{-1}$ (OKUMURA *et al.* 2004), respectively. The sedimentation rate off Ishinomaki was approximately one-third that off Yamoto. Thus, the sedimentation rate in Sendai Bay varies by location. Various sedimentation rates have been reported for different parts of Japan by other studies (all values are expressed as g cm^{-2} $year^{-1}$) : 0.116 ±0.063 (n=5; average ±S.D.), Funka Bay near Hokkaido; 0.26±0.12 (n=3), Sakai-Izumi Port; 0.22 ± 0.17 (n=3),

Yokohama Port; 0.335 (n=1), Nagoya Port; 0.341 (n=1), Nagasaki Port; and 0.552 (n=2), Osaka Port (MINISTRY OF LAND, INFRASTRUCTURE AND TRANSPORT, GOVERNMENT OF JAPAN 2001); 0.2±0.091 (n=6), Harima-Nada (HOSHIKA *et al.* 1983); and 0.27±0.11 (n=7), Tokyo Bay, (FOUNDATION FOR PROMOTING PERSONAL MOBILITY AND ECOLOGICAL TRANSPORTATION 2001). Excluding values from Sendai Bay, the average sedimentation rate is 0.24 g cm^{-2} $year^{-1}$. The sedimentation rate off Ishinomaki was lower than this average and similar to that reported for Funka Bay.

The average water content of sediment from the surface to 60 cm depth off Ishinomaki in Sendai Bay was 49.46 ±3.9% (average ±S.D., Table 1). The value off Yamoto in Sendai Bay is 47.01 ±4.6% (OKUMURA *et al.* 2004). The average reported water content (%) of sediments from Nagoya, Osaka, Nagasaki, Yokohama, and Sakai-Izumi ports is 50.1±6.7, 58.6±7.9, 58.8±6.8, 59.5±10.2, and 63.1±5.0, respectively (MINISTRY OF LAND, INFRASTRUCTURE AND TRANSPORT, GOVERNMENT OF JAPAN 2001). The average water content of sediments from Sendai Bay (off Ishinomaki and Yamoto), less than 50%, is therefore lower than those of sediments from other Japanese ports.

The average ignition loss from the surface to 60 cm depth off Ishinomaki in Sendai Bay was 6.5 ±0.6% (average ±S.D., Table 1). That off Yamoto in Sendai Bay is 5.8 ±0.9% (OKUMURA *et al.* 2004). The average reported ignition loss (%) of sediments from Nagoya, Osaka, Sakai-Izumi, Yokohama, and Nagasaki ports is 6.8±2.1, 8.4±1.5, 8.3±0.8, 9.6±3.5, and 16.0 ±3.3, respectively (MINISTRY OF LAND, INFRASTRUCTURE AND TRANSPORT, GOVERNMENT OF JAPAN 2001). The average ignition loss, like the average water content, is lower in Sendai Bay than in other Japanese port sediments.

Water content and ignition loss are considered indicators of organic matter content. Because sediments in Sendai Bay had lower water content and ignition loss than those reported for sediments from other Japanese ports, the ratio of inorganic matter to organic matter in Sendai Bay sediments is inferred to be higher than that in sediments of other Japanese ports. We infer that inorganic suspended solids from rivers dominantly contributed to sedimentation in Sendai Bay.

3.3. Composition of dioxins in the sediment core

The average of total PCDDs in sediments at 0–4 cm depth (deposited from the early 1980s to 2002) accounted for 85% of the total dioxin concentration (Table 2). The dominant PCDD congeners were tetrachlorodibenzo-*p*-dioxin (1, 3, 6, 8-TeCDD), 1, 3, 7, 9-TeCDD, and octachlorodibenzo-*p*-dioxin (OCDD), which together accounted for 79% of the total PCDD concentration. PCDFs accounted for 5% of the total PCDD + PCDF concentration. Although Co-PCBs accounted for 10% of dioxins, PCB #118, the most abundant Co-PCB congener, accounted for 54% of the total Co-PCB concentration. PCB #105, the next most abundant Co-PCB congener, accounted for 19% of the total Co-PCB concentration. PCB #81 and PCB #169 concentrations were below the detection limit.

1, 3, 6, 8-TeCDD and 1, 3, 7, 9-TeCDD derive from impurities in chloronitrophen (CNP), and OCDD derives from impurities in pentachlorophenol (PCP), pesticides used from the 1960s to the 1990s (CNP) and to the 1970s (PCP) in Japan (YAMAGISHI *et al.* 1981, MASUNAGA *et al.* 2001a). Shipments of CNP products to Miyagi Prefecture, the so-called granary of Japan, were higher than those to any other prefectures in Japan during this period (JAPAN PLANT PROTECTION ASSOCIATION 1963–1995). It is clear that the major source of the dioxins deposited from the early 1980s to 2002 in Sendai Bay, as reported in this study as well as previously (OKUMURA *et al.* 2003, 2004), was impurities in CNP and PCP. However, the total shipment volume of CNP products was higher than that of PCP products in Miyagi Prefecture (JAPAN PLANT PROTECTION ASSOCIATION 1963-1995). Consistent with that observation, 1,3,6,8-TeCDD + 1,3,7,9-TeCDD concentrations in sediment of Sendai Bay reported previously by OKUMURA *et al.* (2003, 2004) were also higher than OCDD concentrations. However, it is difficult to explain why, in

Table 2. Dioxin concentrations in the sediment core sampled from off Ishinomaki in Sendai Bay.

	0–2cm 1997 (2002–1992)		2–4cm 1987 (1992–1981)			0–2cm 1997 (2002–1992)		2–4cm 1987 (1992–1981)	
	conc.	conc. */year	conc.	conc. */year		conc.	conc. */year	conc.	conc. */year
1368-TeCDD	330	34.0	420	39.3	12368/13478-PeCDF	N.D.	–	1	0.1
1379-TeCDD	150	15.5	210	19.6	12478-PeCDF	1	0.1	1	0.1
1378-TeCDD	1	0.1	1	0.1	12479/13467-PeCDF	N.D.	–	N.D.	–
1369/1247/1248-TeCDD	4	0.4	6	0.6	12467-PeCDF	N.D.	–	N.D.	–
1268-TeCDD	1	0.1	2	0.2	14678/12347-PeCDF	N.D.	–	N.D.	–
1237-TeCDD	N.D.	–	1	0.1	13469-PeCDF	N.D.	–	N.D.	–
1234/1246/1249/1238-TeCDD	4	0.4	4	0.4	12348/12378-PeCDF	1	0.1	1	0.1
1236/1279-TeCDD	2	0.2	2	0.2	12346-PeCDF	N.D.	–	N.D.	–
total TeCDDs	492	50.7	646	60.4	12379-PeCDF	N.D.	–	N.D.	–
12468/12479-PeCDD	17	1.8	21	2.0	12367-PeCDF	N.D.	–	N.D.	–
12368-PeCDD	59	6.1	76	7.1	12469/12678-PeCDF	N.D.	–	N.D.	–
12478-PeCDD	N.D.	–	1	0.1	12679-PeCDF	N.D.	–	N.D.	–
12379-PeCDD	23	2.4	27	2.5	12369-PeCDF	N.D.	–	N.D.	–
12469/12347-PeCDD	2	0.2	2	0.2	23468-PeCDF	4	0.4	5	0.5
12378-PeCDD	N.D.	–	1	0.1	12349-PeCDF	N.D.	–	N.D.	–
total PeCDDs	101	10.4	128	12.0	12489-PeCDF	N.D.	–	N.D.	–
123468/124679/124689-HxCDD	25	2.6	29	2.7	23478-PeCDF	N.D.	–	N.D.	–
123679/123689-HxCDD	13	1.3	15	1.4	12389-PeCDF	N.D.	–	N.D.	–
123678-HxCDD	3	0.3	3	0.3	23467-PeCDF	1	0.1	1	0.1
123469-HxCDD	N.D.	–	N.D.	–	total PeCDFs	9	0.9	13	1.2
123789-HxCDD	3	0.3	4	0.4	123468-HxCDF	2	0.2	3	0.3
123467-HxCDD	N.D.	–	N.D.	–	134678/134679-HxCDF	N.D.	–	2	0.2
total HxCDDs	44	4.5	51	4.8	124678-HxCDF	4	0.4	5	0.5
1234679-HpCDD	69	7.1	79	7.4	124679-HxCDF	N.D.	–	N.D.	–
1234678-HpCDD	48	4.9	49	4.6	123478/123479-HxCDF	3	0.3	2	0.2
total HpCDDs	117	12.1	128	12.0	123678-HxCDF	N.D.	–	N.D.	–
OCDD	590	60.8	600	56.1	124689-HxCDF	2	0.2	3	0.3
total PCDDs	1344	138.6	1553	145.1	123467-HxCDF	N.D.	–	N.D.	–
1368-TeCDF	N.D.	–	N.D.	–	123679-HxCDF	N.D.	–	N.D.	–
1378/1379-TeCDF	N.D.	–	N.D.	–	123469/123689-HxCDF	N.D.	–	N.D.	–
1347-TeCDF	N.D.	–	N.D.	–	123789-HxCDF	N.D.	–	N.D.	–
1468-TeCDF	N.D.	–	N.D.	–	123489-HxCDF	N.D.	–	N.D.	–
1247/1367-TeCDF	N.D.	–	N.D.	–	234678-HxCDF	N.D.	–	2	0.2
1348-TeCDF	N.D.	–	N.D.	–	total HxCDFs	11	1.1	17	1.6
1346/1248-TeCDF	N.D.	–	N.D.	–	1234678-HpCDF	10	1.0	11	1.0
1246/1268-TeCDF	N.D.	–	N.D.	–	1234679-HpCDF	N.D.	–	N.D.	–
1478/1369/1237-TeCDF	N.D.	–	N.D.	–	1234689-HpCDF	12	1.2	14	1.3
1678/1234-TeCDF	N.D.	–	N.D.	–	1234789-HpCDF	N.D.	–	N.D.	–
2468/1238/1467/1236-TeCDF	11	1.1	15	1.4	TOTAL HpCDF	22	2.3	25	2.3
1349-TeCDF	N.D.	–	N.D.	–	OCDF	19	2.0	20	1.9
1278-TeCDF	N.D.	–	N.D.	–	total PCDFs	72	7.4	90	8.4
1267/1279-TeCDF	N.D.	–	N.D.	–	total PCDD/Fs	1416	146.0	1643	153.6
1469-TeCDF	N.D.	–	N.D.	–	3,3',4,4'-TeCB(#77)	12	1.2	15	1.4
1249/2368-TeCDF	N.D.	–	N.D.	–	3,4,4',5-TeCB(#81)	N.D.	–	N.D.	–
2467-TeCDF	N.D.	–	N.D.	–	3,3',4,4',5-PeCB(#126)	1	0.1	1	0.1
1239-TeCDF	N.D.	–	N.D.	–	3,3',4,4',5,5'-HxCB(#169)	N.D.	–	N.D.	–
2347-TeCDF	N.D.	–	N.D.	–	total non-*ortho* PCBs	13	1.3	16	1.5
1269-TeCDF	N.D.	–	N.D.	–	2,3,3',4,4'-PeCB(#105)	27	2.8	40	3.7
2378-TeCDF	N.D.	–	N.D.	–	2,3,4,4',5-PeCB(#114)	1	0.1	2	0.2
2348-TeCDF	N.D.	–	N.D.	–	2,3',4,4',5-PeCB(#118)	81	8.4	110	10.3
2346-TeCDF	N.D.	–	N.D.	–	2',3,4,4',5-PeCB(#123)	6	0.6	5	0.5
2367-TeCDF	N.D.	–	N.D.	–	2,3,3',4,4',5-HxCB(#156)	10	1.0	17	1.6
3467-TeCDF	N.D.	–	N.D.	–	2,3,3',4,4',5'-HxCB(#157)	3	0.3	3	0.3
1289-TeCDF	N.D.	–	N.D.	–	2,3',4,4',5,5'-HxCB(#167)	5	0.5	7	0.7
total TeCDFs	11	1.1	15	1.4	2,3,3',4,4',5,5'-HpCB(#189)	2	0.2	4	0.4
13468-PeCDF	N.D.	–	N.D.	–	total mono-*ortho* PCBs	135	13.9	188	17.6
12468-PeCDF	2	0.2	4	0.4	total Co-PCBs	148	15.3	204	19.1
13678-PeCDF	N.D.	–	N.D.	–	total dioxins	1564	161.2	1847	172.6
13479-PeCDF	N.D.	–	N.D.	–	total TEQ	1.711	0.2	2.94	0.3

*: The average annual dioxin concentrations (conc./year) were calculated by dividing dioxins cancentration (conc.) by period of age of each layer in Table 1. The values of conc./year were rounded off to one decimal place.

this study, the 1,3,6,8-TeCDD + 1,3,7,9-TeCDD concentration in the sediment was the same as that of OCDD at 2–4 cm depth, and lower than that of OCDD at 0–2 cm.

Major sources of Co-PCBs are thought to be PCBs in electrical insulating oil (KANNAN *et al.* 1987, TAKASUGA *et al.* 1995) and in fly ash and exhaust gases from incinerators (CZUCZWA and HITES 1984, SAKAI *et al.* 1993). In Kanechlor, a PCB mixture used in Japan, PCB # 118 and PCB # 105 are the major congeners (TAKASUGA *et al.* 1995). Thus, the dominant Co-PCB congeners in sediments from Sendai Bay corresponded to those in this PCB product. PCB # 169, which is derived from combustion (YAO *et al.* 2002), was below the detection limit in sediments from Sendai Bay. From these findings, we infer that the major source of Co-PCBs in Sendai Bay from the early 1980s to 2002 was PCB products and that combustion was much less important.

3.4. Dioxin concentrations from the early 1980s to 2002

Dioxin concentrations in Sendai Bay increased from the mid-1930s and reached a maximum level in the 1987 (OKUMURA *et al.* 2004). However, accurate determination of dioxin concentrations in sediments from the late-1980s could not be measured in that study because the sediments from the late-1980s to 2002 were mixed. In this study, the average concentration in the 1992–2002 layer was 34.0 pg g^{-1} $year^{-1}$ for 1,3,6,8-TeCDD, 15.5 pg g^{-1} $year^{-1}$ for 1,3,7,9-TeCDD, 60.8 pg g^{-1} $year^{-1}$ for OCDD, and 161.2 pg g^{-1} $year^{-1}$ for total dioxins (Table 2). The values in the 1981-1992 layer were 39.3 pg g^{-1} $year^{-1}$ for 1,3,6,8-TeCDD, 19.6 pg g^{-1} $year^{-1}$ for 1,3,7,9-TeCDD, 56.1 pg g^{-1} $year^{-1}$ for OCDD, and 172.6 pg g^{-1} $year^{-1}$ for total dioxins.

Degradation of dioxins is thought to occur by sunlight or in anaerobic environments by aquatic microorganisms (SINKKONEN and PAASIVIRTA 2000). For example, the half-lives of dioxins in sediments are generally more than 100 years in the Baltic Proper (KJELLER and RAPPE 1995), about 35 years in Lake Shinji, Japan (MASUNAGA *et al.* 2001b), and 600 days in Lake Mendota,USA (CLAUDIA and MATSUMURA 1978). Although half-lives of dioxins vary with the aquatic environment or the specific congener, it is reasonable to suppose that fewer dioxins have been degraded in the 1992–2002 layer for the shorter residence time in the sediment than in the 1981-1992 layer. Despite the influence of degradation on the dioxin concentrations, the average annual concentration in the 1992-2002 layer was slightly lower than that in the 1981–1992 layer. In general, the dioxin sedimentation rate increased upward from the mid-1930s, reached a maximum in the mid-1980s, and then decreased slightly upward from the (OKUMURA *et al.* 2004) mid-1980s to 2002.

Shipments of CNP and PCP to Miyagi Prefecture were highest in 1975, when 4700 t of CNP products were shipped, and in 1970, when 3100 t of PCP products were shipped (OKUMURA *et al.* 2004). In 1970, the amount of PCBs used in Japan reached a maximum of 11,100 t (TATSUKAWA 1972). Therefore, the maximum concentrations of 1,3,6,8-TeCDD + 1,3,7,9-TeCDD, OCDD, and Co-PCBs in the sediment did not correspond in time to the peak period of shipments of CNP and PCP products or to the period of maximum use of PCBs (Table 1). Comparing our data with data collected elsewhere in Japan, the maximum concentration of TeCDDs, OCDD, and Co-PCBs in Lake Shinji (MASUNAGA *et al.* 2001b) and Tokyo Bay at 35°33′ N and 139°55′ E (YAO *et al.* 2002), and of total PCDD/Fs in Lake Biwa-South (SAKAI *et al.* 1999), were reported from sediments deposited before the 1980s. Although the timing of the peak period of shipments of CNP and PCP to each prefecture differed slightly, the maximum concentrations of TeCDD, OCDD, and Co-PCBs in these sediments tended to correspond to the peak period of shipments of CNP and PCP products and of PCB use. The time trends of dioxins in Lake Biwa and Tokyo Bay varied with the sampling site. The maximum concentration of OCDD in Tokyo Bay (35°35′ N and 139°55′ E) was reported from sediments deposited during 1979–1981 (YAMASHITA *et al.* 2000). The maximum concentrations of 1,3,6,8- and 1,3,7,9-TeCDD and total PCBs in Tokyo Bay at 35°35′ N and 139°55′ E (Yamashita *et al.* 2000) and the

maximum total PCDD/F concentrations in Lake Biwa-North and the Yodo River offshore region (SAKAI *et al.* 1999) were in sediments deposited after the 1980s. The maximum concentrations of dioxins in these sediments therefore did not correspond in time to the peak period of shipments of CNP and PCP products or of PCB use. The dioxin distribution in Sendai Bay most closely resembled the distributions at these latter sites.

Shipments of CNP and PCP to Miyagi Prefecture were higher weight than those to any other prefecture in Japan (OKUMURA *et al.* 2004). The period of maximum concentrations of 1,3,6,8-TeCDD + 1,3,7,9-TeCDD, OCDD, and Co-PCBs in the sediment of Sendai Bay did not correspond to the peak period of shipments of CNP and PCP products and of PCB use, but was later. It is possible that the dioxin sedimentation rate increased upward in the core. However, from this study, it is clear that the dioxin concentration per year in the 1992-2002 layer was slightly lower than that in the 1981-1992 layer. Dioxin concentrations in the sediment of Sendai Bay, as well as those in sediments elsewhere reported previously (SAKAI *et al.* 1999, Yamashita *et al.* 2000), may gradually decrease in the future. Although the degradation rate of dioxins in sediments of paddy fields and rivers in Miyagi Prefecture and in Sendai Bay is not clear, degradation may have an important role in decreasing dioxin concentrations in sediment of Sendai Bay.

Acknowledgments

This work (B-61) was made possible by a contribution from the project "Integrated Research Program on the Effects of Endocrine Disrupters on Agriculture, Forestry and Fisheries and their Action Mechanisms on Domestic Animals and Fishes" from the Agriculture, Forestry and Fisheries Research Council Secretariat, Ministry of Agriculture, Forestry and Fisheries, Japan.

References

CLAUDIA, T. W., and F. MATSUMURA (1978): Fate of 2,3,7,8-Tetrachlorodibenzo-*p*-dioxin in a model aquatic environment. Arch. Environ. Contam. Toxicol. 7, 349–357.

CZUCZWA, J. M., and R. A. HITES (1984): Environmental fate of combustion-generated polychlorinated dioxins and furans. Environ. Sci. Technol. **18**, 444–450.

FOUNDATION FOR PROMOTING PERSONAL MOBILITY AND ECOLOGICAL TRANSPORTATION (2001): The investigation of dioxins in ports. Tokyo, 93pp (in Japanese).

HANDA, N., and K. OHTA (1983): Sedimentary record of polycyclic aromatic hydrocarbon pollution in Tokyo Bay. Geochemical J., **16**, 60–67 (in Japanese).

HOSHIKA, A., T. SHIOZAWA, and E. MATSUMOTO (1983): Sedimentation rate and heavy metal pollution in sediments in Harima Nada (Harima Sound), Seto Inland Sea. J.Oceanogr. Soc. Japan., **39**, 82–87 (in Japanese).

JAPAN INDUSTRIAL STANDARD (1999a): Test method for density of soil particles. JISA1202.

JAPAN INDUSTRIAL STANDARD (1999b): Test method for water content of soils. JISA1203.

JAPAN INDUSTRIAL STANDARD (2000): Test method for ignition loss of soils. JISA1226.

JAPAN PLANT PROTECTION ASSOCIATION (1963-1995): The shipments of agricultural chemicals. *In* Agricultural chemicals Handbook. Japan Plant Protection Association (ed.), Tokyo (in Japanese).

KANAI, Y., Y. INOUCHI, M. YAMAMURO and T. TOKUOKA (1997): Sedimentation rate and environment in Lake Shinji, Shimane Prefecture. Geochemistry, **32**, 71–85 (in Japanese).

KANNAN, K., S. TANABE, T. WAKIMOTO, and R. TATSUKAWA (1987): A simple method for determining non-*ortho* PCB substituted PCBs in Kanechlors, Aroclors and environmental samples. Chemosphere, **16**, 1631–1634.

KANNAN, K., D. L. VILLENEUVE, N. YAMASHITA, T. IMAGAWA, S. HASHIMOTO, A. MIYAZAKI and J. P. GIESY (2000): Vertical profiles of dioxin-like and estrogenic activities associated with a sediment core from Tokyo Bay, Japan. Environ. Sci. Technol., **34**, 3568–3573.

KJELLER, L.O. and RAPPE, C. (1995): Time trends in levels, patterns, and profiles for polychlorinated dibenzo-*p*-dioxins, dibenzofurans, and biphenyls in a sediment core from the Baltic Proper. Environ. Sci. Technol. **29**, 346–355.

MASUNAGA, S., S. TAKASUGA and J. NAKANISHI (2001a): Dioxin and dioxin-like PCB impurities in some Japanese agrochemical formulations. Chemosphere, **44**, 873–885.

MASUNAGA, S., Y. YAO, I. OGURA, S. NAKAI, Y. KANAI, M. YAMAMURO and J. NAKANISHI, (2001b): Identifying sources and mass balance of dioxin pollution in Lake Shinji Basin, Japan. Environ. Sci. Technol., **35**, 1967–1973.

MATSUMOTO, E. (1983): The sedimentary

environment in Tokyo Bay. Geochemistry, **17**, 27–32 (in Japanese).

MATSUMOTO, E. (1986): The measurement of sedimentation rate in sediments. *In* Manual of Investigation of the Coastal Environment. The Oceanographic Society of Japan (ed.), p. 37–42 (in Japanese).

MATSUMOTO, E. and S. YOKOTA (1978): Accumulation rate and heavy metal pollution in Osaka Bay sediments. J.Oceanogr. Soc. Japan., **34**, 108–115 (in Japanese).

MINISTRY OF THE ENVIRONMENT (2000): Manual of the investigation of dioxins in sediments. Tokyo (in Japanese).

MINISTRY OF LAND, INFRASTRUCTURE AND TRANSPORT, GOVERNMENT OF JAPAN (2001): The investigation of endocrine disrupting chemicals in ports. Waterfront Vitalization and Environment Research Center (ed), Tokyo, 259pp (in Japanese).

OKUMURA, Y., Y. YAMASHITA and S. ISAGAWA (2003): Sources of polychlorinated dibenzo-*p*-dioxins (PCDDs), polychlorinated dibenzofurans (PCDFs), and coplanar polychlorinated biphenyls (Co-PCBs), and their bioaccumulation through the marine food web in Sendai Bay, Japan. J. Environ. Monit., **5**, 610–618.

OKUMURA, Y., Y. YAMASHITA, Y. KOHNO and H. NAGASAKA (2004): Historical trends of PCDD/Fs and Co-PCBs in a sediment core collected in Sendai Bay, Japan. Wat. Res., **16**, 3511–3522.

SAKAI, S., M. HIRAOKA, N. TAKEDA and K. SHIOZAKI (1993): Coplanar PCBs and PCDDs/PCDFs in municipal waste incineration. Chemosphere, **27**, 233–240.

SAKAI, S., S. DEGUCHI, S. URANO, H. TAKATSUKI and K. MEGUMI (1999): Time trends of PCDDs/Fs in Lake Biwa and Osaka Bay (in Japanese). J. Environ. Chem., **9**, 379–390.

SINKKONEN, S. and J. PAASIVIRTA (2000): Degradation half-life times of PCDDs, PCDFs and PCBs for environmental fate modeling. Chemosphere, **40**, 943–949.

TAKADA, H. (1997): Fluxes of land-derived materials to Japanese coastal zones. Bull. Coastal Oceanogr., **34**, 111–117 (in Japanese).

TAKASUGA, T., T. INOUE and E. OHI (1995): All congener specific analytical method for polychlorinated biphenyls (PCBs) with various chromatographic clean-up and HRGC/HRMS. J. Environ. Chem., **5**, 647–675 (in Japanese).

TANIMOTO, T. and A. HOSHIKA (1994): Settling velocity of suspended particles in Osaka Bay and Etauchi Bay. Oceanography in Japan, **3**, 13–20. (in Japanese)

TATSUKAWA, R. (1972) : PCB pollution. P.P.M., **8**, 43–52. (in Japanese).

YAMAGISHI, T., T. MIYAZAKI, K. AKIYAMA, M. MORITA, J. NAKAGAWA, S. HORII and S. KANEKO (1981): Polychlorinated dibenzo-*p*-dioxins and dibenzofurans in commercial diphenyl ether herbicides, and in freshwater collected from the application area. Chemosphere, **10**, 1137–1144.

YAMASHITA, N., K. KANNAN, T. IMAGAWA, D. L. VILLENEUVE, S. HASHIMOTO, A. MIYAZAKI and J. P. GIESY (2000): Vertical profile of polychlorinated dibenzo-*p*-dioxins, dibenzofurans, naphthalenes, biphenyls, polycyclic aromatic hydrocarbons, and alkylphenols in a sediment core from Tokyo Bay, Japan. Environ. Sci. Technol., **34**, 3560–3567.

YAO, Y., S. MASUNAGA, H. TAKADA and J. NAKANISHI (2002): Identification of polychlorinated dibenzo-*p*-dioxin, dibenzofurans, and coplanar polychlorinated biphenyl sources in Tokyo Bay, Japan. Environ. Toxicol. Chem., **21**, 991–998.

Received December 9, 2004
Accepted August 19, 2005

La mer 43 : 43–48, 2005
Société franco-japonaise d'océanographie, Tokyo

Assessment of fine-scale parameterization of deep ocean mixing using a new microstructure profiler

Kanako YOKOTA*, Toshiyuki HIBIYA*, Maki NAGASAWA*, and Shogo TAKAGI**

Abstract : Although global mapping of deep ocean mixing is essential for accurate modeling of global overturning circulation, each direct measurement using a microstructure profiler takes at least several hours so that it is difficult to extend it to the whole basin. To overcome this difficulty, some kind of empirical formula which can predict diapycnal diffusivity in terms of fine-scale parameters is desirable. In the present study, we carried out direct measurements of dissipation rates in the deep ocean at four locations (38°N, 31°N, 28°N, and 22.4°N) on the ship track from Dutch Harbor (the Aleutian Islands) to Honolulu using TurboMAP-D1 (the first domestic microstructure profiler for the deep ocean) to examine the validity of GREGG's empirical formula (GREGG, 1989), one of the most widely used fine-scale parameterization. The dissipation rates directly measured by TurboMAP-D1 were compared with those estimated by incorporating XCP data into GREGG's empirical formula. We find that GREGG's empirical formula tends to overestimate the dissipation rates except at 38°N, although the depth profiles of the dissipation rates are relatively well reproduced. It turns out that the empirical formula proposed by HENYEY *et al.* (1986) which takes into account latitudinal dependence provides much better fit to the directly measured dissipation rates. This warns us that dissipation rates in the deep ocean predicted using GREGG's empirical formula might exhibit spurious latitudinal distribution.

Keywords : *energy dissipation rates, deep ocean mixing, microstructure profiler, fine-scale parameterization*

1. Introduction

The climate is formed through the interactions among the atmosphere, oceans, and land surfaces. One cycle of global ocean overturning circulation is about 1500 years. To predict the long-term climate change, it is absolutely necessary to construct an accurate global overturning circulation model.

In the equilibrium state of the interior ocean, the structure of internal wave field whose vertical scales range from 10 km to 10 m is known to be well described by the GARRETT-MUNK model spectra (GARRETT and MUNK, 1975; CAIRNS and WILLIAMS, 1976). The energy supplied from winds and tides at large scales cascades down to small scales to induce deep ocean mixing. Turbulent mixing in the lower thermocline, in particular, plays an important role in transferring heat from the sea surface down to the deep ocean, reducing the density of cold deep waters and hence causing upwelling of them. Although global mapping of deep ocean mixing is essential for accurate modeling of overturning circulation, each direct measurement using a microstructure profiler takes, at least, several hours so that it is difficult to extend it to the whole basin. To overcome this difficulty, some kind of empirical formula is desired to predict diapycnal diffusivity in terms of fine-scale parameters which are much easier

*Department of Earth and Planetary Science, Graduate School of Science, The University of Tokyo, Tokyo 113–0033, JAPAN
**Faculty of Fisheries, Hokkaido University, Hakodate 041–8611, JAPAN

Corresponding Author's
E-mail: kanako@eps.s.u-tokyo.ac.jp

to observe.

Turbulent mixing in the deep ocean is thought to be strongly linked with the intensity of fine-scale vertical shear as well as density stratification. Since the distribution of fine-scale vertical shear and density stratification can be measured over a large area even within a limited available ship time using expendable current profilers (XCPs) and expendable conductivity, temperature, and depth profilers (XCTDs), global mapping of diapycnal diffusivity becomes possible so long as the reliable empirical formula is available.

Among the existing parameterization, "GREGG's empirical formula" (GREGG, 1989) is most widely used. GREGG's empirical formula is originally based on the results of eikonal calculations by HENYEY *et al.* (1986) given by

$$\langle \epsilon \rangle = F(f, N) \left\langle \frac{N^2}{N_0^2} \right\rangle \left\langle \frac{S_{10}^4}{S_{GM}^4} \right\rangle \quad [\mathrm{Wkg}^{-1}] \quad (1)$$

$$\text{with} \quad F(f, N) = 8.1 \times 10^6 f N_0^2 \cosh^{-1}\left(\frac{N}{f}\right)$$

where $\langle\ \rangle$ denotes the average over large spatial and temporal scales; ϵ is the dissipation rates of turbulent kinetic energy; f is the Coriolis parameter; N_0=3 cycles per hour (cph) is a reference buoyancy frequency; S_{10} is the 10 m scale vertical shear; S_{GM} is the corresponding vertical shear in the GARRETT and MUNK internal wave field (GARRETT and MUNK, 1975; CAIRNS and WILLIAMS, 1976). It should be noted that, because of the f dependence of the relationship (1), the predicted energy dissipation rate diminishes as the latitude decreases (see Figure 1 of GREGG *et al.*, 2003).

GREGG (1989) carried out simultaneous measurements of turbulent energy dissipation rates (ϵ) and 10 m-scale vertical shear (S_{10}) at six locations between 11.5° N and 42° N off both coasts of the continental United States. Although these microstructure measurements were limited to, at most, the top 950 m, insufficient to assess the parameterization of deep ocean mixing, he found no appreciable latitudinal dependence of ϵ and showed that the best fit to the observed vertical profile of ϵ was attained by reducing the relationship (1) to

Table 1 : The locations of microstructure measurements.

		Latitude	Longitude
2003 August Hawaii	St.1	38.00N	165.00W
	St.2	31.00N	162.84W
	St.3	28.00N	160.59W
	St.4	22.40N	158.45W

$$\langle \epsilon \rangle = 2 \times F(f_{34^\circ}, N_0) \left\langle \frac{N^2}{N_0^2} \right\rangle \left\langle \frac{S_{10}^4}{S_{GM}^4} \right\rangle [\mathrm{Wkg}^{-1}] \quad (2)$$

In the present study, based on the microstructure data from the surface down to well below the thermocline obtained using the first domestic microstructure profiler for the deep ocean, we examine the validity of the GREGG's empirical formula (2). First, we carried out direct measurements of dissipation rates down to a depth of ~1600 m on the ship track from Dutch Harbor (the Aleutian Islands) to Honolulu. Then, the directly measured dissipation rates were compared with the dissipation rates estimated by incorporating XCP data into GREGG's empirical formula.

2. Observations

The field experiments were carried out at four locations listed in Table 1 on the ship track of Oshoro-Maru, the training vessel of the Faculty of Fisheries of Hokkaido University in August 2003 (Figure 1). During the cruise, we measured energy dissipation rates using TurboMAP-D1, buoyancy frequency using XCTDs, and vertical shear using XCPs. During each microstructure measurement, we deployed three sets of XCPs and XCTDs.

The instrument package called TurboMAP-D1 (about 2 m long with diameter 0.3 m; see Figure 2) is a free-rising, internally recording, first domestic microstructure profiler for the deep ocean with a shear probe, an FP07 (temperature sensor), a pressure sensor, and an accelerometer which can measure turbulent parameters ($\frac{\partial u}{\partial z}$ and $\frac{\partial T}{\partial z}$) as well as hydrographic parameters (temperature and depth). The accuracy of the shear probe is ±5% with a resolution of 10^{-4} s^{-1}, while the accuracy of FP07 is 0.01℃ with a resolution of 10^{-4}℃. TurboMAP-

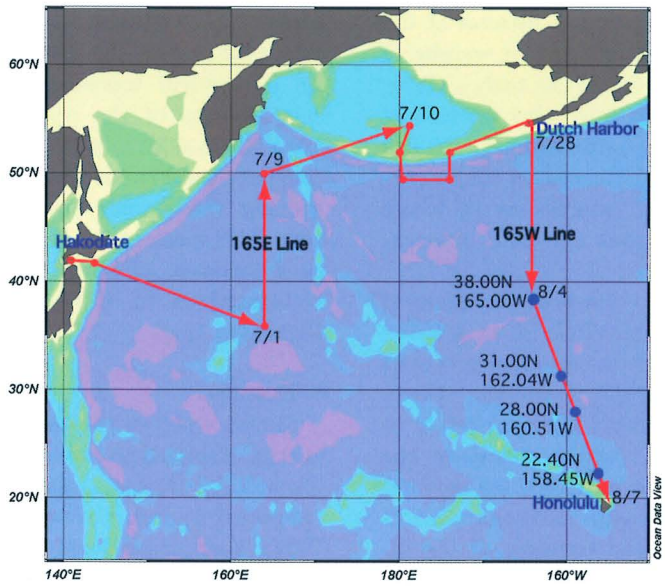

Figure 1 : The ship track of Oshoro-Maru and the locations of field experiments.

Figure 2 : A view of TurboMAP-D1.

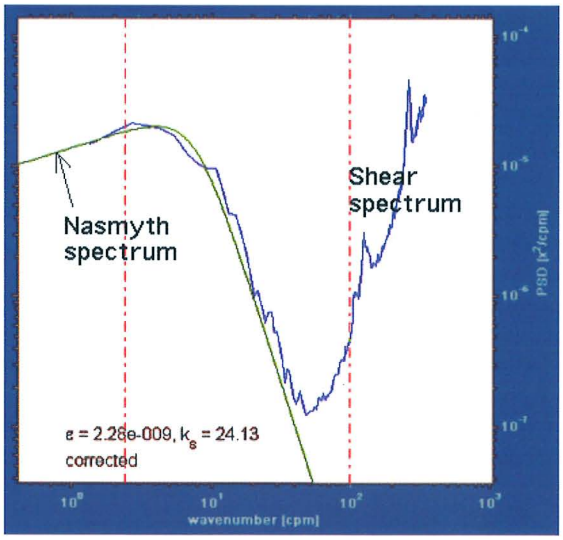

Figure 3 : The Nasmyth universal spectrum (green) corresponding to $\epsilon = 2.28 \times 10^{-9}$ Wkg^{-1} fitted to the observed shear spectrum (blue) for the vertical warenumber band shown by the two red dash-dot lines.

D1 weighs 73 kg in the air, but because of the syntactic foam on the main body, it weighs −1 kg in the water. To minimize the body's vibration thereby permitting low-noise turbulence measurements, a brush is attached near the end of the instrument. Also attached on the instrument is a pinger which enables us to locate TurboMAP-D1 throughout the field observation.

First, TurboMAP-D1 is lowered at a speed of 1.5 ms^{-1} using a winch. When it is lowered down to a depth of ~1600 m, the releaser works to separate TurboMAP-D1 from the winch. Then, TurboMAP-D1 starts uprising freely at a speed of ~0.4 ms^{-1} while recording the microscale vertical shear up to the sea surface. Each microstructure measurement takes about 120 minutes including the recovery of the instrument. Using the microscale shear data, we can calculate the local energy dissipation rates given by

$$\epsilon = \frac{15}{2}\nu\overline{\left(\frac{\partial u}{\partial z}\right)^2} \qquad (3)$$

where ν is the kinetic viscosity (OSBORN, 1980).

The raw data from TurboMAP-D1 is lowpass filtered. Then, the vertical shear spectrum is calculated using FFT. The FFT length is 512 points and 100 points are overlapped. Then, to give one spectrum for the various depth range, the spectrum for all the segments are averaged. The uncontaminated wavenumber range is determined excluding vertical wavenumbers $>10^2$ cpm where the instrumental noise is enhanced and several spikes caused by the instrument's pressure case occur. By fitting Nasmyth spectrum to the observed vertical shear spectrum (OAKEY, 1982), energy dissipation rate is evaluated (see Figure 3).

The XCP, on the other hand, is a free-fall instrument, which can measure horizontal velocity relative to a depth-independent constant from the sea surface down to a depth of ~1600 m by sensing the electric field induced by seawater's horizontal movement in the earth's magnetic field.

Using XCP data, the vertical wavenumber Froude spectra calculated for each depth bin are compared to the corresponding GM76 model (GARRETT and MUNK, 1975; CAIRNS and WILLIAMS, 1976). The spectrum is not meaningful at vertical wavenumbers more than 0.04 cpm because of the uncorrelated instrument noise (NAGASAWA *et al.*, 2002). Therefore, we calculate the Froude number variance by integrating the Froude spectrum up to $k_z=0.04$ cpm. This means that, instead of S_{10}, S_{25} is used as a measure of shear level at high vertical wavenumbers in GREGG's empirical formula (equation (2)).

3. Results

Figure 4 shows the comparison between the energy dissipation rates measured directly by TurboMAP-D1 (ϵ_{Turbo}) and the dissipation rates estimated by incorporating the XCP data into GREGG's empirical formula (ϵ_{Gregg}). We can see that GREGG's empirical formula tends to overestimate the dissipation rates except at 38° N, although the depth profiles of the dissipation rates are relatively well reproduced. This reminds us the fact that, although GREGG's empirical formula is essentially based on HENYEY's eikonal calculations (HENYEY *et al.* 1986), it does not take into account the dependence on latitudes.

Figure 5 shows the comparison between ϵ_{Turbo} and the dissipation rates estimated by incorporating the XCP data into the HENYEY *et al.*'s empirical formula (equation (1)) (ϵ_{HWF}). We can see that, compared to ϵ_{Gregg}, ϵ_{HWF} shows much better agreement with ϵ_{Turbo}. Table 2 shows vertically averaged ratio of ϵ_{Gregg} to ϵ_{Turbo} and that of ϵ_{HWF} to ϵ_{Turbo}. Obviously, ϵ_{Gregg} is overestimated at all the stations, whereas ϵ_{HWF} seems to be rather underestimated, ranging from $0.6\times\epsilon_{Turbo}$ to $1.1\times\epsilon_{Turbo}$.

4. Summary

In the present study, we have examined the validity of GREGG's empirical formula (GREGG, 1989), one of the most widely used fine-scale parameterization to predict energy dissipation rates in the deep ocean. First, we have carried out direct measurements of dissipation rates in the deep ocean at four locations (38° N, 31° N, 28° N, and 22.4° N) on the ship track from Dutch Harbor (the Aleutian Islands) to Honolulu using TurboMAP-D1, the first

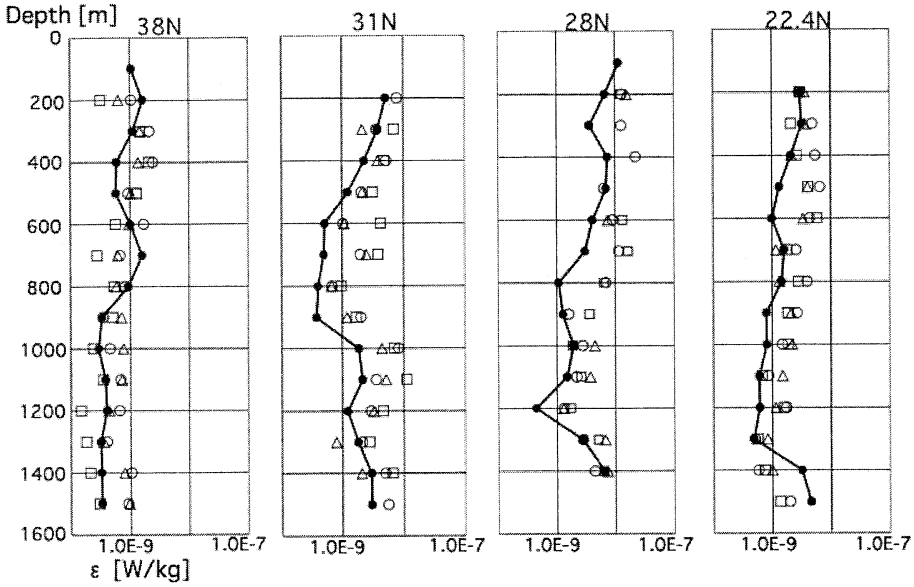

Figure 4 : Depth profile of energy dissipation rate ϵ at each location. The solid line shows ϵ_{Turbo}. Superimposed by circles, triangles and squares are ϵ_{Gregg} calculated using the data from the first, second and third XCP deployment, respectively.

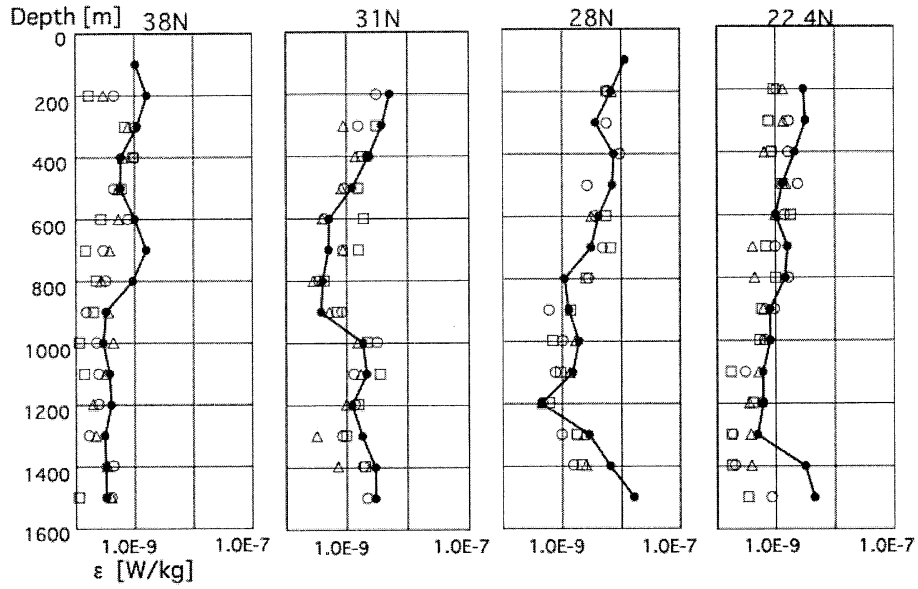

Figure 5 : As in Figure 4 but for the comparison between ϵ_{Turbo} and ϵ_{IIWF}.

domestic microstructure profiler which can reach down to a depth of ~1600 m. The dissipation rates directly measured by TurboMAP-D1 have been compared with the dissipation rates estimated by incorporating XCP data into GREGG's empirical formula.

We have found that GREGG's empirical formula tends to overestimate the energy dissipation rates except at 38° N, although the depth profiles of the dissipation rates are relatively

Table 2 : Comparison between the vertically averaged ratio of ϵ_{Gregg} to ϵ_{Turbo} and that of ϵ_{HWF} to ϵ_{Turbo}.

Latitude[°N]	$\epsilon_{Gregg}/\epsilon_{Turbo}$	$\epsilon_{HWF}/\epsilon_{Turbo}$
38	1.46	0.66
31	2.73	1.07
28	3.07	0.97
22.4	2.52	0.64

well reproduced. Much better agreement with the directly measured values has been attained using HENYEY *et al.*'s empirical formula which takes into account latitudinal dependence of dissipation rates in the deep ocean. This warns us that dissipation rates in the deep ocean predicted using GREGG's empirical formula might exhibit spurious latitudinal distribution.

The result of the present study is offered as an important contribution toward the global mapping of deep ocean mixing which is indispensable for accurate modeling of global thermohaline circulation.

Acknowledgments

The authors would like to express their gratitude to the captain, the officers and crews of T/V Oshoro-Maru of the Faculty of Fisheries of Hokkaido University for their help in collecting data.

References

CAIRNS, J. L., and G. O. WILLIAMS, 1976: Internal wave observations from a midwater float, 2. J. Geophys. Res., **81**, 1943–1950.

GARRETT, C. J. R., and W. H. MUNK, 1975: Space-time scales of internal waves: A progress report. J. Geophys. Res., **80**, 291–297.

GREGG, M. C., 1989: Scaling turbulent dissipation in the thermocline. J. Geophys. Res., **94**, 9686–9698.

GREGG, M. C., T. B. Sanford, and D. P. WINKEL, 2003: Reduced mixing from the breaking of internal waves in equatorial waters. Nature, **422**, 513–515.

HENYEY, F. S., J. A. WRIGHT, and S. M. FLÄTTE, 1986: Energy and action flow through the internal wave field. J. Geophys. Res., **91**, 8487–8495.

NAGASAWA, M., T. HIBIYA, Y. NIWA, M. WATANABE, Y. ISODA, S. TAKAGI and Y. KAMEI, 2002: Distribution of fine-scale shear in the deep waters of the North Pacific obtained using expendable current profilers. J. Geophys. Res., **107**, doi: 10.1029/2002JC001376.

OAKEY, N. S., 1982: Determination of the rate of dissipation of turbulent energy from simultaneous temperature and velocity shear microstructure measurements. J. Phys. Oceanogr., **12**, 256–271.

OSBORN, T. R. 1980: Estimates of local rate of vertical diffusion from dissipation measurements. J. Phys. Oceanogr., **10**, 83–89.

Received, July 5, 2005
Accepted, August 22, 2005

La mer 43 : 49-59, 2005
Société franco-japonaise d'océanographie, Tokyo

Deep Western Boundary Current along the eastern slope of the Kerguelen Plateau in the Southern Ocean: observed by the Lowered Acoustic Doppler Current Profiler (LADCP)

Yoshihiro NARUMI*, Yuji KAWAMURA**, Tomoko KUSAKA*, Yujiro KITADE* and Hideki NAGASHIMA*

Abstract : The Deep Western Boundary Current (DWBC) is considered to flow northwestward along the eastern slope of the Kerguelen Plateau in the Southern Ocean. SPEER and FORBES (1994) estimated the volume transport of DWBC at 6 SV (1SV=10^6 m^3/s) northwestward based on the assumption of a level of no motion at 2500 dbar depth. However, there is no evidence of an existence of such a level in the deep sea over the plateau. To clarify the transport of the current, we tried to observe the current profile by using the Lowered Acoustic Doppler Current Profiler (LADCP) and CTD at a section that crosses isobaths of the plateau. The cross sectional transport is estimated at 10 SV northwestward from the LADCP data, and is about 1.7 times larger than that by SPEER and FORBES (1994) . The geostrophic transport is estimated from the CTD data by adjusting a reference level in order that the total transport coincides with that calculated from the LADCP data. The baroclinic and barotropic transports are estimated at 5 SV southeastward and 15 SV northwestward, respectively.

Keywords *: LADCP, the Kerguelen Plateau, Deep Western Boundary Current (DWBC), Geostrophic Transport*

1. Introduction

The Antarctic Bottom Water (AABW) is produced around the Antarctica. The main three areas in which AABW is produced are considered to be the Weddell-Enderby Basin, the South Pacific Basin and the South Indian Basin. The origin of AABW in the South Indian Basin is recognized as the continental shelf and continental slope is located at the region off Adélie Land. The behavior of this water is influenced by topographical effect of ocean floor, e.g. the Princess Elizabeth Trough and the Kerguelen Plateau.

The AABW in the source region off the Adélie Land (ADLBW: Adélie Land Bottom Water) flows westward along the continental slope (e.g. MANTYLA and REID, 1995; ORSI *et al.*, 1999; BINDOFF *et al.*, 2000), and is prevented by the Princess Elizabeth Trough and some of this turn northwestward along the Kerguelen Plateau. SPEER and FORBES (1994) investigated the Deep Western Boundary Current (DWBC) along the eastern flank of the Kerguelen Plateau from its geostrophic shear and water mass properties. Then this water mass flows to the north of the Antarctic Divergence, and turns eastward due to the influence of the Antarctic Circumpolar Current (ACC) and some of this water forms recirculation (BINDOFF *et al.*, 2000). ORSI *et al.* (1999) also suggested these flow fields based on the horizontal density distribution of the Southern Indian Ocean. SPEER

* Department of Ocean Sciences, Tokyo University of Marine Science and Technology, 4-5-7 Konan, Minatoku, Tokyo 108-8477, Japan
** Present address: Center for Marine Environmental Studies, Ehime University, 2-5 Bunkyotyo, Matsuyama, Ehime 790-8577, Japan

Corresponding to Authors
Telephone: 03-5463-0380 FAX: 03-5463-0378 E-mail: od02109@edu.s.kaiyodai.ac.jp

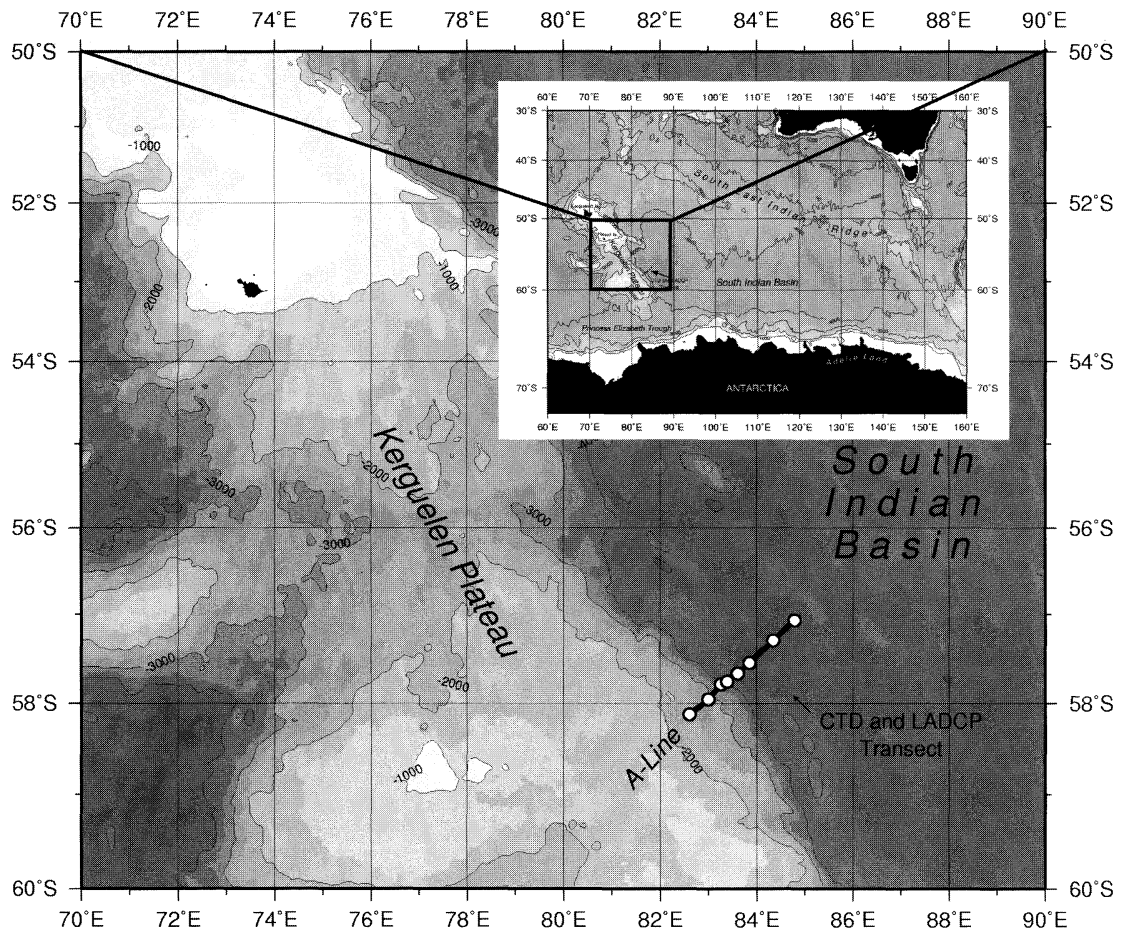

Fig. 1. Locations of CTD and LADCP observation stations (circles) along A-line (Bold line). Contour obtained from ETOPO2 bathymetric data are depicted every 1000 m. Numerals attached to contour stand for depth in m. Shaded areas show depth less than 500 m.

and FORBES (1994) estimated the geostrophic transport of bottom water at 6.0 SV northwestward from the hydrographic observation. The estimated geostrophic transport of DWBC is about 48.9 SV northwestward on the bases of LADCP referenced velocity (DONOHUE *et al.*, 1999). But they don't mention about the current profiles in detail. Thus, it is important that we investigate oceanographic structure and water properties at the region of the Kerguelen Plateau as a part of circulation of AABW at the Southern Indian Ocean.

We provided an observation line crossing the Kerguelen Plateau and carried out Conductivity–Temperature–Depth profilers (CTD) and Lowered Acoustic Doppler Current Profilers (LADCP) observations by Training and Research Vessel Umitaka-Maru in February 2003. In this paper we first describe water mass property from hydrographic data, and then current distribution by LADCP. Finally, we discuss the velocity field and transport of results and conclude with a brief summary.

2. DATA

Hydrographic observation points (Fig. 1) were provided along the line (A-Line) crossing the Kerguelen Plateau followed the study of SPEER and FORBES (1994). The T/R Vessel Umitaka-Maru departed from Port Luis on 3

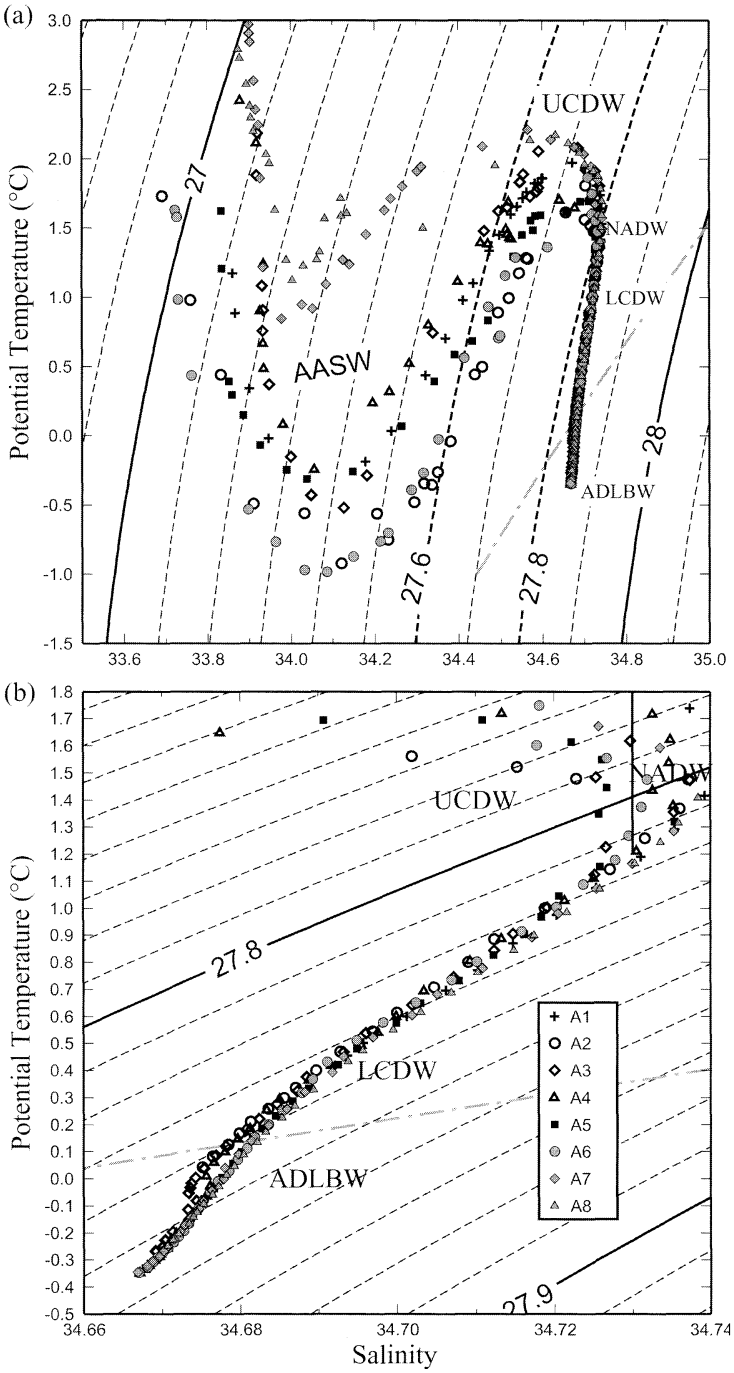

Fig. 2. Potential temperature (℃) −salinity relation of sea water for (a) whole water and (b) that for deep water. Each station is distinguished by a different symbol shown in the legend. The broken and solid lines indicate contours of constant potential density (σ_θ). Isopycnal of σ_θ=27.8 is the boundary of LCDW and UCDW, and follows the saltiest NADW (S>34.73: vertical solid line in (b)). Isopycnal of σ_θ=27.6 indicates the boundary of AASW and UCDW. Dash-dotted line indicates isopycnal of σ_4=46.04 as the boundary of LCDW and ADLBW (AABW).

January 2003, and arrived at the first observation point (Station A1) on 9 January. Observations from Station A1 to Station A8 were carried out for three days.

Temperature and salinity were measured by using Sea-Bird Electronics CTD. Salinity of bottle samples water were measured by using the Guildline AUTOSAL. Then, the conductivity sensor of CTD was calibrated against these bottle samples salinity data. Potential temperature (θ), density in situ (σ_t), potential density (σ_θ) and density at 4000 dbar (σ_4) were calculated from the pressure, the temperature and the calibrated salinity by using the equation of state, UNESCO (1981).

Ocean current velocity was measured by using LADCP, produced by RD Instruments, placed in the frame of CTD. The direction data of LADCP were corrected with International Geomagnetic Field Model 2000, because the current direction data measured by magnetic compass placed in LADCP have azimuth deviation from that by gyrocompass. Next, in order to minimize the effect of CTD motion, we got rid of the data when pitching or rolling is greater than 5 degree. Finally, zonal and meridional velocities are estimated by inverse solutions (VISBECK, 2000) every 20 dbar vertically.

3. Results

3.1 Water properties

Fig. 2 shows potential temperature-salinity relation for each station. The low salinity water covered the surface layer, are known as the Antarctic Surface Water (AASW) defined for the water properties of salinity (S) less than 34.0 with potential temperature (θ) $-1.84℃ < \theta < 2.00℃$ (BINDOFF *et al.*, 2000) or potential density (σ_θ) less than 27.6 (ORSI *et al.*, 1999). The cold AASW ($\theta < 0.5℃$) is found between Station A1 and Station A5, but not at Station A7 and Station A8; the difference between warmer and colder classes of AASW are easily seen on Fig. 2 (a) in the potential density ($27.2 < \sigma_\theta < 27.6$).

Below AASW, the warm and saline water mass that occupies most of the deep layers above the Antarctic Bottom Water (AABW) is the Circumpolar Deep Water (CDW). In the layer of CDW, the saltiest water (S>34.73) originated from the North Atlantic Deep Water (NADW) is found at all stations except at Station A5 as also shown in Fig. 3 (b). SPEER and FORBES (1994) suggested that the salinity field was dominated by the salinity maximum of old NADW. The isopycnal of σ_θ=27.79 (ORSI *et al.*, 1995; REID, 1989) or σ_θ=27.80-27.81 (HEYWOOD *et al.*, 1999) follows about the salinity maxima of the NADW that enters the ACC from the north in the southwestern Atlantic Ocean (REID, 1989). Water column is classified into the upper layer and the lower layer characterized Upper CDW (UCDW) and Lower CDW (LCDW), respectively (SPEER and FORBES, 1994). Details are shown in section 3.2.

Next, in bottom water, the Antarctic Bottom Water (AABW) whose salinity (S) is $34.65 < S < 34.72$ at potential temperature (θ) of $-0.4℃ < \theta < 0.0℃$ (BINDOFF *et al.*, 2000) and $\sigma_4 > 46.04$ (ORIS *et al.*, 1999) is distributed at all stations except Station A1. A little warmer and fresher water mass ($-0.1℃ < \theta < 0.5℃$) is located between Station A2 and Station A4 (near the Kerguelen Plateau) is different from that is located between Station A5 and Station A8 (near the South Indian Basin). This difference is due to the fact that the water of the shore region is fresher and warmer than that of the basin region. In contrast, the property is same in the deeper region from Station A2 to Station A8 at the potential temperature colder than $-0.1℃$.

RODMAN and GORDON (1982) indicated that the property of AABW in the eastern side of Kerguelen Plateau was different from that in the western side, and the potential source of Weddell Sea Bottom Water from the Weddell-Enderby Basin across the Princess Elisabeth Trough is negligible. The AABW whose salinity is lower than 34.68 formed off Adélie Land (ADLBW: Adélie Land Bottom Water) flows cyclonically along the southern and western rims of the South Indian Basin (MANTYLA and REID, 1995). ORSI *et al.* (1999) defined the bottom water the coldest and freshest ($\theta < -1.0$ ℃ and S<34.64) in the southwestern Weddell Sea, the warmest and saltiest ($-0.6℃ < \theta < 0.3$ ℃ and S>34.72) in the northwestern Ross Sea, and the intermediate properties ($-0.8℃ < \theta < -0.4℃$ and $34.62 < S < 34.68$) off the Adélie

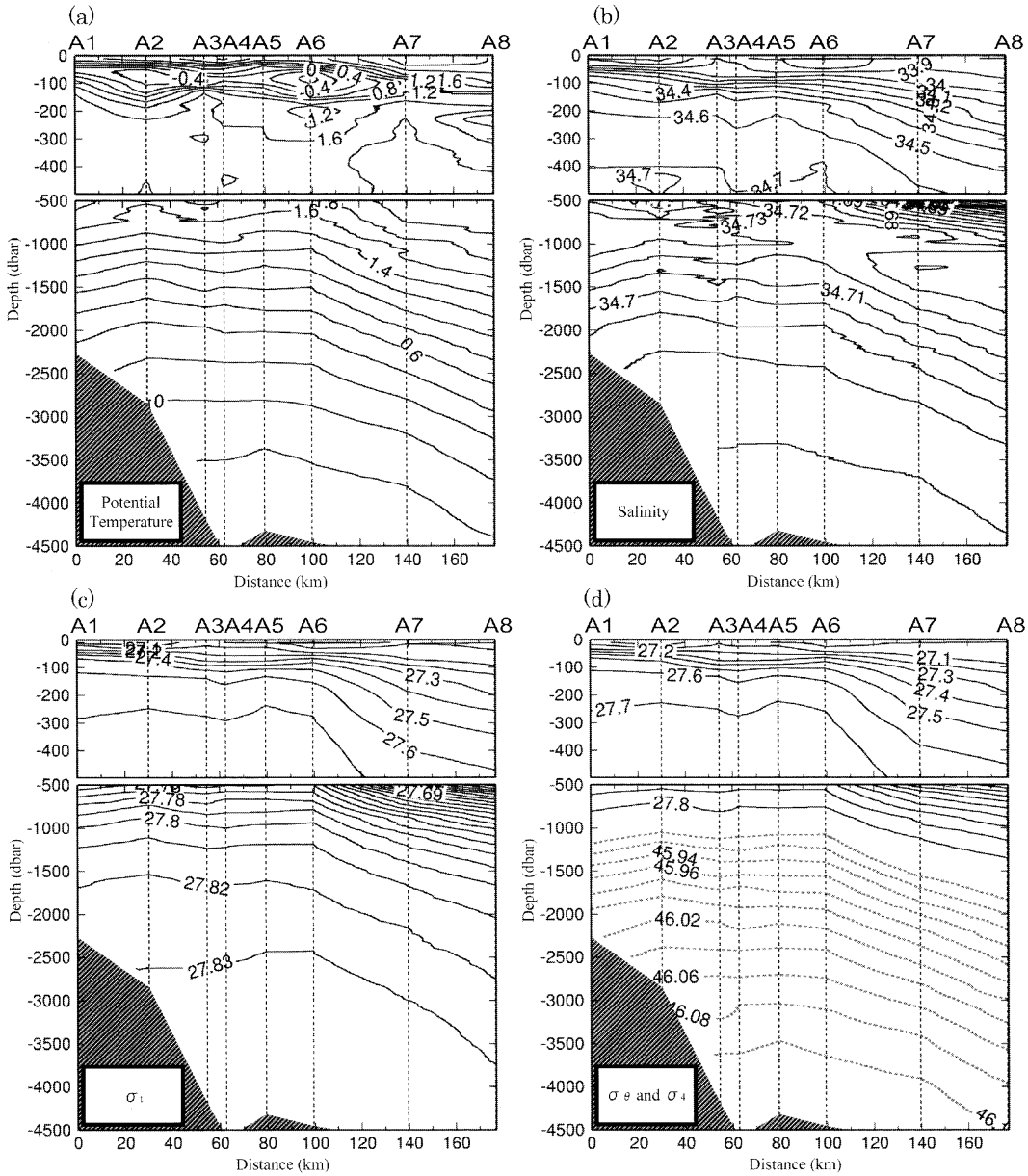

Fig. 3. Vertical sections of (a) potential temperature in ℃, (b) salinity, (c) σ_t and (d) σ_θ (solid lines) or σ_4 (dotted lines). Vertical broken lines indicate observation stations; station numbers are indicated above the plots.

Land (140°–150°E). The AABW in this observation indicates same properties of that off the Adélie Land (ADLBW) by ORSI *et al.* (1999). Moreover, BINDOFF *et al.* (2000) also defined that property of ADLBW was θ <0.5℃ at salinity 34.66<S<34.68, and the sea water is in the present study.

Comparing the properties of AABW in this observation with that in the previous observations mentioned above, there are slight differences in the water properties. ORSI *et al.* (1999) indicated that deep water properties in this

region was $\theta = -0.5$℃ and S>34.67 at the bottom. SPEER and FORBES (1994) also described that the deepest water properties converged on $\theta = -0.5$℃ and S=34.675 to the bottom. But the water property is a little warmer and saltier. SPEER and FORBES (1994) indicated that observed AABW was warmer and saltier than that of previous observation by GORDON *et al.* (1982) at the same density field below 0℃. Consequently, we compare the water properties by SPEER and FORBES (1994) (referred by their Fig. 5) with those in our observation (Fig. 2). In so far as what we compare these figures at the same density field below 0.0℃, the AABW in our observation is a little warmer and fresher than that by SPEER and FORBES (1994), and is almost similar to that by GORDON *et al.* (1982). SPEER and FORBES (1994) assumed the difference suggesting that the AABW sources varied along the southern boundary off the Antarctic as far east as the Ross Sea with the time scale of 20 years or less. Nevertheless their assumption remains a matter for speculation; the differences mentioned above are possible due to the historical changes.

3.2 Distribution of water mass

Fig. 3 shows vertical distribution of potential temperature, salinity, σ_t and σ_θ or σ_4. The water mass colder than 0.0℃ is distributed near 70dbar between Station A1 and Station A6 as shown in Fig. 3 (a). This water is the coldest in this region; the temperature is lower than −0.4℃ between Station A2 and Station A3, especially lower than −0.8℃ at Station A6. In addition, a couple of lens-like temperature structure exists about 70 dbar depth between Station A1 to Station A6. This coldest water is not distributed between Station A7 and Station A8. The contrast between two groups also can be clearly seen in Fig. 2 (a). The warmest water lies around 500 dbar depth. ORSI *et al.* (1995) described that at the position of the southern ACC front there is a distinct temperature gradient along the θ-maximum of the UCDW, as it shoals southward to near 500 dbar (θ>1.8℃). As the water property distribution is clearly different between Station A6 and Station A7, the existence of the southern ACC front is suggested.

The Kerguelen Plateau (70°-80° E) clearly obstructs the path of the southern ACC front and forces it farther to the south (ORSI *et al.*, 1999). East of the plateau, the southern ACC front turns sharply to the north forming a boundary current along its eastern flank (RODMAN and GORDON, 1982; SPEER and FORBES, 1994). Sparrow *et al.* (1996) suggested by Fine Resolution Antarctic Model (FRAM) that the southern ACC front moved northward along the eastern side of the Kerguelen Plateau to about 55° S. ORSI *et al.* (1995) described that property indicators of the southern ACC front were θ>1.8℃ along θ-maximum at the depth deeper than 500 dbar farther north of the front, or θ<0.0℃ along θ-minimum at the depth shallower than 150 dbar farther south of the front. Such water properties are found between Station A6 and Station A7.

Next, as shown in Fig. 3 (b), strong halocline with θ<0.0℃ is found at 70 dbar depth between Station A1 and Station A6. The saltiest water is distributed around 500 dbar depth at Station A1. On the other hand, it is found around 1200 dbar depth at Station A8. Accordingly, a strong salinity gradient exists between 500 dbar and 1200 dbar. This gradient also indicates the existence of the southern ACC front.

Finally we describe the density distribution. As shown in Figs. 3 (c) and (d), the strong pycnocline exists in the layer around 50 dbar between Station A1 and Station A6. In addition, a lens-like structure is conspicuous around this depth between Station A3 and Station A5, and suggests an existence of cyclonic eddy in this region. The strong horizontal gradient is also found in the density field below 100 dbar off shore of Station A6. This suggests that the southward flow exists off the southern ACC front. In contrast, a weak but opposite density gradient in the near-shore region is remarkable. This means an existence of northward flow.

We reconsider the previously described water distribution from the perspective of water property.

The coldest water in this region has the property of the Antarctic Surface Water (AASW) (−1.84℃< θ <2.00℃, S<34.00) (BINDOFF *et al.*, 2000). Below the AASW, UCDW (27.35< σ_θ

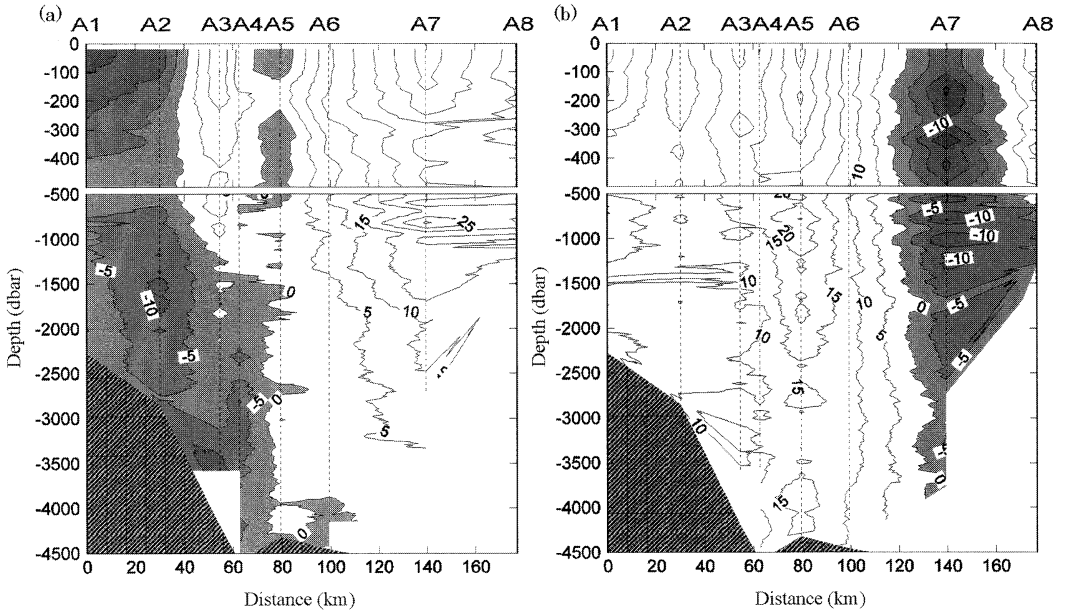

Fig. 4. Vertical sections of (a) eastward and (b) northward current velocity in cm/s measured by LADCP. Contour interval is 5 cm/s. Shaded areas indicate (a) westward and (b) southward current. Locations of observation stations are the same as these in Fig.3.

<27.75) (SIEVERS and NOWLIN, 1984) lies between 100 and 1000 dbar. According to the previous studies, the isopycnal of σ_θ=27.79 (ORSI *et al.*, 1995; REID, 1989) or σ_θ=27.80–27.81 (HEYWOOD *et al.*, 1999) follows the saltiest NADW. In this observation, the saltiest water mass is found around the isopycnal σ_θ=27.80. This isopycnal lies around 700 dbar between Station A2 and Station A6, and lies around 1000 dbar between Station A7 and Station A8. Below UCDW, the LCDW lies above AABW about 2500dbar. ORSI *et al.* (1999) adopted the σ_4=46.04–46.06 (Fig. 3 (d)) as a boundary between LCDW and AABW (ADLBW). ADLBW (θ <0.5 ℃ and 34.66<S<34.68) defined by BINDOFF *et al.* (2000) is found between Station A2 and Station A8 below LCDW.

3.3 Structure of the boundary current

In the vertical distribution of current shown in Fig. 4, the northwestward boundary current exists between Station A1 and Station A4 over the continental slope. Below 500 dbar, the westward current speed higher than 10 cm/s is observed around 1500 dbar depth at Station A2, and around 3500 dbar depth at Station A3. Current flows almost along isobaths between Station A1 and Station A4, although the direction is northeastward above about 1500 dbar between Station A3 and Station A4. Moreover northward flow is observed at Station A5 from bottom to surface, and northeastward extends from Station A5 to Station A6. Such a complicate current structure suggests the existence of a cyclonic eddy, which is already found as a lens-like structure in temperature and density field between Station A1 to Station A5.

The northward current speed is the highest at Station A5, and averaged current speed from surface to bottom is about 19 cm/s. DONOHUE *et al.* (1998) already pointed out that the core of northward boundary current existed around there. Current direction changes from northward to southward from bottom to surface between Station A6 and Station A7 where the southern ACC front exists. The Southward current velocity is more than 30 cm/s at 700 dbar of Station A7.

3.4 Geostrophic volume transport

Evaluating geostrophic current, it is important that the current velocity at the reference

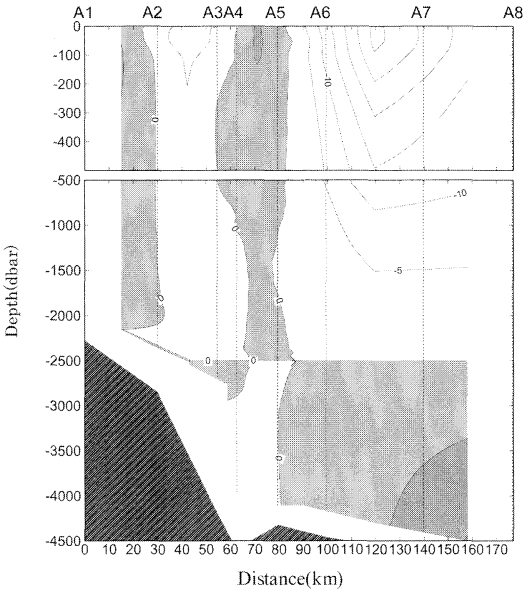

Fig. 5. Vertical section of the geostrophic current in cm/s for the reference level of 2500 dbar between Station A2 and Station A8. The deepest common depth of 2157 dbar is used between Station A1 and Station A2. Shaded areas indicate the northwestward current. Contour interval is 5 cm/s. Locations of observation stations are the same as these in Fig.3.

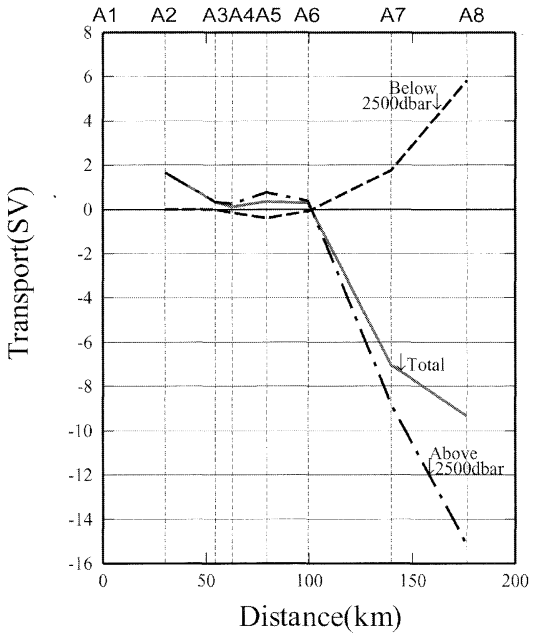

Fig. 6. Cumulative geostrophic transports integrated from Station A1 to Station A8. Positive value indicates the northwestward transport. Solid, dash-dotted and broken lines indicate the transport between surface and bottom (total), above 2500 dbar and below 2500 dbar, respectively.

level is negligible (SPEER and FORBES, 1994). They estimated northwestward geostrophic transports taking a reference at 2500 dbar depth, and obtained the transport of −12 SV (1 SV=10^6 m^3/s) between the reference level and the surface, 6 SV between the reference level and the bottom, and −6 SV in total. We first follow their analysis and choose 2500 dbar depth taking a reference level, and then, compare the current fields and transports by geostrophic calculation taking a reference of level of no motion with those by the direct current observations of LADCP.

As shown in Fig. 5, above the reference level, the northwestward currents are estimated between Station A1 and Station A2, and between Station A4 and Station A5. In contrast to this, southeastward current is estimated between Station A2 and Station A3. Above the reference level, the strong southeastward current is estimated between Station A5 and Station A8, and is larger than 30 cm/s at between Station A6 and Station A7 above 70 dbar. Below the reference level, northwestward current is estimated at between Station A6 and Station A7. The integrated transport (Fig.6) from Station A1 to Station A6 is about 0 sv above and below the reference level (2500 dbar), and much smaller than that between Station A6 and Station A8 (Table. 1). The transport on the plateau between Station A1 and Station A6 is smaller than that obtained by SPEER and FORBES (1994), because the northward transport associated with the cyclonic eddy prevails between Station A2 and Station A3. Northwestward transport exists between Station A6 and Station A8 below the reference level. Comparing this transport with their resolution; our estimate between Station A6 and Station A8 is about 6 SV, and coincided with their estimate (referred to their Fig. 4; the integrated transport of northeastern part about 100 km from reversals of transport below reference level, SPEER and FORBES, 1994).

We compare geostrophic transport taking a reference of level of no motion at 2500 dbar

Table. 1. Northwestward geostrophic transports in Sv (1 SV=10^6 m^3/s) below 2500 dbar, above 2500 dbar and between surface and bottom, respectively, as function of station (row) and geostrophic reference technique (column).

	A1–A6	A6–A8	A1–A8(total)
	from surface to bottom		
LNM*	0.2	−9.5	9.3
LADCP**	38.0	−39.5	−1.5
	above 2500 dbar		
LNM*	0.3	−15.5	−15.2
LADCP**	28.0	−31.5	−3.5
	below 2500 dbar		
LNM*	−0.1	6.0	5.9
LADCP**	10.0	−8.0	2.0

* Taking a reference of a Level of no motion at 2500 dbar.

** Matching geostrophic transport with that measured by LADCP between adjacent stations.

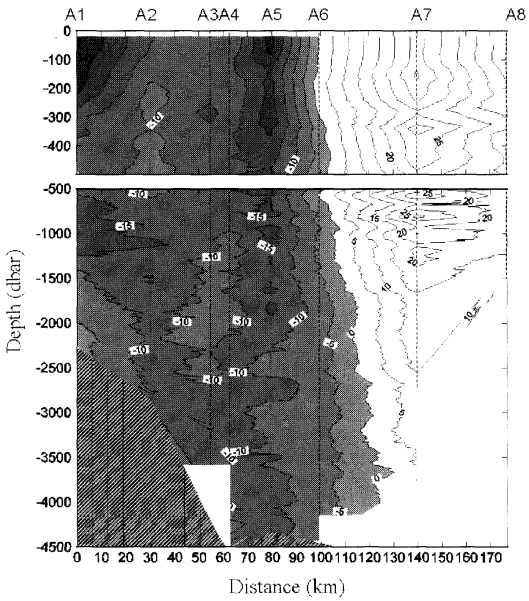

Fig. 7. Vertical section along the section (A-line) of current in cm/s observed by LADCP. Contour interval is 5 cm/s. Shaded areas indicate the northwestward current. Locations of observation stations are the same as these in Fig. 3.

(Fig. 5) with LADCP data (Fig. 7). The geostrophic transport taking a reference of level of no motion indicates that the the northwestward current is located between Station A6 and Station A8. On the other hand, direct current observations of LADCP the

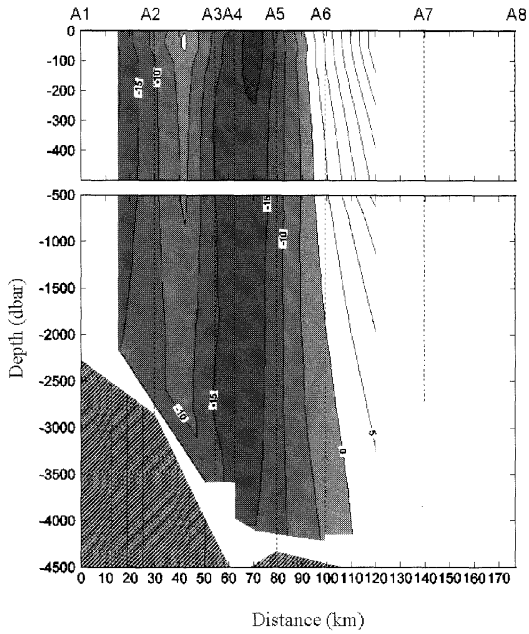

Fig. 8. Vertical section of the geostrophic current velocity in cm/s. The current is estimated by matching its total transport with that measured by LADCP between adjacent stations. Contour interval is 5 cm/s. Shaded areas indicate the northwestward current. Locations of observation stations are the same as these in Fig. 3.

northwestward current indicated that DWBC is located between Station A1 and Station A6.

The estimates based on a level of no motion are only based on the baroclinic flows referring to structure of density fields. DONOHUE *et al.* (1998) also suggested that the geostrophic transports based on a level of no motion would consequently underestimate the transport in the DWBC. Geostrophic calculations only yield velocity shear, and knowledge of the absolute velocity at any depth is required to estimate the barotropic component (HEYWOOD *et al.*, 1999).

Thus, in the present analysis, the geostrophic transport is estimated by matching its total transport with that by LADCP data between adjacent stations (Fig. 8). The current distribution shown in Fig. 9 is almost similar to these by the direct current observations of the LADCP as shown in Fig. 8. The integrated transport from Station A1 to Station A6 measured by the LADCP is about 10.0±1.3

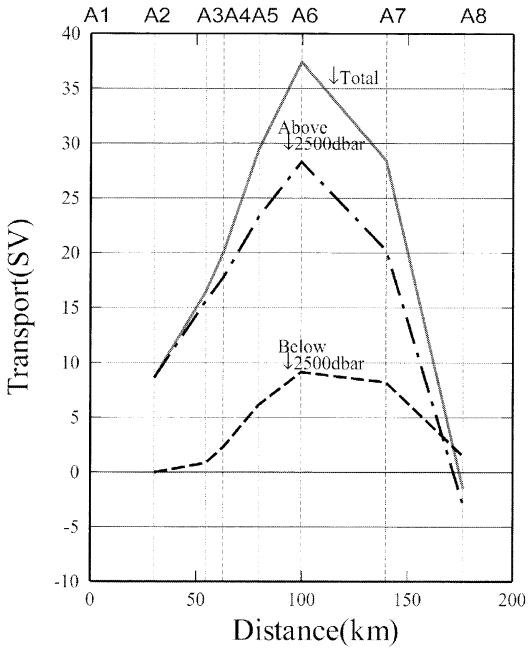

Fig. 9. Cumulative transports by cross-section LADCP velocity integrated from Station A1 to Station A8. Positive value indicates the northwestward transport. Solid, dash-dotted and broken lines indicate the transport between surface and bottom (total), above 2500 dbar and below 2500 dbar, respectively.

SV (Table. 1). As mentioned above, SPEER and FORBES (1994) and we estimate the DWBC transport at 6.0 SV based on the level of no motion at 2500 dbar. Thus, our own estimate is about 1.7 times larger than that by theirs. In addition, the DWBC is located between Station A6 and Station A8 by the geostrophic transport estimate taking a reference of no motion at 2500 dbar (Fig. 5), but that exist between Station A1 and Station A6 by the direct current observations of LADCP (Fig. 7).

4. Discussion

In consequence of matching the geostrophic fields to direct current observations by using LADCP, we can estimate the barotropic and baroclinic transports of DWBC. Barotropic transports are evaluated by the surface flow of the geostrophic current between adjacent stations by the method mentioned above. The barotropic and baroclinic transports between Station A6 and Station A7 are about 19.3 SV northwestward and 40.3 SV southeastward, respectively, and show that the southeastward transport of the ACC at the northern region of the southern ACC front. The northwestward barotropic and baroclinic transports are negligible and 4.3 SV between Station A2 and Station A3, and 4.4 SV and 1.0 SV between Station A3 and Station A4, respectively. This indicates the evidence of eastward flow due to the clockwise vortex around these stations. This vortex also appears in the distribution of temperature, salinity and density fields. A couple of lens-like structure of temperature exists about 70 dbar between Station A1 and Station A6. In this region around 70 dbar, the constricted part of temperature is located between Station A3 and Station A4 and distributes saline and high-density water; fresher and low-density water is distributed in the other region. The barotropic and baroclinic transports estimated are at 15.2 SV northwestward and 5.2 SV southwestward, respectively, between Station A1 and Station A6 below 2500 dbar where the DWBC exists. Accordingly, the geostrophic calculation based on the level of no motion at the 2500 dbar gives transports smaller than that based on direct current measurement by LADCP, because the barotropic transport at the level is not taken into account.

DONOHUE *et al.* (1998) used the method similar to that in present study and estimated transport below 500 dbar where potential temperature is lower than 1.0℃. They estimated the northwestward transport of 48.9±9.4 SV. Our calculation for the same temperature range and obtained the northwestward transport of 22.3±4.1 SV, which is less than a half of their estimation. Unfortunately, we cannot compare the current distribution directly with theirs, because they do not show the distribution in detail. But one of the reasons of the difference is probably due to difference of the observation line and period.

Acknowledgments

We would like to thank the captain Yoshio Koike, officers, crew and scientists of 9th cruise of the T/R Vessel Umitaka-Maru of Tokyo University of Marine Science and Technology from Port Luis to Fremantle. The

hydrographic observations are supported by any scientists, especially, the primary researcher of doctor Takashi Ishimaru. We also thank doctor Masao Nemoto for helpful discussions. We are very grateful to reviewer for their fruitful and constructive comments. Logistical support was provided by a Grant-in-Aid for Scientific Research (A) (14255012) from Japan Society for the Promotion of Science (JSPS).

References

BINDOFF, N.L., M.A. ROSENBERG and M.J. WARNER (2000) : On the circulation and water masses over the Antarctic continental slope and rise between 80 and 150° E. Deep-Sea Res. II, **47**, 2299-2326.

DONOHUE, K.A., G.E. HUFFORD and M.S. MCCARTNEY (1998) : Sources and transport of the Deep Western Boundary Current east of the Kerguelen Plateau. Geophys. Res. Lett., **26** (**7**), 851-854.

GORDON, A.L., E.J. MOLINELLI, and T.N. BAKER (1982): Southern Ocean Atlas. Columbia University Press, New York, 34pp

HEYWOOD, K.J., M.D. SPARROW, J. BROWN and R.R. DICKSON (1999) : Frontal structure and Antarctic Bottom Water Flow through the Princess Elizabeth Trough, Antarctica. Deep-Sea Res. I, **46**, 1181–2000.

MANTYLA, A.W. and J.L. REID (1995) : On the origins of deep and bottom waters of the Indian Ocean. J. Geophys. Res., **100**, 2417–2439.

ORSI, A.H., G.C. JOHNSON, and J.L. BULLISTER (1999): Circulation, mixing and the production of Antarctic Bottom Water. Prog. Oceanogr., **43**, 55–109.

ORSI, A.H., T. WHITEWORTH III and W.D. NOWLIN Jr., (1995) : On the meridional extent and fronts of the Antarctic Circumpolar Current. Deep-Sea Res. I, **42**, 641–673.

REID, J.L. (1989) : On the total geostrophic circulation of the South Atlantic Ocean: flow pattern, tracers and transports. Prog. Oceanogr., **23**, 149–244.

RODMAN, M.R., and A.L. GORDON (1982) : Southern Ocean bottom water of the Australian-New Zealand sector. J. Geophys. Res., **87**, 5771–5778.

SIEVERS, H.A. and W.D. NOWLIN Jr., (1984) : The stratification and water masses at Drake Passage. J. Geophys. Res., **89** (**C6**), 10489–10514.

SPARROW, M.D., K.J. HEYWOOD, J. BROWN and D.P. STEVENS (1996) : Current structure of the South Indian Ocean. J. Geophys. Res., **101**, 6377–6392.

SPEER, K.G., and A. FORBES (1994) : A deep water boundary current in the Indian Ocean. Deep-Sea Res. I, **41**, 1289–1303.

UNESCO (1981) : Tenth report of the joint panel on oceanographic tables and standards. UNESCO Technical Papers in Marine Science, Number 36, UNESCO, Paris, 1–45.

VISBECK, M. (2000) : Deep Velocity Profiling using Lowered Acoustic Doppler Current Profiler: Bottom Track and Inverse Solutions. J. Ocean. Tech., **19** (**5**), 794–807.

Received June 28, 2005
Accepted September 16, 2005

La mer 43 : 61–62, 2005
Société franco-japonaise d'océanographie, Tokyo

資　料

第43巻第1–2号掲載欧文論文の和文要旨

柳哲雄[*]・日野貴明[**]：黄河河川水プルームの挙動に関する短期・季節・潮汐周期変動

黄河河川水プルームの挙動に関する短期・季節・潮汐周期変動を，2002年1年間のNOAAの可視画像を使って調べた。その結果，黄河河川水プルームは河口を出た後，ライゾウ湾から渤海湾へと岸を左手に見て広がること，大潮時の広がり面積は小潮時より広いこと，季節変動はほとんどないことがわかった。これは，黄河河川水プルームは主に，ラグランジェ的な潮汐残差流により広がっていて，強い潮流による底質の再懸濁がその広がり面積に影響を与えているためである。

（[*]九州大学応用力学研究所　〒816–8580 春日市春日公園6 [**]九州大学大学院総合理工学府大気海洋システム学専攻　〒816–8580 春日市春日公園6）

Prasert Tongnunui[*]・佐野光彦[*]・黒倉　壽[*]：タイ王国トラン県シカオ湾に生息するモトギスとホシギスの食性

タイ王国トラン県シカオ湾において，2003年5月から2004年4月までに採集した892個体（127個体の稚魚と765個体の成魚）のモトギスと，734個体（159個体の稚魚と575個体の成魚）のホシギスの標本を用いて，両種の食性を明らかにした。両種の稚魚においては，成長に伴って主要な餌生物が変化することがわかった。小型の稚魚（標準体長40㎜以下）は主に動物プランクトンのカラヌス類などを採餌するのに対し，大型の稚魚（41～129㎜）では主に多毛類やエビ類などを食べていた。一方，両種の成魚（130㎜以上）の主要な餌生物は，大型稚魚のものと同様に多毛類とエビ・カニ類であり，全胃内容物体積に占める割合は合計70%以上であった。また，これらの餌の割合には明瞭な季節変化は認められなかった。さらに，調査期間中，稚魚や成魚の餌組成がモトギスとホシギスの間で明確に異なることもなかった。

（[*]東京大学大学院農学生命科学研究科農学国際専攻　〒113–8657　東京都文京区弥生1–1–1）

Mohamed Néjib Daly Yahia[1)], Ons Daly Yahia–KEFI, Sami Souissi, Fadhila Maamouri and Patricia Aissa. チュニス湾および隣接するラグーン（ガール・エル・メル湖及び南チュニス湖）（南地中海）におけるTintinnids (Ciliophora, Tintinnina) と毒化の可能性のある独立栄養渦鞭毛藻（Dinophyceae）の関係

チュニス湾とそれにつながる2つのラグーン（ガール・エル・メル湖と南チュニス湖）においてTintinnids及び毒化の可能性がある独立栄養の渦鞭毛藻類のサンプリングを毎月行った。得られた種組成から，Tintinnidsのラグーン群衆は隣接する海域の群衆構造の影響を強く受けていることが示唆された。Tintinnidsの出現種数はチュニス湾で61種，ガール・エル・メル湖で15種，南チュニス湖で12種であったが，少なくともどちらか一方の湖に出現した種はチュニス湾でも出現した。調査海域における主要種である*Favella ehrenbergi, Tintinnopsis* spp, *Stensemella nivalis* のブルームは，*Dinophysis acuminata, Alexandrium* sup, *Prorocentrum lima* の出現と関連しながら生じるものと推測された。これらの仮説をクラスター解析により検討した結果，優占種であるTintinnidsのいくつかの種と毒化の可能性がある渦鞭毛藻類との間の関係において同一性が認められた。

（– Laboratoire de Biosurveillance de l'Environnement. Groupe de Recherche en Hydrologie et Planctonologie. Département des Sciences de la Vie. Faculté des Sciences de Bizerte, Republic of Tunisia. 7021, Zarzouna, Bizerte.
Fax : 216 72 590 566 –
E-mail : nejib.daly@fsb.rnu.tn）

奥村　裕[*]・長坂洋光[**]・河野洋一[***]・神山孝史[*]・鈴木敏之[*]・山下　洋[****]：仙台湾石巻沖で採取した底泥中ダイオキシン類の堆積速度－1980年代以降について－

仙台湾石巻沖において1980年代以降の底泥中ダイオキシン類（ダイオキシン，ジベンゾフラン，コプラナーPCB）濃度を調査した。ダイオキシンが全ダイオキシン類濃度の約85%を占めており，中でも3種類のダイオキシン異性体（1,3,6,8–TCDD + 1,3,7,9–TCDD + O_8CDD）の合計が全ダイオキシン濃度の79%と優占していた。これら異性体は農薬の不純物と考えられており，80年代以降も農薬の不純物が仙台湾におけるダイオキシンの主要な起源であると考えられた。ダイオキシン類の堆積速度は，1992–2002の堆積層より1981–1992の堆積層でわずかに高く，表層ほど低くなる傾向があった。また，石巻沖における懸濁粒子の堆積速度は他の港湾地域より低い傾向にあった。水分含量，強

熱源量の結果より石巻沖では川からの無機粒子が他の港湾地域に比べ底泥の堆積に寄与していると考えられた。

(*(独) 水産総合研究センター・東北区水産研究所 〒985-0001 宮城県塩釜市新浜町3-27-5 **国土環境株式会社環境創造研究所 〒421-0212 静岡県志太郡大井川町利右衛門1334-5 ***(財) 日本食品分析センター 〒206-0025 東京都多摩市永山6-11-10 ****京都大学フィールド科学教育研究センター舞鶴水産実験所 〒625-0086 京都府舞鶴市字長浜無番地)

横田華奈子*・日比谷紀之*・長澤真樹*・高木省吾：本邦初の深海乱流計を用いた乱流パラメタリゼーションの有効性の検証**

密度躍層内の乱流混合は，深層海洋大循環のパターンや強さをコントロールする重要な物理現象であり，そのグローバルなマッピングに向けてエネルギー消散率ϵの見積もりは不可欠な課題となる。しかしながら，深海乱流計を用いたϵの直接観測には少なくとも2時間を必要とするため、それをグローバルに展開することは甚だ困難である。これを解決するためには，観測のより容易なファインスケールの物理パラメータからϵを見積もるというパラメタリゼーションが必要となる。従来，このパラメタリゼーションとして，10mスケールの鉛直シアーからϵを見積もるGREGGの式(GREGG, 1989) が広く使われてきたが，その有効性についてはまだ十分に確かめられていなかった。本研究では，我が国では初めてとなる深海乱流計(TurboMAP-D1) を用いてϵの直接観測を行い，GREGGの式を用いて見積もったϵと比較することによって，このパラメタリゼーションの有効性を検証した。その結果，GREGGの式はϵの深度分布を比較的よく再現するが，特に低緯度において，ϵの値を全体的に過大評価してしまうことが明らかになった。また，この不一致はϵの緯度依存性を考慮したHENYEY *et al.* (1986) のパラメタリゼーションを用いることによって解消できることが示された。このことは，GREGG の式に基づいて見積もったエネルギー消散率が見かけの緯度分布を示してしまう可能性のあることを示している。

(*東京大学大学院理学系研究科地球惑星科学専攻 〒113-0033 東京都文京区本郷7-3-1 **北海道大学水産学部 〒041-8611 函館市港町3-1-1)

鳴海吉洋*・川村有二・日下朋子*・北出裕二郎*・長島秀樹*: 南大洋インド洋セクターにおけるケルゲレン海堆のDeep Western Boundary Currentについて: LADCP観測から得られた結果**

Deep Western Boundary Current (DWBC) は，南大洋インド洋セクターケルゲレン海堆の東側斜面に存在する北西向きの流れである。その流量は，2500dbarを無流面とした地衡流計算から約6 SV (1 SV=10^6m^3/s) と見積もられている (Speer and Forbes, 1994)。この流れを明らかにするために，2003年1月，ケルゲレン海堆の等深線に直交する形で測線を設け，CTDおよびLADCP観測を実施した。LADCPデータからその流量を見積もったところ北西向き10SVとなり，Speer and Forbes (1994)が見積もった流量の1.7倍であることがわかった。また，地点間の地衡流計算による流量とLADCPデータによる流量が等しくなるよう基準面を設定した。この地衡流計算の結果からDWBCの傾圧，順圧流量を見積もったところ，それぞれ北西向き-5，15SVとなった。以上のことから，無流面に基づく地衡流計算によるDWBCの見積もりでは，その順圧流量が過小評価される。

(*東京海洋大学海洋科学部海洋環境学科 〒108-8477 東京都港区港南4-5-7 **現在： 愛媛大学沿岸環境科学研究センター 〒790-8577 愛媛県松山市文京町2-5)

La mer 43: 63-68, 2005
Société franco-japonaise d'océanographie, Tokyo

学 会 記 事

1. 2005年3月28日（月）東京海洋大学海洋環境棟会議室において幹事会が開かれた。
   1．日本学術会議会員候補者の情報提供について
   2．日仏会館科学シンポジウムの開催
   3．ケルゲレン諸島学術調査関連
   4．2005年度「日仏共同研究」
   5．日仏関連学会連絡協議会

2. 2005年5月27日（金）東京海洋大学海洋環境棟会議室において幹事会および評議員会が開かれた。
   1．平成16年度事業報告
   2．平成16年度決算報告及び監査報告
   3．平成17年度事業計画（案）
   4．平成17年度予算（案）審議
   5．日仏共同シンポジウムの実施

3. 新入会員

氏 名	所 属	紹介者
山田昌郎	独立行政法人 港湾空港技術研究所 構造強度研究室 〒239-0826 横須賀市長瀬3-1-1	森永 勤
長岩理史	東京海洋大学海洋環境学科 海洋生物学講座 〒108-8477 東京都港区港南4-5-7	山口征矢
小野敦史	東京海洋大学 海洋環境保全学専攻 海洋生物学講座 浮遊生物学研究室 〒108-77 東京都港区港南4-5-7	荒川久幸
渡部俊広	独立行政法人 水産総合研究センター 水産工学研究所 漁業生産工学部 漁法研究室 〒314-0421 茨城県鹿島郡波崎町海老台	森永 勤

4. 所属・住所変更（受付順）

下田 徹 〒907-0451 沖縄県石垣市桴海大田148-446
西海区水産研究所 石垣支所

高橋正征 〒783-8502 高知県南国市物部乙200
高知大学大学院黒潮海洋科学研究科

愛澤政二 〒105-0001 東京都港区虎ノ門2-5-4
末広ビル
(株)イーエムエスアイ

小林 貴 〒225-8502 横浜市青葉区鉄町1614
桐蔭横浜大学 医用工学部

奥田邦明 〒085-0802 北海道釧路市桂恋116
独立行政法人 水産総合研究センター
北海道区水産研究所

和田 明 〒102-0073 東京都千代田区九段北4-2-1
市ヶ谷東急ビル609号室 日本大学大学院
総合科学研究科 環境科学専攻

寺崎 誠 〒164-8039 東京都中野区南台1-15-1
東京大学海洋研究所

門谷 茂 〒160-0813 札幌市北区13条西8
北海道大学大学院環境研究室
海洋生物生産環境コース

落合正宏 〒769-2193 徳島県さぬき市志度1314-1
徳島文理大学工学部 環境システム工学科

高橋 暁 〒737-0797 広島県呉市広末広2-2-2
産業技術総合研究所
中国センター地質情報研究部門
沿岸海洋研究グループ

日仏海洋学会誌「うみ」投稿規定

1. 「うみ」(欧文誌名 La mer) は日仏海洋学会の機関誌として，和文または欧文により，海洋学および水産学ならびにそれらの関連分野の研究成果を発表する学術雑誌であり，同時に研究者間の情報交換の役割をもつことを目的としている。
2. 「うみ」は，原則として年4回発行され，投稿（依頼原稿を含む）による原著論文，原著短報，総説，学術資料，書評その他を，編集委員会の審査により掲載する。これらの著作権は日仏海洋学会に帰属する。
3. 投稿は日仏海洋学会会員，および日仏海洋学会正会員に準ずる非会員からとする。共著者に会員を含む場合は会員からの投稿とみなす。
4. 用語は日，仏，英3カ国語のいずれかとする。ただし，表および図の説明の用語は仏文または英文に限る。原著論文には約200語の英文または仏文の要旨を別紙として必ず添える。なお，欧文論文には約500字の和文要旨も添える。ただし，日本語圏外からの投稿の和文要旨については編集委員会の責任とする。
5. 原稿はすべてワードプロセッサを用いて作成し，本文・原図とも2通（正，副各1通）ずつとする。副本は複写でよい。本文原稿はすべてA4判とし，白紙にダブル・スペース（和文ワープロでは相当間隔）で記入する。表原稿および図の説明原稿は本文原稿とは別紙とする。
6. 投稿原稿の体裁形式は「うみ」最近号掲載論文のそれに従う。著者名は略記しない。記号略号の表記は編集委員会の基準に従う。引用文献の表示形式は，雑誌論文，単行本分載論文（単行本の一部引用も含む），単行本などの別による基準に従う。
7. 原図は版下用として鮮明で，縮尺（版幅または1/2版幅）に耐えられるものとする。
8. 初稿に限り著者の校正を受ける。
9. すべての投稿原稿について，1編あたり5万円の論文掲載料を申し受けます。
10. 会員に対しては10印刷ページまでの掲載を無料とする。会員の投稿で上記限度を超える分および非会員投稿（依頼原稿を除く）の印刷実費はすべて著者負担（1万円/ページ）とする。ただし，カラー印刷を含む場合には，別に所定の費用（1ページあたり9万円）を著者（会員，非会員とも）負担とする。
11. すべての投稿原稿について，1編あたり別刷り50部を無料で請求できる。50部を超える分は請求により50部単位で有料で作製される。別刷り請求用紙は初稿校正と同時に送付される。
12. 原稿の送り先は下記の通りとする。なお著者（共著の場合は代表者）連絡先のe-mailアドレス並びにFAX番号を付けることとする。

〒108-8477 東京都港区港南4-5-7
東京海洋大学海洋科学部海洋環境学科（吉田 次郎気付）
日仏海洋学会編集委員会
e-mail：jiroy@s.kaiyodai.ac.jp

執 筆 要 領

1. 原稿

(1) 和文原稿の場合：ワードプロセッサを使用し，A4版の用紙におよそ横30字，縦25行を目安に作成すること。
(2) 欧文原稿の場合：ワードプロセッサを使用し，A4版の用紙にダブルスペース25行でタイプし，十分な英文添削または仏文添削を経て提出すること。
(3) 和文原稿，欧文原稿いずれの場合も，要旨，表原稿および図版説明原稿はそれぞれ本文原稿とは別紙とする。
(4) 最終原稿提出の際に，印刷原稿とともに原稿，表，図版が保存されたフロッピーディスク，CD-R/RW，MO等での提出を依頼する。この場合，原稿はMicrosoft WORD，Just System 一太郎，PDFの原稿のみに限る。また，表，図版はこれら原稿ファイルの中に取り込むか，bmp，jpg等の一般的な画像ファイルに保存したものに限る。なお，電子媒体は返却しない。

2. 原稿記載の順序

(1) 原著（和文原稿）：原稿の第1ページ目に表題，著者名，研究の行われた所属機関，所在地，郵便番号を和文と英文で記載する。研究終了後所属機関が変わった場合は現所属機関も記載する。連絡先（共著の場合は連絡先とする著者を明示する）の住所，電話番号，ファックス番号，E-mailアドレスも記す。最後にキーワード（4語以内），ランニングヘッドを英文で記載すること。第2ページ目に欧文要旨（欧文表題，著者名を含む）を200語以内で記す。本文は第3ページ目から，「緒言」「資料」「結果」「考察」「謝辞」「文献」「図版の説明」などの章立てあるいは項目で順に記載する。基本的には最近号掲載論文の体裁形式を参考にして投稿原稿を作成すること。原稿には通しのページ番号を記入すること。

(2) 原著（欧文原稿）：原稿の第1ページ目に表題，著者名，研究の行われた所属機関，所在地，郵便番号を記載する。研究終了後所属機関が変わった場合は現所属機関も記載する。最後にキーワード（4語以内），ランニングヘッドを記載すること。第2ページ目に欧文要旨（欧文表題，著者名を含む）を200語以内で記す。本文は第3ページ目からとする。「Introduction」「Data」「Results」「Discussion」「Acknowledgement」「References」「Figure Caption」などの章立てで順に記載する。基本的には投稿原稿の体裁形式は最近号掲載論文を参考にして作成すること。最終ページに和文の表題，著者名，連絡先著者住所，電話番号，ファックス番号，E-mailアドレスおよび約500字以内の和文要旨を添える。原稿には通しのページ番号を記入すること。

(3) 原著短報，総説：和文ならびに欧文原稿とも原著論文に準ずる。

(4) 学術資料，書評：特に記載に関する規定はないが，すでに掲載されたものを参考にすること。

3. 活字の指定

原稿での活字は10.5pt～12ptを目安に設定し，英数字は半角フォントを用いること。学名はイタリック，和文原稿での動植物名はカタカナとすること。句読点は（。）および（，）とするが，文献リストでは（.）および（,）を用いること。章節の題目，謝辞，文献などの項目はボールドまたはゴシックとする。

4. 文献

文献は本文および図表に引用されたもののすべてを記載しなければならない。和文論文，欧文論文共に筆頭著者のアルファベット順（同一著者については，単著，共著の順とし，それぞれ発表年の古い順）にまとめ，以下の例に従って記載する。

(1) 論文の場合

有賀祐勝,前川行幸,横浜康継（1996）：下田湾におけるアラメ群落構造の経年変化.うみ, **34**, 45–52.

YANAGI, T. T. TAKAO and A. MORIMOTO (1997): Co-tidal and co-range charts in the South China Sea derived from satellite altimetry data. La mer, **35**, 85–93.

(2) 単行本分載論文（単行本の一部引用の場合）

村野正昭（1974）：あみ類と近底層プランクトン.海洋学講座10　海洋プランクトン（丸茂隆三編），東京大学出版会，東京，p.111–128.

WYNNE, M. J. (1981): Pheaophyta: Morphology and classification. *In* the Biology of Seaweeds. LOBBAN, C. S. and M. J. WYNNE (eds.), Blackwell Science, Oxford, p.52–85.

(3) 単行本の場合

柳　哲雄（1989）：岸海洋学—海の中でものはどう動くか—. 恒星社厚生閣，東京，154pp.

SVERDRUP, H. U., M. W. JOHNSON and R. H. FLEMING (1942): The Oceans: Their Physics, Chemistry and General Biology. Prentice-Hall, Englewood Cliffs, New York, 1087pp.

(4) 本文中での文献の引用

本文中での文献の引用方法はすでに発行された雑誌を参考にするが，基本的には次の形式に従う。

①GREVE and PARSONS(1977)

②（AVIAN and SANDRIN, 1988），

③YANAGI *et al.*（1997）は……（3名以上の共著の場合）

④……示されている（例えば，YANAGI *et al.*, 1997）（3名以上の共著の場合）

5. 図，表および写真

(1) 図，表および写真とその説明はすべて英文または仏文を用いる。

(2) 図，表はそのまま写真製版用の草稿となるような明瞭なもので，A4版の上質紙に作製したもの（写真は，正原稿についてもオリジナルとは別にA4版の用紙にコピーしておくことが望ましい）のみを受け付ける。カラー図を希望する場合はその旨明記する。この場合，別に所定の費用を著者負担とする。

(3) 写真は光沢平滑印画紙に鮮明に焼き付けたものを受け付ける。カラー写真の印刷を希望する場合はその旨明記する。この場合，別に所定の費用を著者負担とする。

(4) 図，表および写真は刷り上がり時に最大横が14cm，縦が20cm（説明文を含む）以内であることを考慮して作製すること。

(5) 図（写真を含む）には，Fig. 1, Fig. 2, ……のように通し番号をつけ，一つの図中に複数の図を含む場合はFig. 3 (a), Fig. 3 (b), ……のように指定する。本文中での引用は和文原稿の場合も「Fig. 1にみられるように……」のようにすること。

(6) 表には，表題の次（表の上のスペース）に説明をつけ，表ごとに別紙とし，Table 1, Table 2,.....のように通し番号をつけること。

(7) 図，表および写真は1枚ごとに著者名，通し番号をつけること。また，本文中での挿入箇所を最終提出原稿の該当箇所右欄外に朱書きすること。

(8) 図，写真の説明は別紙にまとめること。

(9) 地図にはかならず方位と縮尺または緯度，経度を入れること。

6. 単位系

原則としてSI単位を用いること。塩分は実用塩分単位（Practical Salinity Unit： psuまたは PSU）を用いる場合は単位なしとする。

Information for Contributors

1. The scientific journal,"La mer," the official organ of Japanese-French Oceanographic Society (JFOS), is published quarterly. "La mer" is open to all researchers in oceanography, fisheries and related sciences in the world. The journal is devoted to the publication of original articles, short contributions, reviews, book reviews, and information in oceanography, fisheries and related fields. Submission of a manuscript will imply that it has not been published or accepted for publication elsewhere. The editorial board decides the acceptance of the manuscript on the basis of peer-reviews and is responsible for its final editing. The Society reserves the copyright of all articles in the Journal.
2. *Submission*: Manuscripts must be written in French, English or Japanese. Authors are requested to submit their original manuscript and figures with one copy to the Editor in chief.
3. *Publication charges*: Each accepted article is charged 50,000 yen for publication. For members, there will be no page charge for less than ten printed pages, and 10,000 yen will be charged per page for the excess, except for color pages. For nonmembers there is a publication charge of 10,000 yen per printed page except for color pages. Color illustrations will be provided at cost.
4. *Proofs and reprints*: Fifty reprints of each article will be provided free of charge. Additional reprints can be provided in blocks of 50 copies. Proofs will be sent to the corresponding author. A reprint order form will be sent with the proofs.
5. Manuscripts should be sent to

   Editor in Chief of "La mer"
   Jiro Yoshida
   Department of Ocean Sciences
   Tokyo University of Marine Science and Technology
   Konan, Minato-Ku, Tokyo, Japan 108-8477.
   jiroy@s.kaiyodai.ac.jp

Manuscript Preparation

1. General
   1) Manuscripts must be typed with double-spacing on one side of A4 size white paper with wide margins.
   2) Figures, tables, and figure captions should be prepared separate from the main text.
   3) Authors should submit an electronic copy of their paper with the final version of the manuscript. The electronic copy should match the hardcopy exactly and should be stored in CD-R/W or FD. MS-WORD (Windows) and PDF formats are accepted.
2. Details
   1) The first page of the manuscript should include the title, author's full names and affiliations including Fax numbers and E-mail addresses. The corresponding author should be designated. Key words (up to four words) and running head should be written at the bottom of the page.
   2) An abstract of 200 words or less in English or French should be on the second page.
   3) The main text should start on the third page. Please adhere to the following order of presentation: main text, acknowledgements, appendices, references, figure captions, tables. All pages except the first page must be numbered in sequence.
   4) Mathematical formulae should be written with a wide space above and below each line. Syst e me International (SI) units and symbols are preferred.
   5) All references quoted in the text should be listed separately in alphabetical order according to the first author's last name. Citations must be complete according to the following examples:

   Article: YANAGI, T. T. TAKAO and A.MORIMOTO (1997): Co-tidal and co-range charts in the South China Sea

derived from satellite altimetry data. La mer, **35**, 85–93.

Chapter: WYNNE, M.J. (1981): Pheaophyta: Morphology and classification. *In* the Biology of Seaweeds. LOBBAN, C.S. and M. J. WYNNE (eds.), Blackwell Science, Oxford, p. 52–85.

Book: SVERDRUP, H. U., M. W. JOHNSON and R. H. FLEMING (1942): The Oceans: Their Physics, Chemistry and General Biology. Prentice-Hall, Englewood Cliffs, New York, 1087pp.

6) *Illustrations*: All illustrations should be provided in camera-ready form, suitable for reproduction (which may include reduction) without retouching. Photographs, charts and diagrams are all to be referred to as "Fig(s)." and should be numbered consecutively in the order to which they are referred. They should accompany the manuscript, but should not be included within the text. All figures should be clearly marked on the back with the figure number and the author's name. All figures are to have a caption. Captions should be supplied on a separate sheet.

7) *Photographs*: Original photographs must be supplied as they are to be reproduced (e.g. black and white or color). If necessary, a scale should be marked on the photograph. Please note that photocopies of photographs are not acceptable. Half-tone illustrations should be kept to a minimum.

8) *Color illustrations*: The printing cost of color illustrations must be borne by authors or their institution. Authors will receive information about the cost on acceptance of the manuscript.

9) *Tables*: Tables should be numbered consecutively and given a suitable caption on top and each table typed on a separate sheet.

賛助会員

アレック電子株式会社	神戸市西区井吹台東町７－２－３
株式会社イーエムエス	神戸市中央区多聞通３－２－９
有限会社英和出版印刷	文京区千駄木４－20－６
株式会社内田老鶴圃　内田　悟	文京区大塚３－34－３
財団法人海洋生物環境研究所	千代田区神田神保町３－29　帝国書院ビル５Ｆ
株式会社川合海苔店	大田区大森本町２－31－８
ケー・エンジニアリング株式会社	台東区浅草橋５－14－10
国土環境株式会社	横浜市都筑区早渕２－２－２
三洋測器株式会社（環境情報研究所）	渋谷区恵比須南１－２－８
株式会社高岡屋	台東区上野６－７－22
テラ株式会社	世田谷区代沢４－44－２　下北沢ビル２Ｆ
日本海洋株式会社	北区栄町９－２
渡邊機開工業株式会社	愛知県渥美郡田原町神戸大坪230

日仏海洋学会入会申込書

（正会員・学生会員）

	年度より入会	年　月　日申込
氏　名 ローマ字		年　月　日　生
住　所　〒 勤務先　機関名 電　話　E-mail:		
自　宅　住　所　〒 電　話　E-mail:		
紹介会員氏名		
送付金額　円	送金方法	
会誌の送り先（希望する方に○をつける）	勤務先　自　宅	

（以下は学会事務局用）

受付	名簿 原簿	会費 原簿	あて名 カード	学会 記事

入会申込書送付先：〒150-0013 東京都渋谷区恵比寿 3-9-25

（財）日仏会館内

日 仏 海 洋 学 会

郵便振替番号：00150−7−96503

2005年5月25日印刷
2005年5月28日発行

う　み　　第43巻 第1・2号

定価　¥5,000

編集者　吉田次郎
発行所　日仏海洋学会
財団法人　日仏会館内
東京都渋谷区恵比寿3-9-25
郵便番号：150-0013
電話：03（5421）7641
振替番号：00150-7-96503
印刷者　佐藤一二
印刷所　㈲英和出版印刷社
東京都文京区千駄木4-20-6
郵便番号：113-0022
電話：03（5685）0621

本雑誌に関する問い合わせ　電話番号 03(5463)0462

う　み

第 43 巻　第 1-2 号

2005年 5 月

日仏海洋学会